SHRP-A-401

Low-Temperature Cracking: Field Validation of the Thermal Stress Restrained Specimen Test

Hannele K. Kanerva
Ted S. Vinson
Huayang Zeng

Department of Civil Engineering
Oregon State University

Strategic Highway Research Program
National Research Council
Washington, DC 1994

SHRP-A-401
Contract A-033A
ISBN 0-309-05808-2
Product No.: 1021

Program Manager: *Edward T. Harrigan*
Project Manager: *Rita Leahy*
Program Area Secretary: *Juliet Narsiah*

June 1994

key words:
asphalt concrete
asphalt
cold climates
cracking
low-temperature cracking
pavements
temperatures
thermal cracking

Strategic Highway Research Program
National Research Council
2101 Constitution Avenue N.W.
Washington, DC 20418

(202) 334-3774

1500/NAP/694

Acknowledgments

The research described herein was supported by the Strategic Highway Research Program (SHRP). SHRP is a unit of the National Research Council that was authorized by section 128 of the Surface Transportation and Uniform Relocation Assistance Act of 1987.

This project, entitled "Performance Related Testing and Measuring of Asphalt-Aggregate Interactions and Mixtures," was conducted at the Institute of Transportation Studies, University of California at Berkeley, with Carl L. Monismith as Principal Investigator.

The work reported herein has been conducted as a part of Project A-003A of the Strategic Highway Research Program (SHRP).

The support and encouragement of R. Gary Hicks, Co-principal Investigator on the Low-Temperature Cracking Subtask, is gratefully acknowledged.

Contents

List of Figures

List of Tables

Abstract

The purpose of the field validation program was to evaluate the thermal stress restrained specimen test (TSRST) as the accelerated performance test to predict low-temperature cracking of asphalt concrete mixtures.

Construction histories, cracking observations, and temperature data were collected for five test roads. In addition, a validation program was conducted at the U.S. Army Cold Regions Research and Engineering Laboratory (USACRREL). The laboratory test program consisted of performing the TSRST on specimens fabricated in the laboratory with original materials from the test roads and asphalt concrete pavement specimens cut from the actual test sections. In addition, the field pavements were monitored for crack history and, where possible, crack initiation.

TSRST fracture temperature correlated with field cracking temperature and crack frequency. TSRST results can be used to predict field low-temperature cracking of asphalt-aggregate mixtures. Preliminary models to predict cracking frequency and temperature for the test roads were developed.

Executive Summary

The purpose of the field validation program reported herein was to analyze the performance of the thermal stress restrained specimen test (TSRST) as the accelerated performance test (APT) to predict low-temperature cracking of asphalt concrete mixtures. Performance-based specifications can be developed from a model that uses TSRST results to represent the effect of mixture properties on low-temperature cracking.

Five test roads were selected for the field validation of the TSRST. Two of the roads are in Fairbanks, Alaska; one is in Elk County, Pennsylvania; and two are in Peraseinajoki and Sodankyla, Finland. Construction histories, cracking observations, and temperature data were collected for the test results. In addition, a validation program was conducted at the Frost Effects Research Facility (FERF) of the U.S. Army Cold Regions Research and Engineering Laboratory (USACRREL). The environmental conditions at the FERF could be precisely controlled, and an extensive instrumentation system located there could be used for temperature and crack detection.

The laboratory test program consisted of a set of TSRST experiment designs for specimens that were fabricated in the laboratory with original materials from the test roads and asphalt concrete pavement specimens cut from the actual test sections. Elapsed time, temperature, and tensile load were recorded with the TSRST system.

Correlations of TSRST fracture temperature with field cracking temperature and crack frequency were investigated. Cracking behavior of the test roads could be explained with TSRST fracture temperatures for Alaska, Pennsylvania, Peraseinajoki and USACRREL. In Sodankyla, other factors besides mixture properties affected low-temperature cracking.

TSRST results can be used to predict field low-temperature cracking of asphalt-aggregate mixtures. Preliminary models to predict cracking frequency and temperature for the test roads were developed. Thus, it should be possible to develop a model that would predict low-temperature cracking response for all climate conditions.

1

Introduction

1.1 Background

It is inevitable that low-temperature cracking will occur in pavements constructed in the cold regions of the world. Esch and Franklin (1989) state that all pavements in Alaska, with the possible exception of those in the south-coastal areas, can be expected to suffer from thermal-contraction cracking. Therefore, it is imperative that design engineers involved in establishing the requirements for pavements identify an asphalt concrete mixture that will minimize low-temperature cracking without compromising other performance characteristics, such as resistance to rutting.

Three approaches may be employed to identify the low-temperature cracking resistance of an asphalt concrete mixture: *(1)* regression equations, *(2)* mechanistic prediction, and *(3)* laboratory simulation tests.

Regression Equations Based on an analysis of data from 26 airfields in Canada, Haas et al. (1987) established the following regression equation to predict the average transverse crack spacing in a pavement structure:

$$\text{TCRACK} = 218+1.28\ \text{ACTH}+2.52\ \text{MTEMP}+30\ \text{PVN}-60\ \text{COFX} \qquad (1.1)$$

in which

TCRACK = transverse crack average spacing in meters,
MTEMP = minimum temperature recorded on site in °C,
PVN = McLeod's dimensionless pen-vis number (PVN),
COFX = coefficient of thermal contraction in mm/1000 mm/°C, and
ACTH = thickness of the asphalt concrete layer in centimeters.

The PVN in equation (1.1) (determined from the penetration at 25°C and the kinematic viscosity at 135°C) is an indicator of temperature susceptibility of the asphalt cement

(McLeod 1972, and 1987). As the PVN decreases for a given grade of asphalt, the temperature susceptibility increases. Consequently, as the PVN decreases, the average crack spacing increases. Further, crack spacing increases with pavement age and minimum temperature but decreases with pavement thickness.

Equation (1.1) may not be applicable to airfields in the subarctic and arctic. The 26 airfields evaluated were located below 50° north latitude. Fifteen were coastal-associated airports. Approximately half of the observations were made for pavement overlays. Finally, extracted asphalt cement properties were used to develop the regression equation(s).

Mechanistic Prediction This approach may be visualized in Figure 1.1. Specifically, low-temperature cracking occurs in the surface layer when the thermally induced tensile stress (due to the pavement's tendency to contract with decreasing temperature) equals the tensile strength of the asphalt concrete mixture. The thermally induced tensile stress is generally calculated from a pseudo-elastic beam-analysis equation of the following form (Hills and Brien 1966):

$$\sigma(\dot{T}) = \alpha \sum_{T_o}^{T_f} S(t,T) \cdot \Delta T \qquad (1.2)$$

in which

$\sigma(\dot{T})$	=	accumulated, thermal stress for a particular cooling rate,
α	=	coefficient of thermal contraction
T_o, T_f	=	initial and final temperature, respectively,
$S(t,T)$	=	asphalt concrete mix stiffness (modulus), time- and temperature-dependent, and
ΔT	=	temperature increment over which S(t,T) is applicable.

The approximate solution suggested by equation (1.2) may yield reasonable results provided that two input parameters are correctly measured or assumed: *(1)* the coefficient of thermal contradiction, and *(2)* the asphalt concrete mix stiffness. The tensile strength of the asphalt concrete mix may be estimated or measured in the laboratory in either direct or indirect tension.

The determination of both the asphalt concrete mix stiffness and the tensile strength requires that the rate of cooling in the field (and the associated development of tensile stresses and strength) must be related to a rate of loading or deformation in the laboratory (or in the case of a creep test, a time after initial loading). To date, a procedure to accomplish this task has not been convincingly demonstrated to the pavement engineering community. Further, in the calculation of thermal stress, the thermal contraction coefficient is generally assumed to be 2 to 2.5×10^{-5} per °C. Recent measurements of the thermal contraction of mixes with high void contents or mixes employing modified asphalt cement suggest that this assumption could be in error by a factor of two or three. Further, age conditioning of the specimens for the determination of the mix stiffness or tensile strength has not been considered in the application of this approach. Finally, several researchers have noted that any approach that

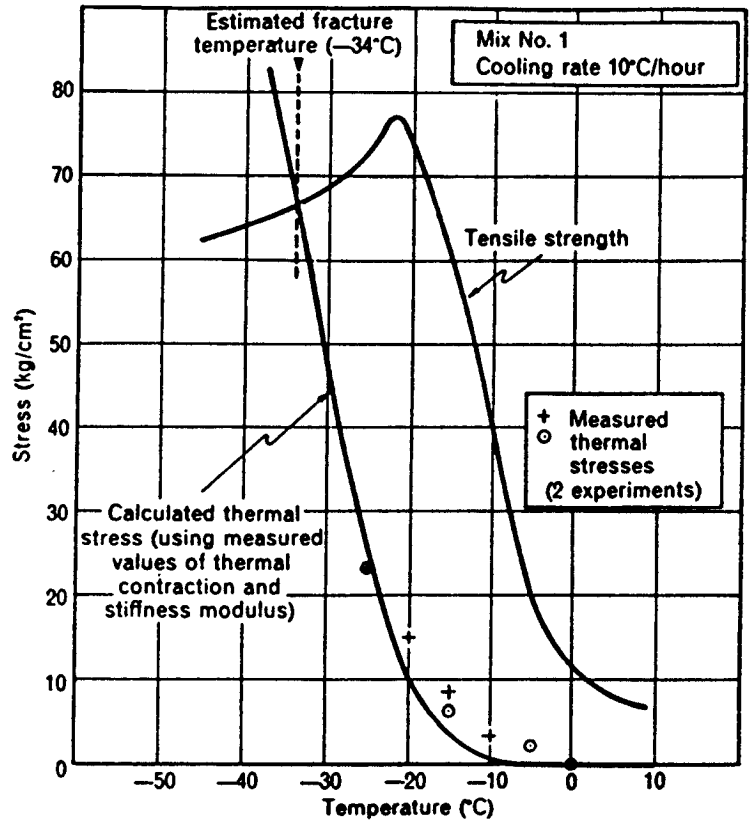

Figure 1.1. Estimating the fracture temperature of asphalt concrete (Hills and Brien 1966)

is fundamentally related to a measurement of the stiffness of the mix will not be acceptable for mixtures that employ modified asphalt cements.

Simulation Measurement. Monismith et al. (1965) were the first to suggest that the thermally induced stress, strength, and temperature at failure could be measured in a laboratory test that simulated the conditions to which a pavement slab was subjected in the field. The basic requirement for the test system is that it maintain the test specimen at constant length during cooling. Initial efforts involved the use of fixed frames constructed from invar steel (Monismith et al. 1965; Fabb 1974; Janoo 1989; Kanerva and Nurmi 1991). In general, these devices were not satisfactory because as the temperature decreased, the load in the specimen caused the frame to deflect to such a degree that the stresses relaxed and the specimen didn't fail! Arand (1987) substantially improved the test system by inserting a displacement feedback loop, which ensured that the stresses in the specimen would not relax because the specimen length was continuously corrected during the test.

A recent version of this system is shown in Figure 1.2. The system consists of a load frame, screw jack, computer data acquisition and control system, low-temperature cabinet, temperature controller, and specimen-alignment stand. A beam or cylindrical specimen is mounted in the load frame, which is enclosed by the cooling cabinet. The chamber and specimen are cooled with vaporized liquid nitrogen. As the specimen contracts, linearly variable differential transducers (LVDTs) sense the movement and a signal is sent to the computer, which, in turn, causes the screw jack to stretch the specimen back to its original length. This closed-loop process continues as the specimen is cooled and ultimately fails. Measurements of elapsed time, temperature, deformation, and tensile load are recorded with a data acquisition system. This system is called the Thermal Stress Restrained Specimen Test (TSRST).

A typical result from a TSRST is shown in Figure 1.3. The thermally induced stress gradually increases as temperature decreases, until the specimen fractures. At the break point, the stress reaches its maximum value—the fracture strength, a corresponding fracture temperature. The slope of the stress-temperature curve, dS/dT, increases until it reaches a maximum value. At colder temperatures, dS/dT becomes constant, and the stress-temperature curve is linear. The transition temperature divides the curve into two parts—relaxation and nonrelaxation. As the temperature approaches the transition temperature, the asphalt cement becomes stiffer, and the thermally induced stresses are not relaxed beyond this temperature for a specified rate of cooling.

1.2 Purpose

The purpose of the field validation program reported herein is to analyze the performance of the TSRST as the accelerated performance test (APT) to predict low-temperature cracking of asphalt concrete mixes. Performance-based specifications may be based on a model that uses TSRST results to represent the effect of mix properties on low-temperature cracking.

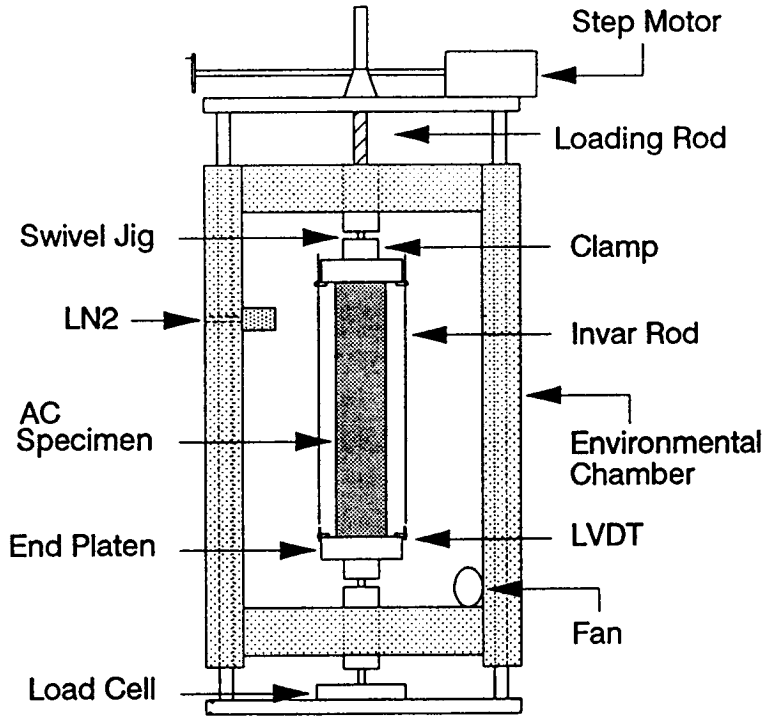

Figure 1.2. Schematic of TSRST system

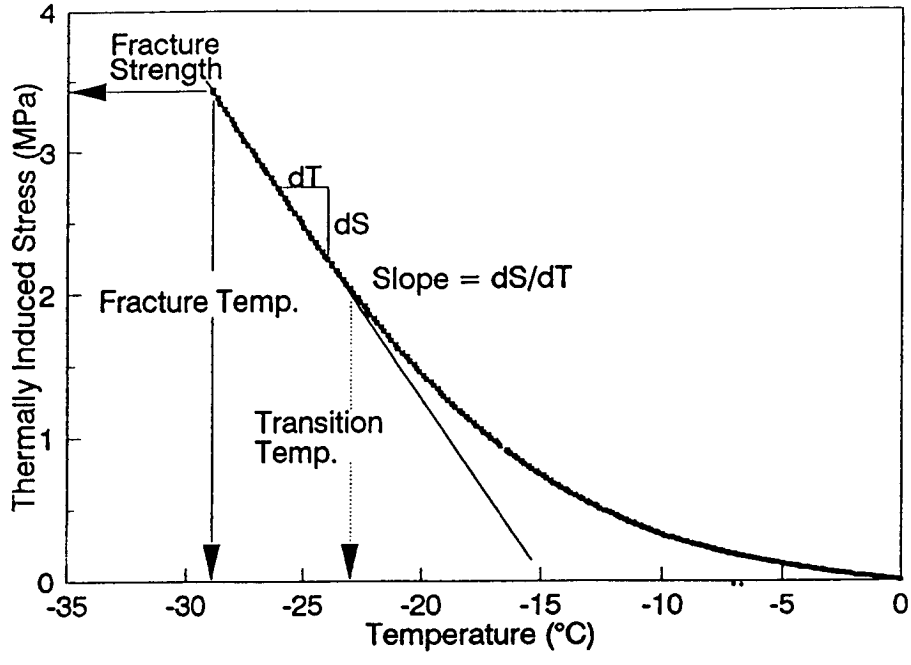

Figure 1.3. Typical TSRST results for monotonic cooling

Several test roads were selected for the field validation of the laboratory results. In addition, a validation program was conducted at the Frost Effects Research Facility (FERF) of the U.S. Army Cold Regions Research and Engineering Laboratory (USACRREL). The environmental conditions at the FERF could be precisely controlled and an extensive instrumentation system located there could be used for temperature and crack detection.

This research is part of Strategic Highway Research Program (SHRP) Contract A-003A, Subtask C.3. A major goal of SHRP is to relate asphalt binder properties to field performance of asphalt concrete mixes. One of the primary products will be the development of performance-based specifications for asphalt-aggregate mixes.

2

Experiment Designs

The experiment consisted of field observations for the test roads and performance of TSRSTs on specimens fabricated from original materials and cut from pavement in the field. Information for each test road and the laboratory testing program is given in the following sections.

2.1 Field Experiments

Five test roads were selected for the validation effort. Two of the roads are in Fairbanks, Alaska; one is in Elk County, Pennsylvania; and two are in Peraseinajoki and Sodankyla, Finland. In addition, several test sections were constructed in the FERF of the USACRREL in Hanover, New Hampshire.

Information for the test roads contained in the following sections was obtained from the local road authorities, excluding the Pennsylvania test road and the USACRREL test sections. The information for the Pennsylvania test road is based on a report by P. S. Kandhal et al. (1984), and the information for the USACRREL test sections was obtained from a report by H. K. Kanerva et al. (1992).

2.1.1 Alaska

Alaska Department of Transportation (DOT) pavement sections in Fairbanks were selected for the test program after they experienced severe low-temperature cracking in the first winter. The first section is on 23rd Avenue [305 m (1,000 ft) east of Peger Road intersection] under the project name 23rd Avenue Extension. The road carries primarily light traffic (average daily traffic = 3,175) and consists of one lane in each direction and a center turn lane. The total width of the asphalt concrete pavement is 15.8 m (52 ft). The second section is on Peger Road [30 m (100 ft) north of Chena River Bridge] under the project name Geist Extension — College to Peger. This road consists of two lanes, and the

total width of the paved surface is 9.7 m (32 ft). Both sections were paved in September 1988.

The pavement structure for the roads (from bottom to top) consists of 910 mm (3 ft) clean gravel (P_{200} < 6 percent) insulation layer, 152 mm (6 in.) crushed-gravel subbase, 152 mm (6 in.) crushed-gravel base course, and a 51 mm (2 in.) asphalt concrete wearing course on 23rd Avenue, and a 76 mm (3 in.) asphalt concrete wearing course on Peger Road.

Materials used in these asphalt concrete pavements were crushed gravel from the Sealand pit and AC-5 asphalt from the Mapco, North Pole Refinery. The asphalt cement properties are given in Table 2.1. Target gradations and asphalt contents were nearly identical; the only difference was that the Peger Road mix design used the 75-blow Marshall procedure, whereas the mix design for 23rd Avenue used the 50-blow procedure. Mix designs are given in Appendix A. The actual aggregate gradations and asphalt contents did not meet the specifications, however, and tender mix characteristics and, subsequently, premature raveling were observed. The actual mix proportions are given in Appendix A. For both projects, the target mixing temperature varied between 134°C and 140°C (274°F and 284°F), and target compaction temperature varied between 124°C and 128°C (255°F and 262°F).

During construction of both projects, the air temperature was approximately 4.4°C (40°F). On Peger Road, roller checking was a problem, and hairline cracking could be observed transverse to the rolling direction. This was at least partially due to the out-of-specification tender mix.

2.1.2 Pennsylvania

The six test sections in Pennsylvania were constructed in Elk County during September 1976 using AC-20 asphalt cements from different sources. The research was undertaken with the cooperation of the Federal Highway Administration, U.S. Department of Transportation, as a long-term durability project (Kandhal 1984).

The test sections are on Traffic Route 219 North of Wilcox, between stations 100+00 and 219+43. The average daily traffic (ADT) on the two-lane, 6.1 m (20 ft) wide highway is 3,700. The sections researched consisted of a 38 mm (1.5 in.) resurfacing of the existing structurally sound pavement. The pavement cross-section is as follows, from bottom to top:

1. 254 mm (10 in.) crushed aggregate base and 76 mm (3 in.) penetration macadam (1948)

2. 76 mm (3 in.) binder and 25 mm (1 in.) coarse sand mix (1962)

3. surface treatment (1974)

4. 38 mm (1.5 in.) bituminous concrete wearing course (1976)

The subgrade consists of a silty soil (American Association of State Highway and Transportation Officials [AASHTO] Classification A-4).

A plan view of the test sections is given in Figure 2.1. Each test pavement was approximately 610 m (2,000 ft) long. Mix composition and compaction levels were held reasonably constant for all test sections. The only variable was the asphalt type or source. The mix was composed of a gravel coarse aggregate and natural sand; its composition and Marshall design data are given in Appendix A.

The mixing temperatures for each test section were adjusted to obtain a mixing viscosity of 170 ± 20 mm^2/s (170 ± 20 cSt). The mix temperatures generally ranged from 146°C to 154°C (295°F to 310°F) . The compaction was completed before the mix cooled down to 79°C (175°F).

Cores taken from each test section were analyzed for mix composition and density. The mix composition conformed to the job mix formula. The average bulk specific gravity was 2.223, and air void content was 4.4 percent.

The six asphalts were supplied by five refineries. The properties of the asphalts are given in Table 2.2.

2.1.3 Peraseinajoki, Finland

The test roads in Finland are part of the Asphalt Pavement Research Program (ASTO) funded by the Government of Finland (Saarela 1991).

The test road between Peraseinajoki and Alavus is part of Highway 672. Paving of the 50 mm (1.97 in.) thick asphalt concrete surface took place in June 1990. The average daily traffic on the two-lane, 7 mm (23 ft) wide road is 1,500.

A 200 mm (7.9 in.) thick crushed-rock base course was added to the existing pavement structure before paving with the wearing course. The existing structure consists of a 350 mm (13.8 in.) thick crushed-rock base course and filter sand layer of 350 mm (13.8 in.) in embankment and 100 mm (3.9 in.) in cut sections. The old wearing course was removed before reconstruction.

The plan view of the six test sections is given in Figure 2.2. Different asphalt cements were used in each section, and the asphalt content varied from 5.6 to 5.8 percent. The asphalt cements were refined by Neste Oil, except B120LD, which was refined by Nynas (Sweden). The asphalt cement properties are given in Table 2.3. The crushed-rock aggregate and mixture gradation were the same for all sections. The mix compositions are given in Appendix A.

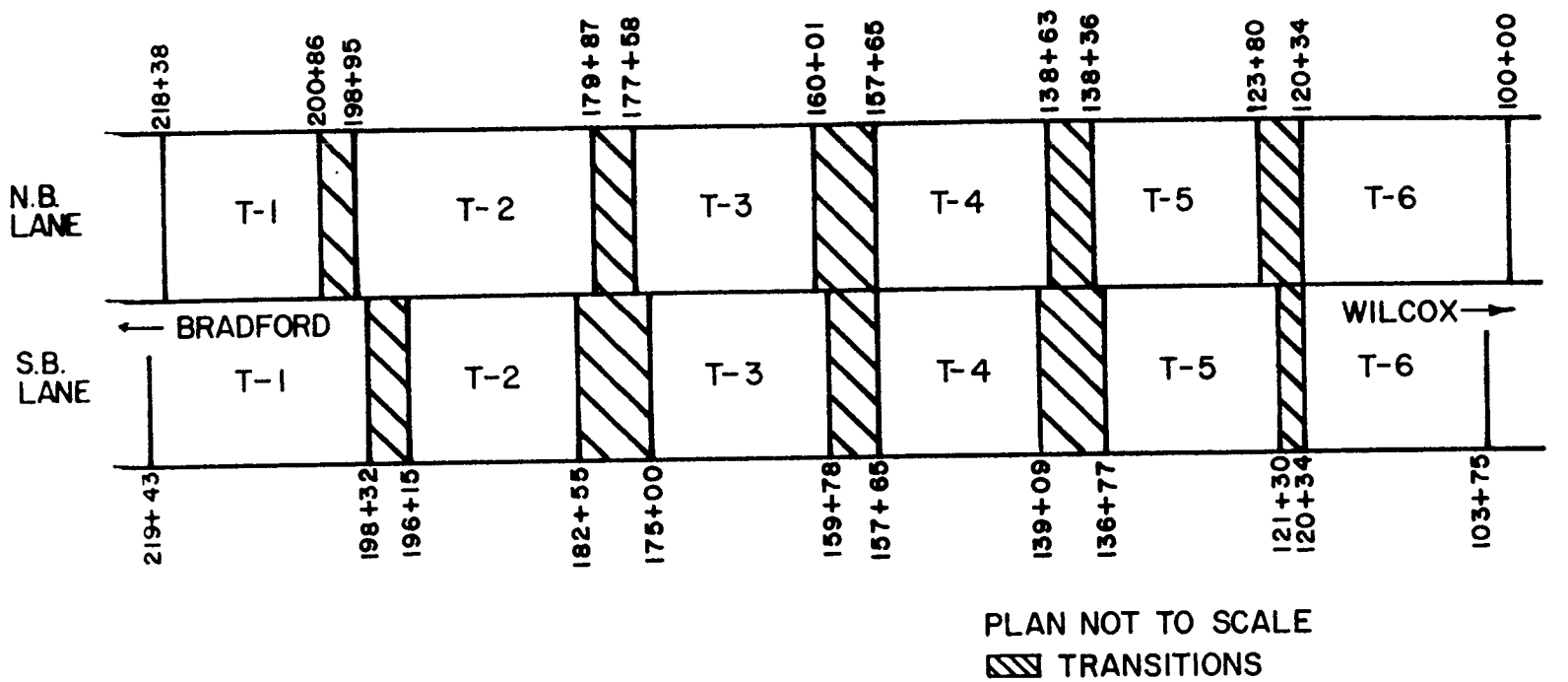

Figure 2.1. Pennsylvania test sections (stations are given in feet)

Table 2.1. Asphalt properties for Alaska test sections (Esch, 1990)

Property	AC-5	AC-2
Original Asphalt		
Pen @ 77°F	162	249
Vis @ 148°F (Poise)	468	275
Vis @ 275°F (cSt)	258	154
PVN	-0.33	-.069
TFOT Aged Residue		
Vis @ 140°F (Poise)	696	412

Table 2.2. Asphalt properties for Pennsylvania test sections (Kandhal 1984)

Property	T-1	T-2	T-3	T-4	T-5	T-6
Original Asphalt (0.1 mm)						
Pen @ 77°F	42	64	72	65	54	80
Pen @ 39.2°F (100g, 5 sec)	2.0	7.4	6.2	6.7	3.4	7.5
Vis @ 140°F (Poise)	2710	2284	1764	1705	1759	1982
Vis @ 275°F (cSt)	420	402	393	355	356	406
PI (Pen 39.2 & Pen 77)	-2.77	-0.71	-1.51	-1.04	-2.23	-0.14
PVN	-1.04	-0.70	-0.61	-0.86	-1.03	0.45
TFOT Aged Residue (0.1 mm)						
Pen @ 77°F	26	38	45	38	37	44
Vis @ 140°F (Poise)	563	569	556	5.27	464	575
Viscosity Ratio	1.34	1.42	1.41	1.48	1.30	1.42

Note: °C = 5/9 (°F - 32)

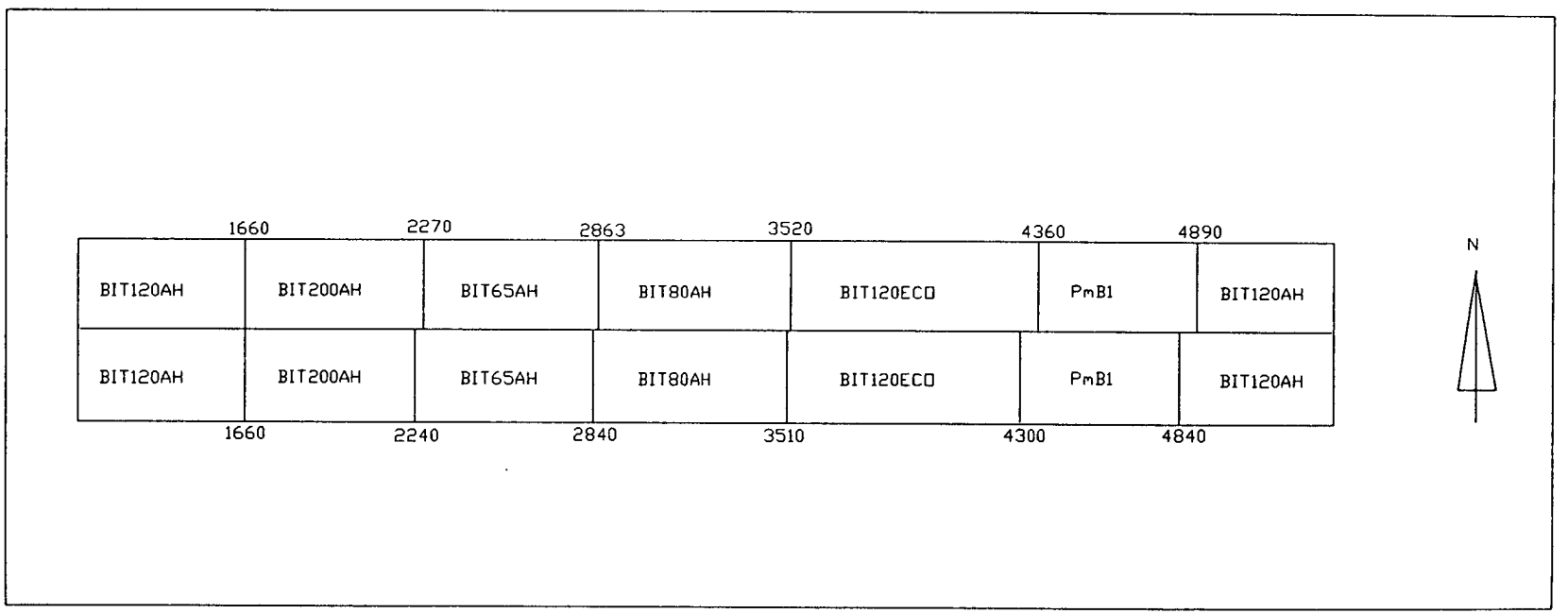

Figure 2.2. Peraseinajoki test sections (stations are given in meters)

Table 2.3. Asphalt properties for Peraseinajoki and Sodankyla test sections (tested by Neste Oil, Bitumen, in Finland)

Property	BIT 120AH	B 120LD	BIT 120ECO	BIT 120ARC	BIT 65AH	BIT 80AH	BIT 200AH	PmB1	BIT 150AH
Original Asphalt									
Pen @ 77°F (0.1 mm)	104	120	120	129	61	84	153	130	138
Pen @ 41°F (100g, 5	12	14	12	20	9	10	15	18	19
sec)	1170	1140	742	727	2990	2030	652		662
Vis @ 140°F (Poise)	363	295	226	225	573	487	278		222
Vis @ 275°F (cSt)	-25	-24	-23	-30	-20	-22	-26	-23	-30
Fraass Brittle Point (°C)	-1.03	-1.00	-1.43	-0.08	-0.25	-0.94	-1.48	-0.47	-0.48
PI (Pen 41 & Pen 77)	-0.32	-0.48	-0.91	-0.83	-0.91	-0.13	-0.28		-0.78
PVN									
TFOT Aged Residue									
Pen @ 41°F (100g, 5	9	9	9	14	7	8	13	13	14
sec)	2520	2300	2260	2650	7230	4930	1420		1860
Vis @ 140°F (Poise)	-23	-22	-22	-30	-21	-22	-26	-23	-26
Fraass Brittle Point (°C)	2.2	2.0	3.0	3.6	2.4	2.4	2.2		2.8
Viscosity Ratio									

Note: °C = 5/9 (°F - 32)

2.1.4 Sodankyla, Finland

The test road is located 10 km (6.2 mi.) South of Sodankyla on Highway 4. The construction of the asphalt concrete wearing course took place in July 1990. The average daily annual traffic on this two-lane, 8.5 m (27.9 ft) wide highway is 2,000.

Before paving, a crushed-rock base course of 7.9 in. (200 mm) and a filter layer of varying thickness was added to the existing pavement structure. The existing oil-gravel wearing course was crushed and left in the base course.

The test sections do not extend across the entire width of the road; they are limited to one lane only, as illustrated in the layout of the sections in Figure 2.3. The aggregate and mix gradation was the same in all sections. Nine different asphalt cements were used, and the asphalt content varied from 5.4 to 5.7 percent by weight of the mix. The mix compositions are given in Appendix A. Some of the asphalt cements were same products as in the Peraseinajoki test sections. The properties of asphalt cements are given in Table 2.3.

2.1.5 USACRREL

A test program was performed in the FERF, under SHRP Contract A-003A, Subtask C.3. The facility consists of test basins, where environmental conditions, such as temperature and moisture content, can be controlled. A plan view of the FERF is shown in Figure 2.4. Basins TC-1...TC-4, TB-11, and TB-12 were used in the program. A comprehensive report of the USACRREL experiment is given in a companion report by Kanerva et al. (1992).

The test program consisted of two phases. In the Phase I program, three length/width ratios and two slab thicknesses were used with one asphalt concrete mixture. In the Phase II program, four different asphalt cements were used with a fixed geometry of the test section. The same mix design and aggregate were used in both phases.

The desired geometry and thickness of the pavement slabs to evaluate low-temperature cracking in newly placed asphalt concrete were not known when the layout of the test sections was developed. Therefore, a set of slabs with different dimensions was identified for the Phase I program. A 2.7 m (9 ft) wide, 61.0 m (200 ft) long, 51 mm (2 in.) thick section was constructed to represent field conditions as closely as possible. Two 1.2 m (4 ft) wide, 21.3 m (70 ft) long, 51 mm (2 in.) thick sections and two 1.2 m (4 ft) wide, 39.3 m (129 ft) long, 76 mm (3 in.) thick sections were constructed to analyze the effect of the ratio of the width and length of the pavement slab and the thickness of the pavement on cracking. The layout of the Phase I program is presented in Figure 2.5.

The Phase II program focused on the low-temperature performance of different asphalt cements. In this phase, four 61 m (200 ft) long, 1.2 m (4 ft) wide, 51 mm (2 in.) thick sections were constructed. Each section contained a different asphalt cement, as illustrated in Figure 2.5.

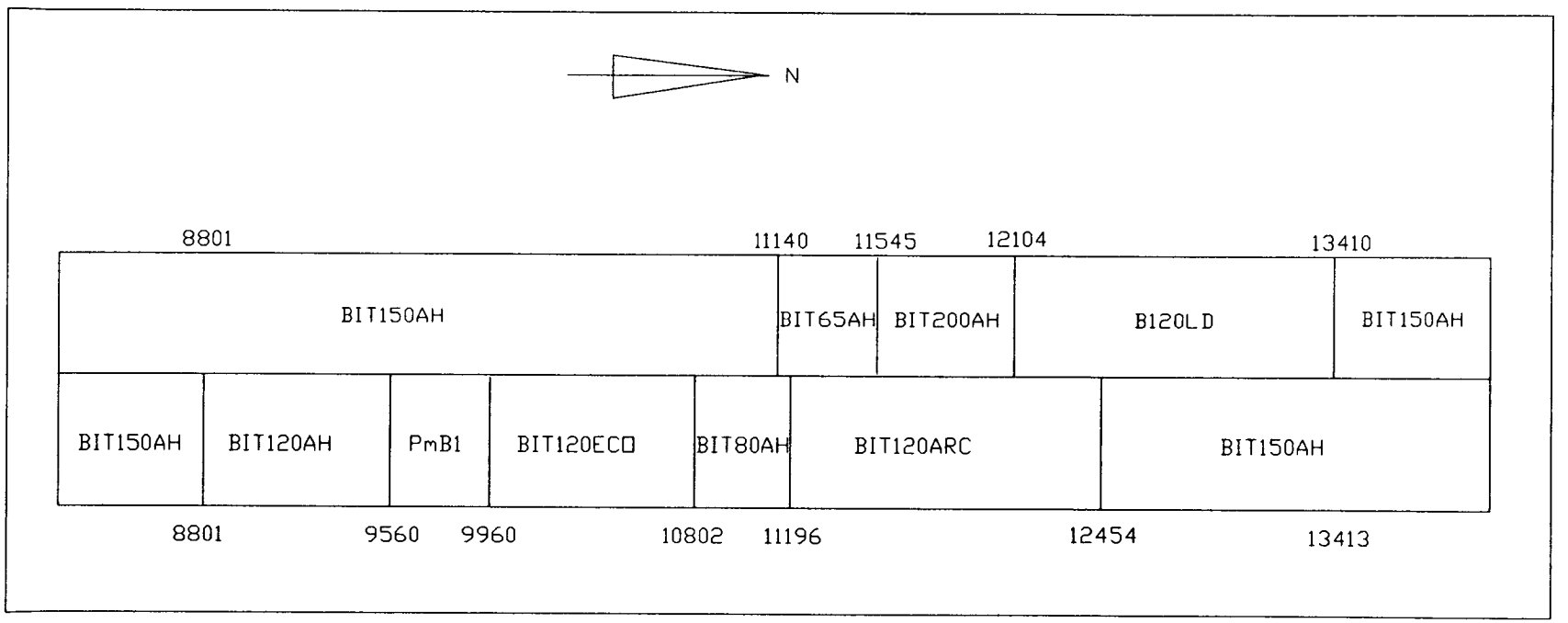

Figure 2.3. Sodankyla test sections (stations are given in meters)

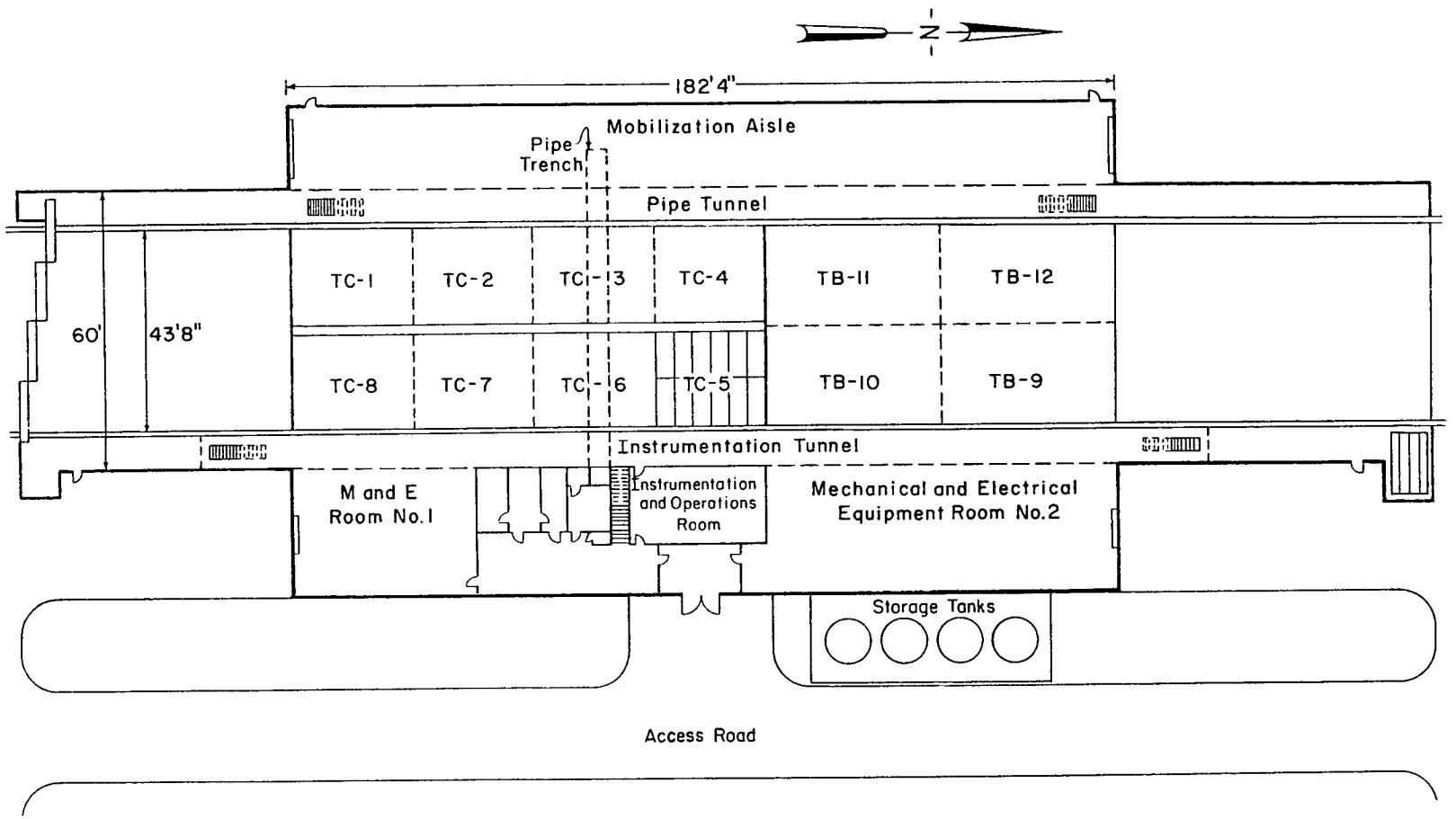

Figure 2.4. Frost Effects Research Facility at USACRREL (Eaton 1992)

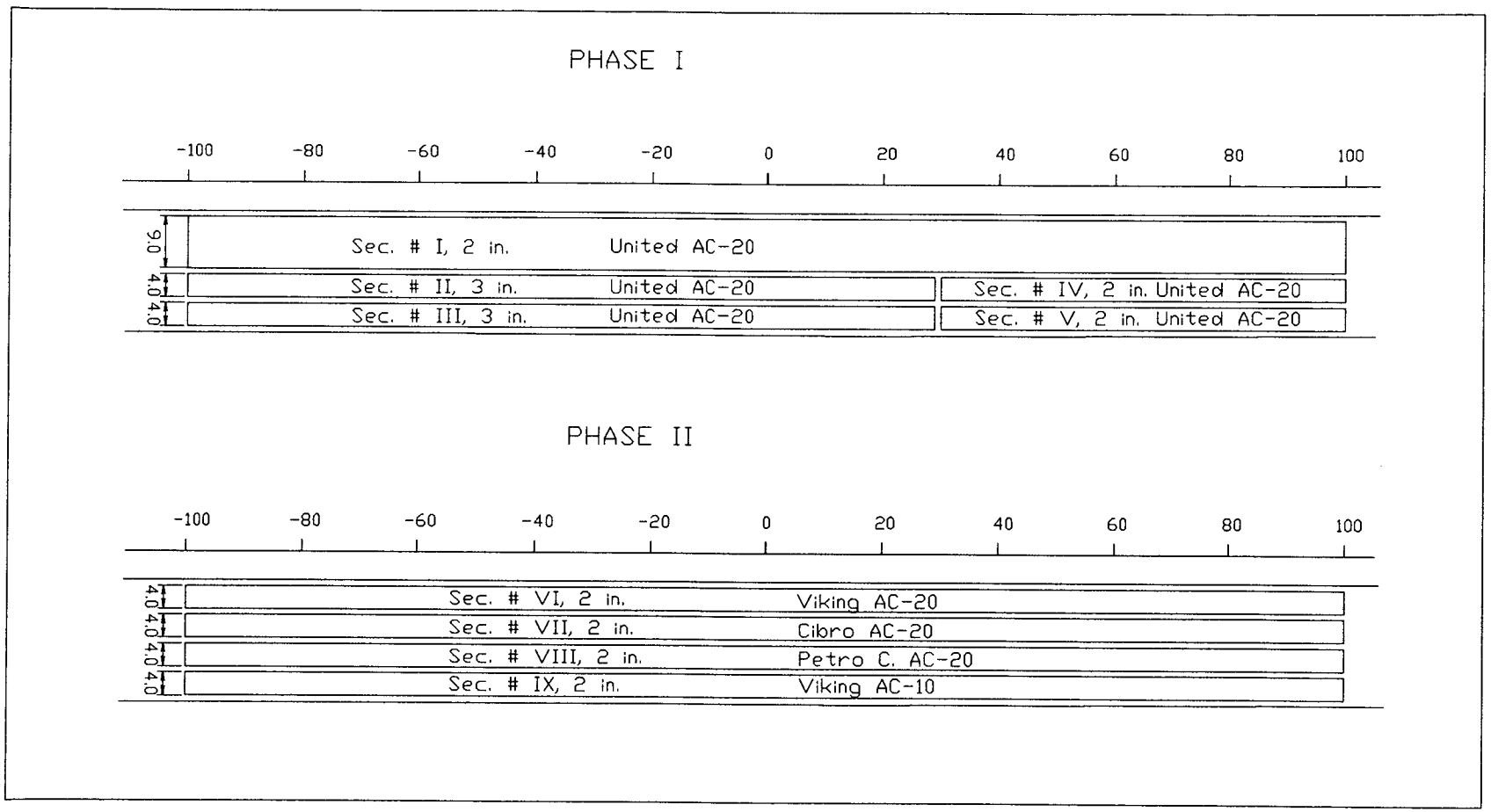

Figure 2.5. Layout of test sections at USACRREL (stations are given in feet)

The subgrade for the pavement structure consisted mainly of silt and partly of four concrete slabs, all at different elevations, as shown in Figure 2.6. A concrete transition block was placed at the interface of the concrete slabs and silt subgrade. A crushed-gravel subbase was placed over the base such that the uppermost concrete slab had 76 mm (3 in.) of aggregate cover. The subbase was placed and compacted at the northern end on plywood boards and a geotextile (to protect the existing subgrade) in two 227 mm (9 in.) thick layers. At the southern end, the subbase was placed directly on the concrete slabs in one layer. One layer of 51 mm (2 in.) thick, high-bearing-capacity board insulation (DOW STYROFOAM Brand Plaza Deck Insulation) was installed between the subbase and the 305 mm (12 in.) crushed-gravel base course. Vertical insulation was placed at the ends of the horizontal insulation from the top of the insulation to the surface of the base course (see Figure 2.6). The wet density of the base course was measured with a nuclear density gauge. The mean density was 2273 kg/m^3 (142.0 lb/ft^3), and standard deviation was 37 kg/m^3 (2.3 lb/ft^3). The mean moisture content was 3.4 percent (standard deviation 0.4 percent).

The Phase I paving took place on June 12, 1991. One lift of 19 mm (3/4 in.) minus asphalt concrete mix was placed. The Marshall mix design and the actual mix composition are given in Appendix A. The aggregate used was crushed stone from Tilcon's pit, West Lebanon, New Hampshire. The natural sand came from Hartland Pit, Hartland, Vermont. The asphalt cement used was an AC-20 produced by the United Refining Company, Warren, Pennsylvania. Its properties are given in Table 2.4.

The sections were constructed according to the layout presented in Figure 2.5. The mixture temperature measured on the grade varied from 152°C to 154°C (305°F to 310°F). Compaction commenced when the temperature reached 107.2°C (225°F) and was completed at 46°C (115°F). The mean density determined in the laboratory for core samples was 2,446 kg/m^3 (152.5 lb/ft^3), Rice specific gravity of 2.600, and mean air void content of 6.0 percent.

The Phase II sections (VI to IX) were paved on September 14, 1991. The aggregate used was from the same batch as the aggregate used for Phase I. The following asphalt cements were used, as given in Table 2.3 and Figure 2.5: AC-20 and AC-10 from Viking Asphalt of Newington, New Hampshire; AC-20 from Petro Canada of Montreal, Canada; and AC-20 from Cibro of Albany, New York. The physical properties of the asphalt cements are given in Table 2.4 and Figure 2.5. Based on the extraction/gradation results, the mixes were not identical in Phases I and II. The actual mix compositions for each phase are given in Appendix A. The mean specific gravities and void contents for the core samples are given in Table 2.4, and the mixing and compaction temperatures are given in Table 2.5.

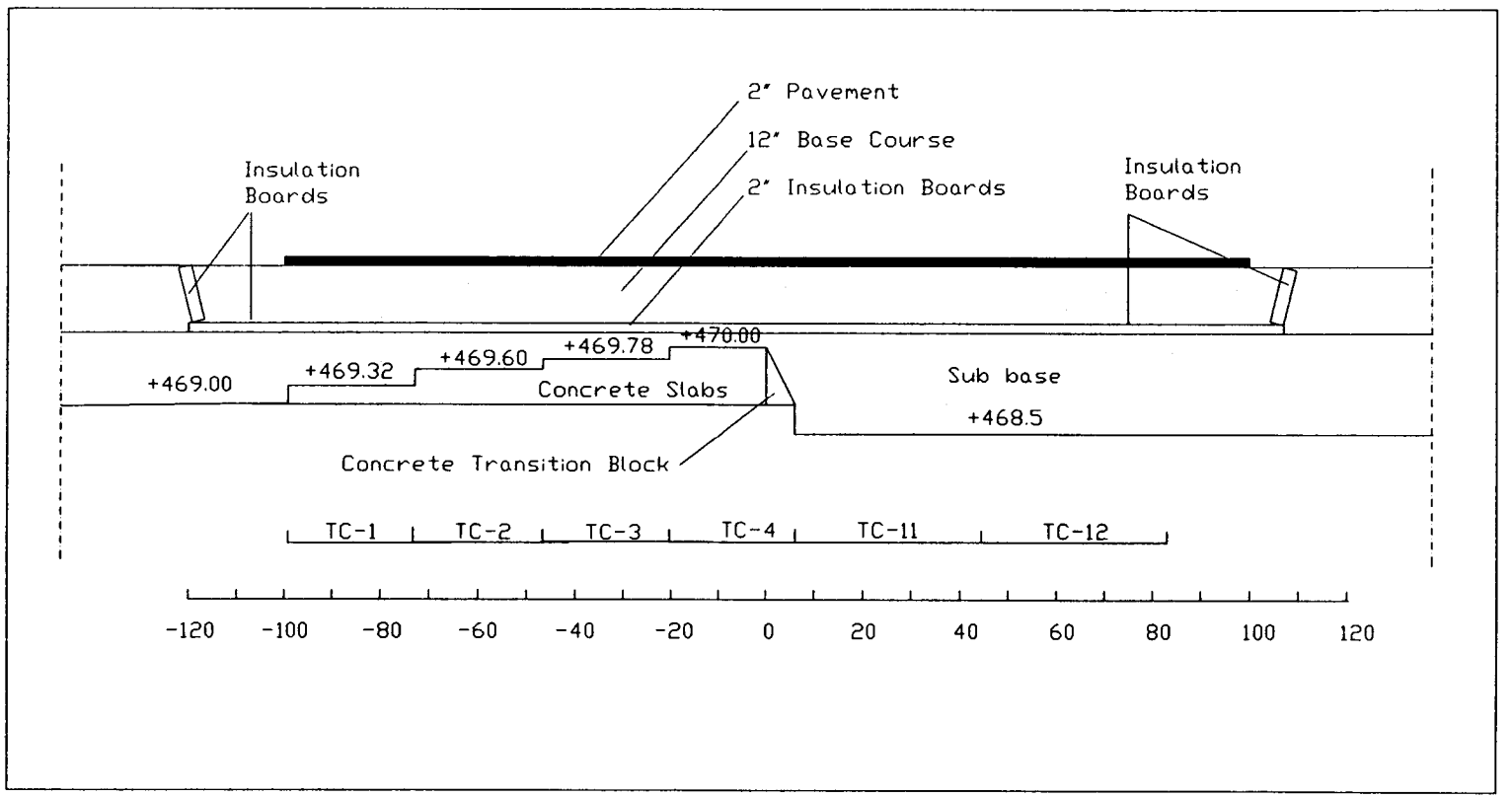

Figure 2.6. Cross-section of the test sections at USACRREL

Table 2.4. Asphalt properties for USACRREL test sections (tested for SHRP by Southwestern Laboratories, Houston, Texas)

Property	AC-20 United	AC-20 Viking	AC-20 Cibro	AC-20 Petro C.	AC-10 Viking
Original Asphalt					
Pen @ 77°F (0.1 mm)	68	76	96	69	122
Pen @ 39.2°F (100g, 5 sec)	6	7	11	8	12
Vis @ 140°F (Poise)	1939	2087	1784	2145	1067
Vis @ 275°F (cSt)	397	366	394	423	293
PI (Pen 39.2 & Pen 77)	-1.4	-1.38	-0.74	-0.66	-1.17
PVN	-0.66	-0.66	0.29	0.57	-0.47
TFOT Aged Residue (0.1 mm)					
Pen @ 77°F (0.1 mm)	---	50	61	42	77
Pen @ 39.2°F (100g, 5 sec)	---	5	9	7	10
Vis @ 140°F (Poise)	---	4267	3515	5044	2076
Vis @ 275°F (cSt)	---	501	530	603	401
PI (Pen 39.2 & Pen 77)	---	-1.13	0.07	0.52	-0.36
PVN	---	-0.64	-0.36	-0.56	-0.51
Viscosity Ratio	---	2.04	1.97	2.35	1.95

Note: °C = 5/9 (°F - 32)

Table 2.5. Mixture properties from Cores for USACRREL test sections

Section	Asphalt	Rice Specific Gravity	Specific Gravity GmbSSD	Void Content SSD (%)	Asphalt Content (% total Weight)
I...V	United AC-20	2.60	2.44	6.0	5.2
VI	Viking AC-20	2.59	2.44	5.6	5.2
VII	Cibro AC-20	2.61	2.44	6.7	5.5
VIII	Petro C. AC-20	2.59	2.41	6.6	5.4
IX	Viking AC-10	2.67	2.43	9.0	5.2

Table 2.6. Field mixing and compaction temperatures for USACRREL test sections

		Mixing Temperature		Compaction Temperature	
Section	Asphalt	(°C)	(°F)	(°C)	(°F)
I...V	United AC-20	152	305	107-46	225-115
VI	Viking AC-20	154	310	110-49	230-120
VII	Cibro AC-20	154	310	110-43	230-110
VIII	Petro AC-20	152	305	127-49	260-120
IX	Viking AC-10	149	300	121-60	250-140

2.2 Laboratory Experiments

2.2.1 Tests

The laboratory test program consisted of a series of experiments using the TSRST system on laboratory-prepared specimens and specimens obtained from pavement sections.

A schematic picture of the test system is given in Figure 2.7. The system consists of a load frame, screw jack, computer data, acquisition and control system, low-temperature cabinet, temperature controller, and specimen alignment stand. A cylindrical specimen is mounted in the load frame, which is enclosed by the cooling cabinet. The chamber and specimen are cooled with vaporized liquid nitrogen. As the specimen contracts, linear variable differential transformers (LVDTs) sense the movement and a signal is sent to the computer, which, in turn, causes the screw jack to stretch the specimen back to its original length. This closed-loop process continues as the specimen is cooled and ultimately fails. Throughout the test, measurements of elapsed time, temperature, deformation, and tensile load are recorded with the data acquisition system (Jung 1992).

Different cooling rates were used in testing. A cooling rate of 10°C/h (18°F/h) represents the proposed standard procedure for the TSRST, whereas 1°, 2°, or 5°C/h represent the actual cooling rates for the test roads.

2.2.2 Materials

2.2.2.1 Alaska

The original asphalt cement (Mapco AC-5 from North Pole Refinery) from the same year that the paving took place was used to fabricate the laboratory samples. Also, Mapco AC-2.5 was used as a reference asphalt, since it is normally used in the Fairbanks area. The aggregate was sampled from the same pit (Sealand pit) from which the aggregate used in the test roads pavements was sampled.

In addition, six slabs were sawed from the test sections as illustrated in Figures 2.8 and 2.9. Slabs 1A, 1B, 2A, and 2B were sawed from the left-turn lane of 23rd Avenue. The three lanes were placed in two strips (see Figure 2.8). Slabs 1A and 1B were from the severely cracked southbound strip of the left-turn lane. The thickness of the slabs was 57 mm (2.25 in.). Slabs 2A and 2B were from the uncracked part of the left-turn lane, where the thickness appeared to be 44 mm (1.75 in.). Slabs 3A and 3B were from Peger Road. The thickness of these slabs was 102 mm (4 in.). The slabs were cut after the first winter and stored at ambient laboratory temperature for 10 months before testing.

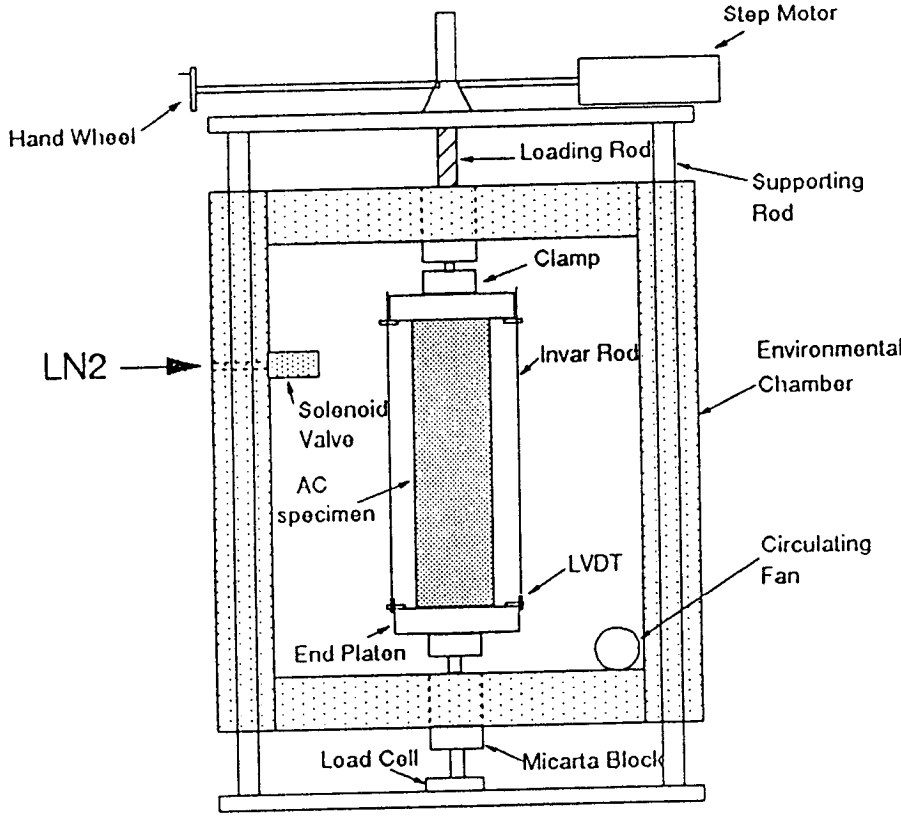

Figure 2.7. Thermal stress restrained specimen test system (Jung 1992)

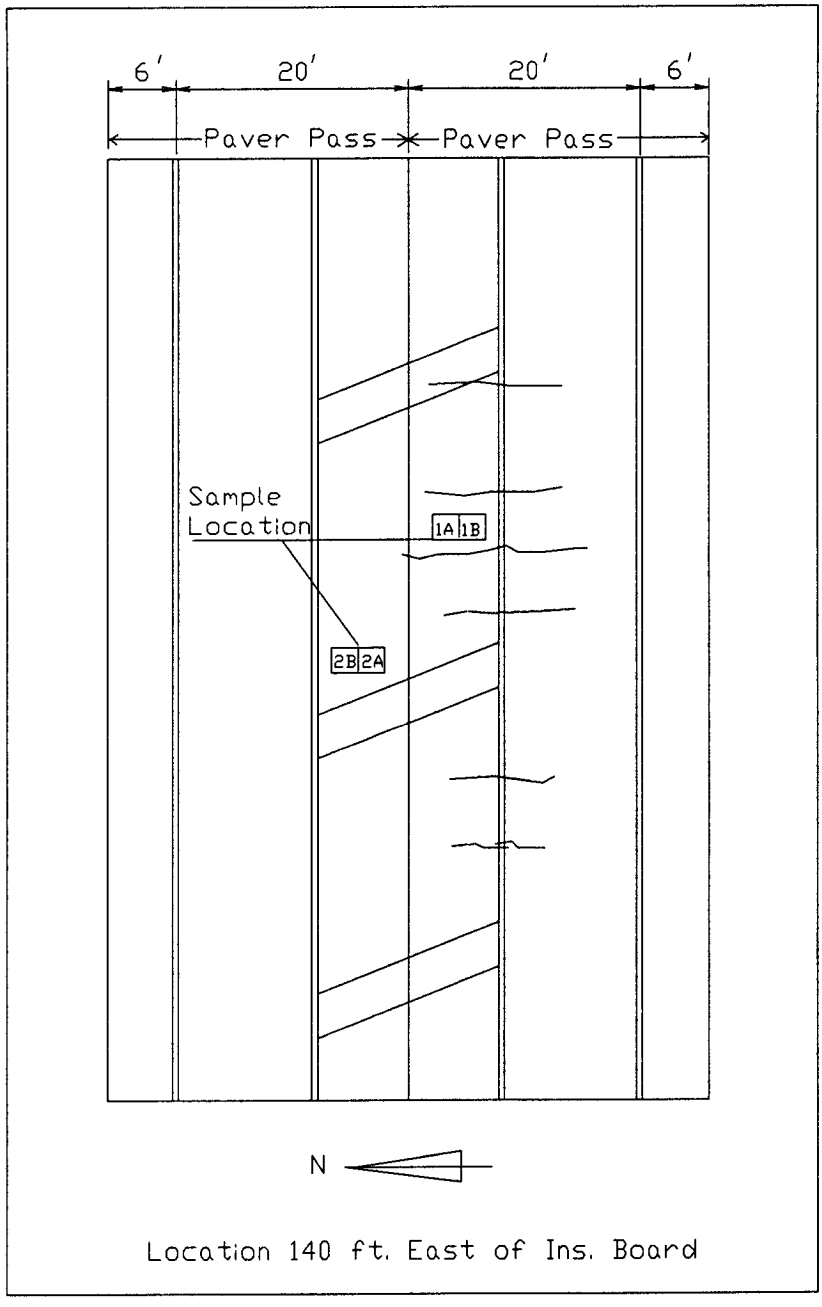

Figure 2.8. Crack map of sampling site for 23rd Avenue, Fairbanks, Alaska (Esch 1990)

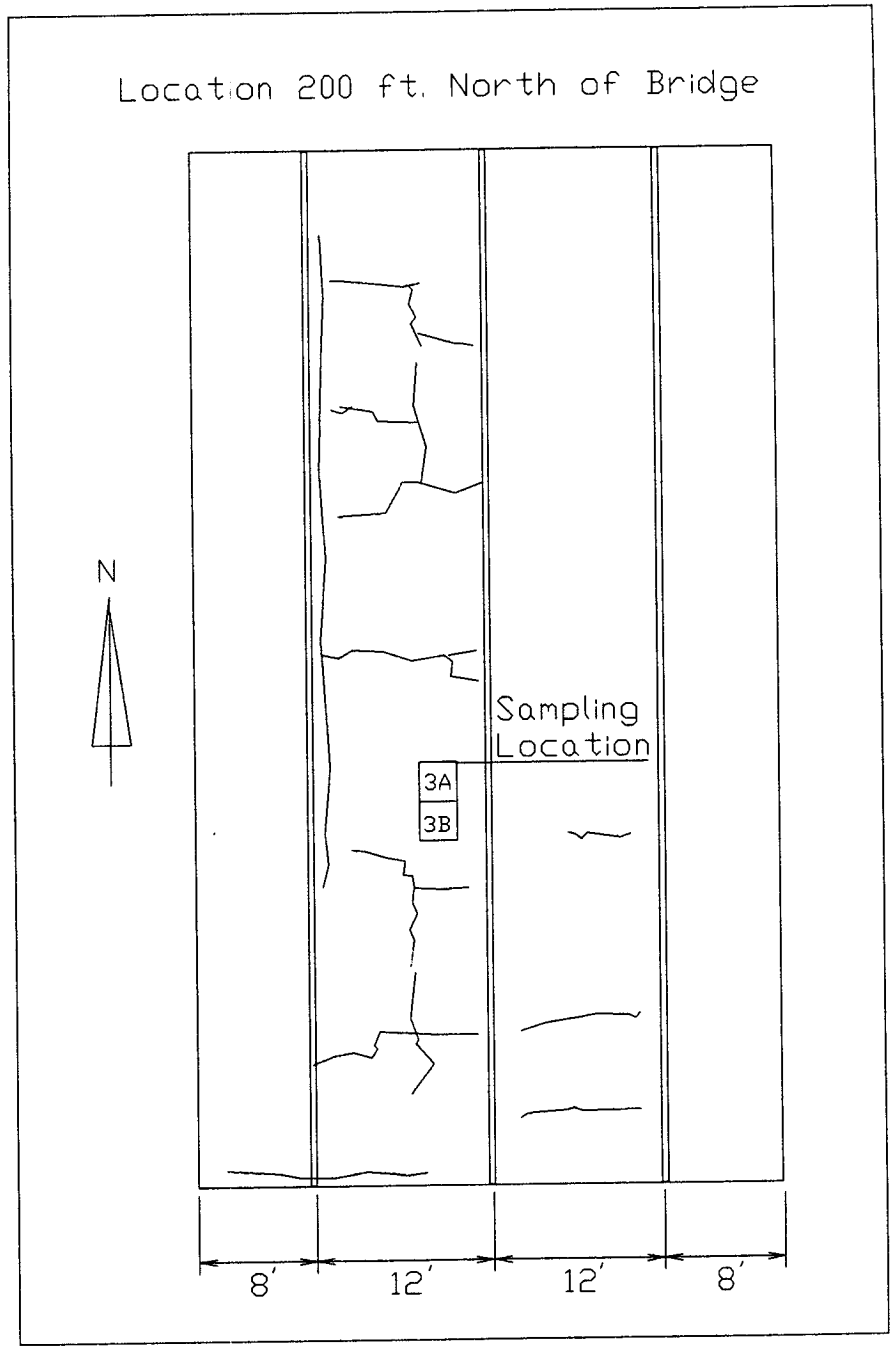

Figure 2.9. Crack map of sampling site for Peger Road, Fairbanks, Alaska (Esch 1990)

2.2.2.2 Pennsylvania

Original asphalt cements (given in Table 2.2) sampled during the construction of the test sections were used to fabricate the laboratory specimens. The aggregate was sampled from a deposit similar to the one from which the original aggregate was sampled in the summer of 1991. The material in the pits (located 11 miles from each other) is glacial gravel and has exhibits considerable variability. No field slabs were available.

2.2.2.3 Peraseinajoki, Finland

Asphalt cements used in the test sections in Peraseinajoki were refined by Neste Oil, Finland. They were the same asphalt products as those used in the Sodankyla test road. The asphalts described in Table 2.3 were sampled in Sodankyla while the paving of the test road took place. Aggregate was sampled from the same piles as the original aggregate was taken and stored in drums a few weeks after the construction in Peraseinajoki. The aggregate was divided into three fractions (0-6 mm, 6-12 mm, 12-20 mm) and natural sand. In addition, the limestone filler was sampled. (The filler was used to replace part of the fines in the mixture.)

2.2.2.4 Sodankyla, Finland

The asphalt cements used in Sodankyla were refined by Neste Oil except the B120LD, which was refined by Nynas (Sweden). The asphalts listed given in Table 2.3 were sampled from the truck during unloading. The aggregate used in the mixing plant consisted of one fraction sampled from the pile during construction. In addition, samples of the limestone filler were obtained.

Field samples were compacted at the mixing plant during construction. Mixture for the slabs were collected from the truck by digging under the surface layer in several locations. A 51 mm (2 in.) thick, 380 × 1200 mm (15 × 47 in.) slab was compacted in a plywood mold using a static laboratory rolling-wheel compactor. Compaction commenced when the viscosity of the asphalt was 280 mm^2/s (280 cSt).

2.2.2.5 USACRREL

The material was sampled from the cold feed conveyor during mixing. Samples of each of the following asphalt cements were obtained from the tanks: AC-20, United Refining Company, Warren, Pennsylvania; AC-20 and AC-10, Viking Asphalt, Newington, New Hampshire; AC-20, Petro Canada, Montreal, Canada; and AC-20, Cibro, Albany, New York.

In addition, 156 2-in. cores and 24 343 × 457 mm (13.5 × 18 in.) asphalt concrete slabs were sawed from test sections VI to IX, as illustrated in Figure 2.10. Slabs taken from

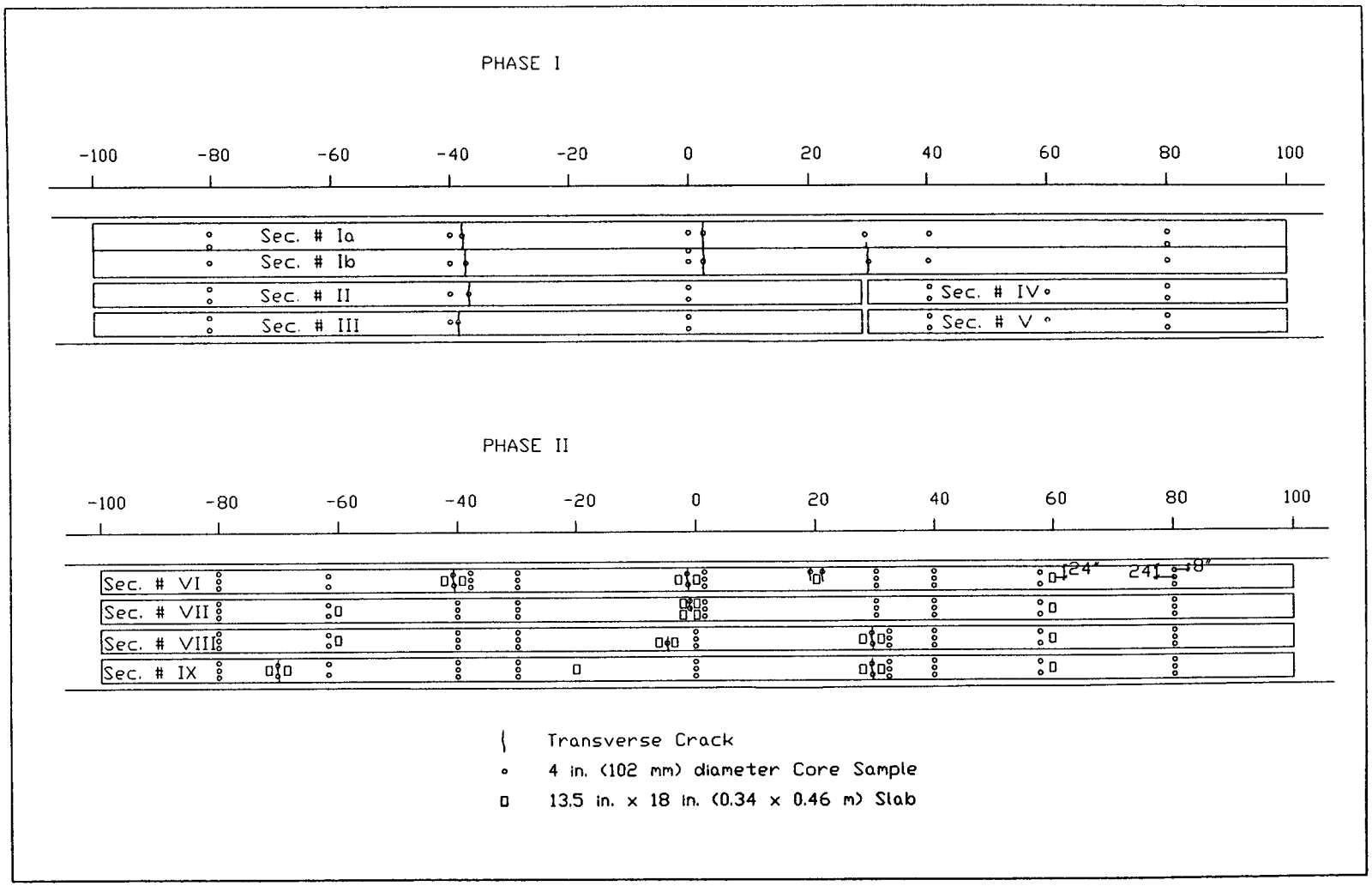

Figure 2.10. Layout of samples for the USACRREL test sections

sections I to V were damaged during transportation to the Oregon State University (OSU) laboratory.

2.2.3 Sample Preparation

Using the original asphalt cements and aggregates, 140 × 140 × 406 mm (5.5 × 5.5 × 16 in.) beams were compacted with a California kneading compactor. The mix compositions used were as close to the actual mix compositions in the field as possible. Detailed information sheets containing the mix design, the compaction procedure, and mixing and compaction temperatures for each beam are given in Appendix B. One-half of the loose mix samples were aged at 135°C (275°F) for 4 hours before compaction. This aging procedure is termed short-term oven-aging (STOA). After the beams were compacted and cooled, four 57.1 mm (2.25 in.) diameter cylinders were cored, or 51 × 51 mm (2 × 2 in.) beams were sawed from the compacted beams. Both cylinders and beams were used in the test program because the TSRST protocol was changed during the field validation program. The specific gravity and air void content were determined for each cylinder. The values are given in Appendix B.

Field samples (asphalt concrete slabs) were collected from the test roads, except for Pennsylvania, where the test sections were already overlaid. Beam specimens were sawed from the Alaskan and Finnish slabs. The dimensions of the beams were 51 × 51 mm (2 × 2 in). (For samples AK1F3 and AK1F4 the dimensions were 38 × 38 mm [1.5 × 1.5 in.].) Cylindrical specimens were prepared from the USACRREL slabs. A 38.1 mm (1.5 in.) diameter drill was used. The specific gravities and void contents were determined for the cylinders. The values are given in Appendix C.

The length of all the laboratory and field cylinders and beams were 254 mm (10 in.). The information about shape, origin, and aging procedure for each specimen is given together with the test results in Appendix D.

3

Test Results

The field validation program results consist of temperature data and cracking observations on the test roads and TSRST results for the laboratory and field samples. The results for each test road are given in the following paragraphs.

3.1 Alaska

3.1.1 Field Results

The temperature data and the cracking observations presented herein were obtained from the Alaska Department of Transportation (Esch 1990).

3.1.1.1 Temperature Data

The critical cooling event of the first winter (1989) occurred on January 31. Air temperature dropped from -33°C to -43°C (-28°F to -46°F). Pavement surface temperatures were measured at the Coldstream Valley site, 14.5 km (9 miles) northwest of the test sections. A maximum hourly cooling rate of 0.7°C/h (1.3°F) was measured between January 21 and 31, during a period when pavement surface temperatures ranged from -35°C to -40°C (-31°F to -40°F).

3.1.1.2 Cracking Observations

The three lanes on 23rd Avenue were placed in two strips, as illustrated in Figure 2.8. The southbound strip experienced severe transverse cracking in the first winter, whereas the northbound strip did not crack at all. The cracking interval of the southbound lane was locally as small as 1.5 m (5 ft).

The Peger Road section was placed in two phases, as shown in Figure 2.9. Cracking occurred in both lanes. However, the cracking was more frequent in the westbound lane and, in addition to the transverse cracks, several longitudinal cracks were observed. The cracking interval varied from 1.8 to 2.4 m (6 to 8 ft). Crack maps in the vicinity of the sampling sites are illustrated in Figures 2.8 and 2.9.

In addition to low-temperature cracking, premature raveling of the roads was observed. Examination by Alaska DOT engineers indicated that raveling was due to the gap-graded (out-of-specification) materials and low asphalt contents.

3.1.2 Laboratory Results

The TSRST results and test variables for each specimen are given in Appendix D. The mean values for each data set are summarized in Table 3.1. The specimens made with asphalt cement AC-5 represent both 23rd Avenue and Peger Road. The specimens made with AC-2.5 represent a control section (associated with many other roads in Fairbanks that did not exhibit severe low-temperature cracking). The specimens were 51 × 51 mm (2 × 2 in.) beams, and specimens were tested in unaged condition.

3.1.3 Data Analysis

The TSRST fracture temperatures for the field specimens from southbound and northbound lanes of 23rd Avenue and Peger Road and for the laboratory-fabricated specimens are given in Figure 3.1. By visual inspection, the fracture temperatures of the laboratory-fabricated samples for the AC-5 and AC-2.5 mixtures do not differ much from each other. Based on this finding, the low-temperature cracking of the test sections is not explained by the use of AC-5 asphalt instead of AC-2.5. (AC-2.5 is commonly used in Fairbanks area, and severe low-temperature cracking of asphalt pavements is not normally observed.) However, it can be seen from Figure 3.1, that the fracture temperatures for the field samples are warmer than for the laboratory-fabricated samples, which may explain the cracking of the pavements. The warmer fracture temperatures indicate stiffer mixture, which may be due to the aging of the pavements in service and/or to excessive aging of the mixture during mixing. Furthermore, the TSRST fracture temperature for the intact northbound lane of 23rd Avenue is colder than for the severely cracked southbound lane of the 23rd Avenue and Peger Road, which may explain the differences in performance of the pavement sections. Statistical analysis was performed to investigate whether these hypotheses could be confirmed.

The fracture temperatures of the test sections were compared with each other by testing the difference between two means ($\bar{X}_1$, $\bar{X}_2$). It was assumed that the populations are normally distributed. Since the variances of the populations are unequal, an approximate procedure was used as follows (Scheaffer 1990):

Table 3.1. Summary of TSRST results for Alaska sections

Laboratory Samples

Asphalt Cement	Mean Voids (VPAR) (%)	Mean Fracture Stress/ Std. Dev. (psi)	(kPa)	Mean Fracture Temperature/ Std. Dev. (°F)	(°C)	Number of Observations
Cooling Rate 18°F/h (10°C/h)						
AC-5	2.2/1.1	511/73	3522/500	-14.4/4.2	-25.8/2.3	4
AC-2.5	3.0/0.1	538/179	3708/1231	-18.8/5.3	-28.2/2.9	4
Cooling Rate 1.8°F/h (1°C/h)						
AC-5	2.7/0.8	683/21	4708/147	-22.7/1.8	-30.4/1.0	2
AC-2.5	2.6/0.2	612/34	4220/234	-24.0/0.3	-31.1/0.1	2

Field Samples

Asphalt Cement	Mean Voids (VPAR) (%)	Mean Fracture Stress/ Std. Dev. (psi)	(kPa)	Mean Fracture Temperature/ Std. Dev. (°F)	(°C)	Number of Observations
Cooling Rate 1.8°F/h (1 C/h)						
23rd South	4.5/0.6	397/140	2738/965	-16.1/1.4	-26.7/2.6	2
23rd North	5.4/1.4	471/19	3247/133	-20.7/0.1	-29.3/0.1	2
Peger Tr.	3.0/0.4	453/38	3131/260	-17.0/2.3	-27.2/1.3	4
Peger Par.	2.5/0.2	497/33	3423/230	-17.3/2.7	-27.4/1.5	4

Tr. = samples were taken transverse to the direction of traffic
Par. = samples were taken parallel to the direction of traffic

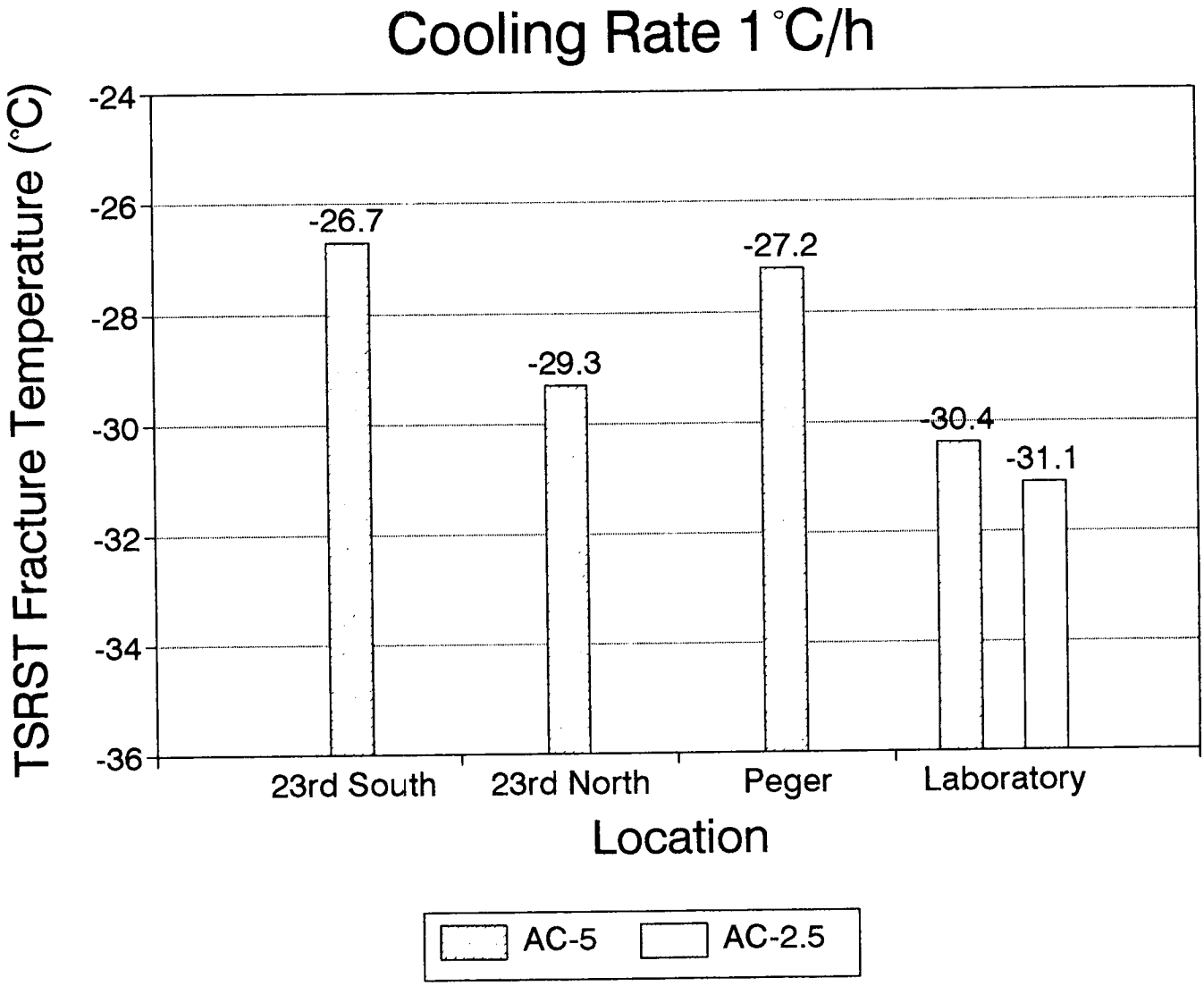

Figure 3.1. TSRST fracture temperatures for Alaska test sections

First, the t-statistic was calculated:

$$t = \frac{\bar{X}_1 - \bar{X}_2 - D_0}{\sqrt{\frac{S_1^2}{N_1} + \frac{S_2^2}{N_2}}}$$

This statistic has approximately a *t* distribution under the null hypothesis $H_0: \mu_1 - \mu_2 = D_0$, with degrees of freedom given by the integer part of

$$df = \frac{(S_1^2 + S_2^2)}{\left[\frac{S_1^2}{n_1 - 1}\right] + \left[\frac{S_2^2}{n_2 - 1}\right]}$$

where S_1^2 and S_2^2 are the sample variances.

For the hypothesis: fracture temperature (obtained using 10°C/h cooling rate) of the laboratory-fabricated specimens containing AC-5 equals fracture temperature of laboratory specimens containing AC-2.5 (FrT(AC-5) - FrT(AC-2.5) = 0), the t-statistic is 1.27 and the degrees of freedom (df) is 3. The p-value in the two-sided t-test is 0.175, and consequently the hypothesis is accepted (limit for rejection of the hypothesis for 5 percent significance is p-value < 0.025). In other words, there is no significant difference between the fracture temperatures of the mixes containing AC-5 or AC-2.5 asphalt cements. Similarly, for laboratory-fabricated specimens tested using a slow cooling rate of 1°C/h, the t-statistic is 0.99 and degrees of freedom is 1. The p-value for this hypothesis is 0.25, and in this case, too, the hypothesis is accepted. Thus, the use of the asphalt AC-5 instead of AC-2.5 does not explain the severe low-temperature cracking of the test sections.

The same analysis was performed for the hypothesis: fracture temperature of all field samples (asphalt cement AC-5) equals fracture temperature of the laboratory specimens for the AC-5 mixture. The t-statistic for the analysis is -1.39 and the degrees of freedom is 3. The p-value is consequently 0.13 and the hypothesis is accepted. Hence, there is no significant difference between the fracture temperatures of the field specimens and of the laboratory-fabricated specimens.

For the hypothesis: fracture temperature of southbound lane of 23rd Avenue equals fracture temperature of the northbound lane, the t-statistic is 2.71, the degree of freedom is 1 and the p-value is 0.13. In this case, too, the hypothesis is accepted, indicating no significant difference between the fracture temperatures.

Finally, the hypothesis that the fracture temperature for Peger Road pavement samples sawed transverse to the direction of the traffic equals the fracture temperature of samples parallel to the direction of the traffic (to investigate the effect of roller checking on the fracture temperature) was tested. The t-statistic for the analysis is 0.21 for 3 degrees of freedom, and

the p-value is greater than 0.4. Accordingly, the hypothesis is accepted; thus, the roller checking did not affect the fracture temperature.

Based on these findings, the TSRST ranked samples in the correct order, but there was no statistical evidence for the differences in fracture temperatures between the populations. With regard the minimum pavement surface temperature in the field, the TSRST fracture temperatures were approximately 10°C (20°F) warmer and, accordingly, cracking could be anticipated for all test sections. However, the temperature distribution in the asphalt concrete pavement layer is not known.

3.2 Pennsylvania

The temperature and cracking observations presented in the following paragraphs were reported by Kandhal et al. (1984).

3.2.1 Field Results

3.2.1.1 Temperature Data

The Pennsylvania Department of Transportation had a thermocouple installation site 7 miles north of the project. The system was capable of recording hourly air temperature and asphalt pavement temperature 51 mm (2 in.) below the surface. According to the recorded data, the critical rapid cooling is believed to have occurred in the first winter, on January 28 and 29, 1977. The air temperature dropped 14°C (25°F) in 2 hours. Rapid cooling of the pavement 51 mm (2 in.) below the surface occurred 12 hours later, a drop of 5°C (9°F) in 1 hour. The minimum air temperature recorded was -29°C (-20°F) whereas the pavement temperature reached -23°C (-10°F). The 1976-1977 Air Freezing Index was determined to be 1509 degree days. Low ambient temperatures prevailed at the site during the second (1977-1978) and third (1978-1979) winters. The minimum temperatures were -18°C (-27.8°F) and -25°C (-31.7°F) respectively.

3.2.1.2 Cracking Observations

When the pavements were constructed in September 1976, no visual difference could be seen among the six test pavements. After the first winter, two test sections (T-1 and T-5) developed excessive low-temperature cracking, while the other sections did not have any transverse cracks. After three severe winters, sections T-1 and T-5 developed more cracks, while the other sections did not develop any significant cracking. After 5 years, sections T-2, T-4 and T-6 gradually developed cracking to different degrees, while section T-3 had no transverse cracking. The Cracking Index with time, defined as (full cracks + 0.5 Half Cracks + 0.25 Partial Cracks) / 500 ft (152.4 m), is given in Table 3.2.

Table 3.2. Cracking Index with time for Pennsylvania test sections

Year	T-1	T-2	T-3	T-4	T-5	T-6
1977	51	0	0	0	38	0
1978	69	0	0	0	50	0
1979	76	-	-	-	54	-
1981	92	9	0	12	64	7

Cracking Index = (Full + 1/2 × Half + 1/4 × Partial)Cracks / 500 ft

Table 3.3. Summary of TSRST results for Pennsylvania test sections

Asphalt Cement	Mean Voids (VPAR) (%)	Mean Fracture Stress/ Std. Dev. (psi)	Mean Fracture Stress/ Std. Dev. (kPa)	Mean Fracture Temperature/ Std. Dev. (°F)	Mean Fracture Temperature/ Std. Dev. (°C)	Number of Observations
Cooling Rate 18°F/h (10°C/h)						
T-1	1.5	529	3645	-2.7	-19.3	1
T-2	0.4/0.5	466/25	3211/172	-8.9/0.2	-22.7/0.1	2
T-3	1.4/0.7	564/162	3887/431	-11.2/2.3	-24.0/1.3	2
T-4	1.9/0.1	595/133	4102/227	-13.7/0.5	-25.4/0.3	2
T-5	2.8/1.1	557/14	3840/96	-3.6/0.9	-19.8/0.5	2
T-6	0.7/0.2	670/159	4619/408	-16.4/1.6	-26.9/0.9	2
Cooling Rate 9°F/h (5°C/h)						
T-1	1.7	347	2396	-1.3	-18.5	1
T-2	0.3/0.3	680/24	4689/166	-17.1/0.0	-27.3/0.0	2
T-3	1.3/0.4	647/20	4462/137	-15.3/0.9	-26.3/0.5	2
T-4	0.6/0.5	533/122	3673/840	-11.7/2.2	-24.3/1.2	2
T-5	1.0/1.0	579/25	3942/174	-4.9/0.3	-20.5/0.1	2
T-6	0.8/0.4	675/0.3	4655/2	-17.5/1.0	-27.5/0.6	2

3.2.2 Laboratory Results

The TSRST results and test variables for each specimen are given in Appendix D. The mean values for each data set are given in Table 3.3. The specimens were laboratory-produced 51 × 51 × 305 mm (2 × 2 × 10 in.) beams and were tested in the unaged condition.

3.2.3 Data Analysis

In the Pennsylvania data set, the actual moments of cracking, and, therefore, the cracking temperatures in the field, are not known. However, minimum air and pavement temperatures for the first as well as for the most severe winter are available. The mean TSRST fracture temperatures (cooling rate 5°C/h (9°F/h) for the test sections and the minimum pavement temperature in the field are given in Figure 3.2. The TSRST fracture temperatures of field sections T-1 and T-5 (that experienced severe low-temperature cracking) are warmer than the minimum pavement temperature of -23°C (-10°F). At the same time, the TSRST fracture temperatures for all the other sections that resisted low-temperature cracking are colder than the minimum pavement temperature. Hence, the cracking behavior of the test sections may be explained totally by the TSRST fracture temperatures.

To investigate the relationship between the Cracking Index for pavement age from 1 to 5 years in Table 3.2 and the TSRST fracture temperature, a multiple regression analysis was performed. The analysis was performed with the mean TSRST fracture temperatures of the tests with a cooling rate of 5°C/h (9°F/h) (FrT5) and 10°C (18°F/h) (FrT10). According to the analysis, there is convincing evidence that the fracture temperature is associated with the Cracking Index (p-value in the two-sided t-test is less than 0.0001). The following model was chosen to represent the Cracking Index (CI) as a function of the TSRST fracture temperature (FrT), based on the smallest error of CI estimate:

Mean{CI} =	-156.88 -	4216.63 / FrT5
S.E.	15.5	353.50
p-value in two-sided t-test		
	<0.0001	<0.0001

R^2 = 89%, Error of CI Estimate 10.95,

where CI = (Full + 0.5 × Half + 0.25 × Partial Cracks)/500 ft,
FrT5 = fracture temperature (°C), cooling rate 5°C/h.

The predicted CI versus the TSRST fracture temperature is plotted in Figure 3.3.

Adding the natural logarithm of age of the pavement improves the model (the p-value is less than 0.005 in extra sum-of-squares F-test), which is given as follows:

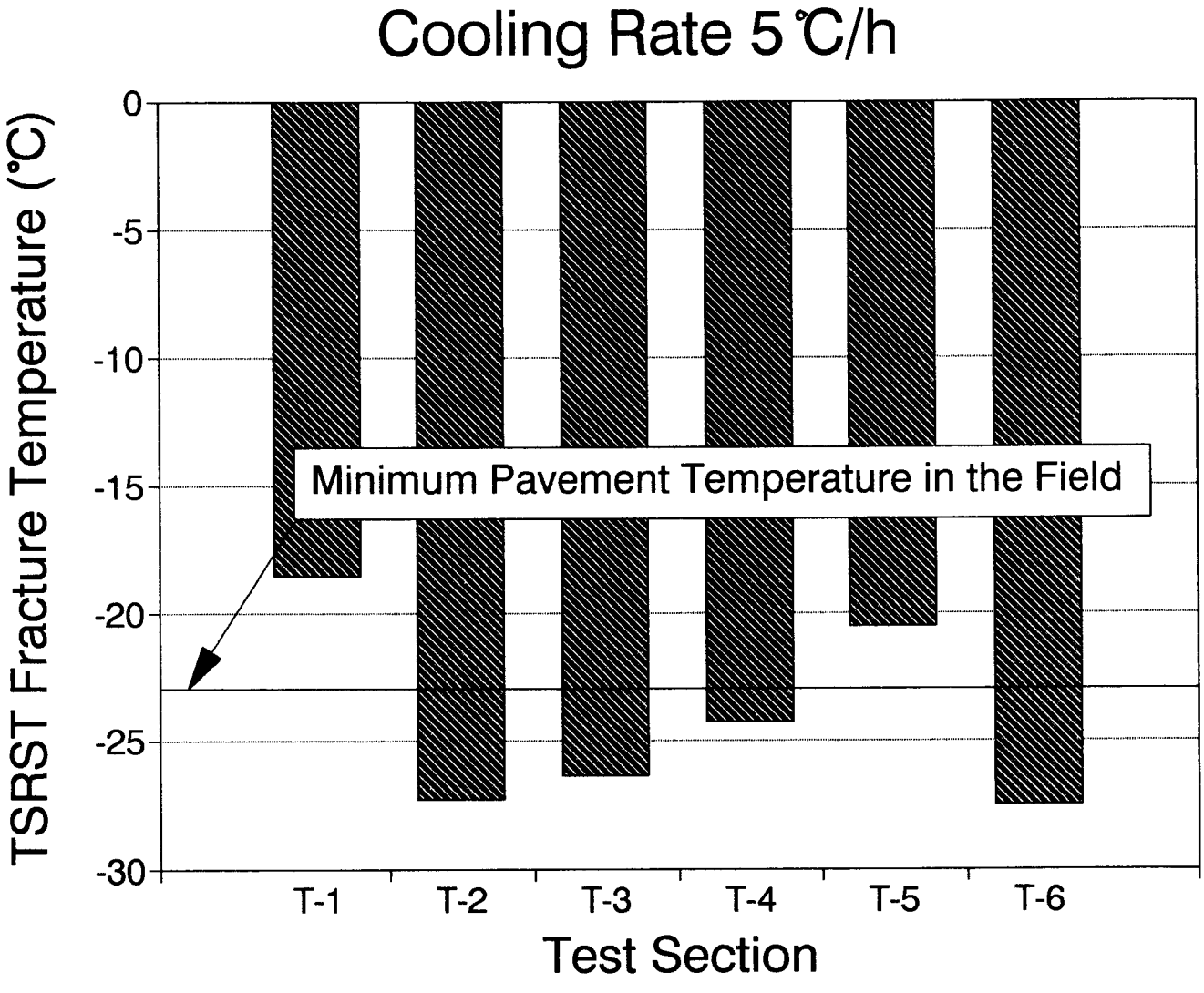

Figure 3.2. TSRST fracture temperatures and minimum pavement temperature for Pennsylvania test sections

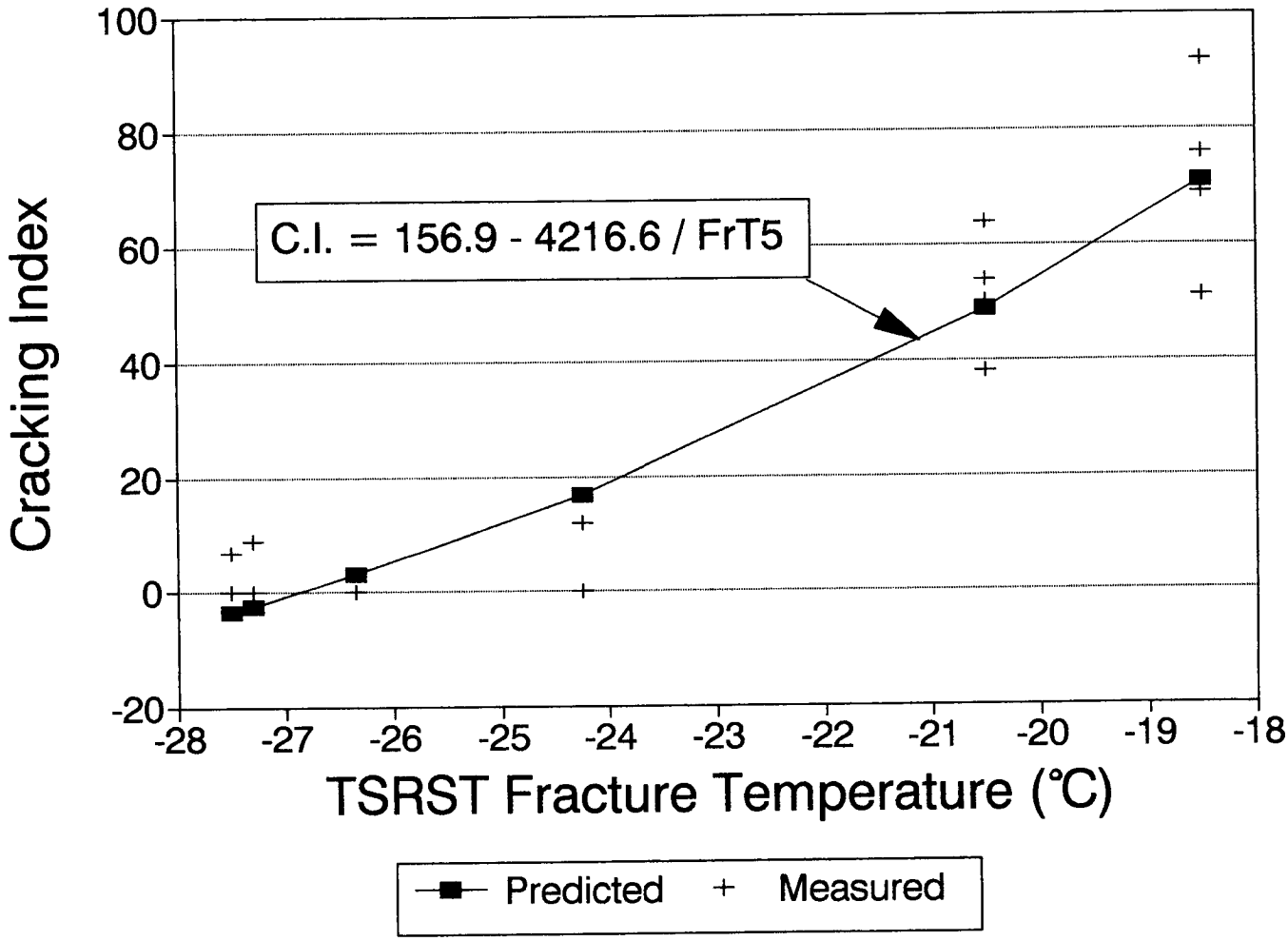

Figure 3.3. Cracking Index versus TSRST fracture temperature for Pennsylvania test sections

Mean{CI}	=	-162.56 -	4160.39/FrT5 +	10.15ln(Age)
S.E.		12.69	286.54	3.13
p-value in two-sided t-test				
		<0.0001	<0.0001	0.0048

R^2 = 93%, Error of CI Estimate 8.86,

where CI = (Full + 0.5 × Half + 0.25 × Partial Cracks)/500 ft,
FrT5 = fracture temperature (°C), cooling rate 5°C/h,
Age = age of pavement (years).

Cracking Indices as a function of time for sections T-1 and T-5 are given in Figure 3.4.

3.3 Peraseinajoki, Finland

3.3.1 Field Results

The temperature data and the cracking observations were obtained from the Technical Research Center of Finland (Kurki 1991).

3.3.1.1 Temperature Data

A temperature data logger was installed at a representative location for the test sections. Temperature was measured using thermocouples at the surface, at a depth of 25 mm (1 in.), at the bottom of the asphalt concrete layer, and in the air every 30 minutes. The coldest recorded air temperature was -30°C (-22°F), and the coldest temperature in the pavement was -20°C (-4°F). The maximum recorded cooling rate was 0.7°C/h (1.3°F/h). The Freezing Index for the period of November 9, 1990, to March 25, 1991, was 661 degree centrigrade days (1190 degree Fahrenheit days).

3.3.1.2 Cracking Observations

No low-temperature cracks were observed in any of the six test sections during the first two winters.

3.3.2 Laboratory Results

Since no cracks were observed in the Peraseinajoki test road, no specimens were prepared in the laboratory. However, because the asphalt cement is the most significant factor influencing low-temperature cracking (Jung and Vinson 1992), the laboratory test results for the Sodankyla specimens could be used to represent the Peraseinajoki sections. (The asphalts are the same, both test roads have a well-graded aggregate, and the asphalt contents are within 0.4 percent.) A summary of the Sodankyla test results adapted for Peraseinajoki are given in Table 3.4.

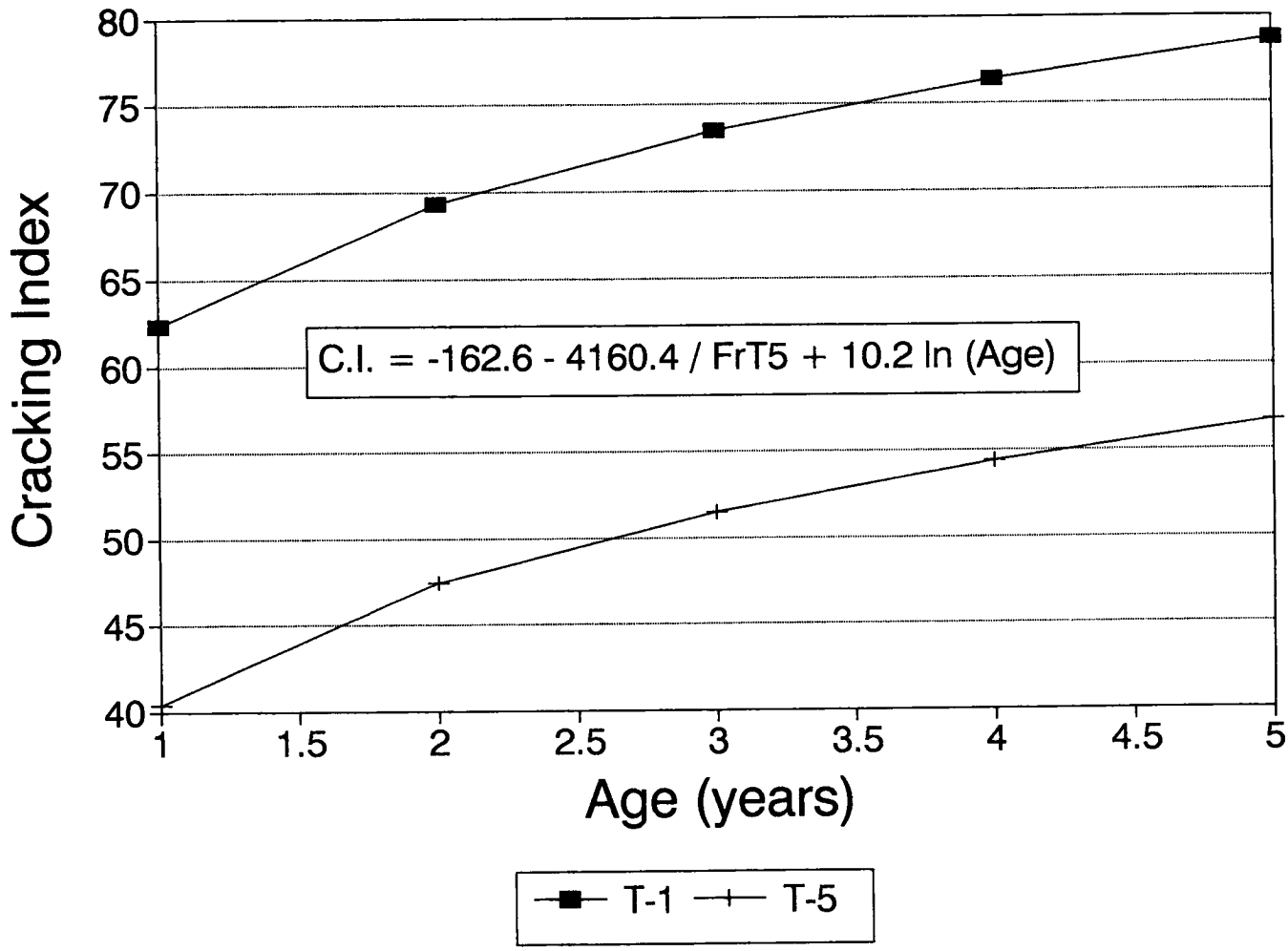

Figure 3.4. Predicted Cracking Index versus time for Pennsylvania sections T-1 and T-5

Table 3.4. Summary of TSRST results for Peraseinajoki sections (adapted from Sodankyla sections)

Asphalt Cement	Mean Voids (VPAR) (%)	Mean Fracture Stress/ Std. Dev. (psi)	Mean Fracture Stress/ Std. Dev. (kPa)	Mean Fracture Temperature/ Std. Dev. (°F)	Mean Fracture Temperature/ Std. Dev. (°C)	Number of Observations
Cooling Rate 18°F/h (10°C/h)						
BIT120AH	1.6/0.1	285/123	1962/845	-24.3/1.7	-31.3/1.0	2
BIT120ECO	1.2/0.1	523/104	3607/720	-20.0/4.8	-28.9/2.7	2
BIT65AH	1.6/0.2	489/127	3369/879	-19.0/1.9	-28.4/1.1	2
BIT80AH	1.5/0.1	402/5	2768/33	-18.0/2.9	-27.8/1.6	2
BIT200AH	2.0/0.4	642/7	4425/48	-28.9/0.4	-33.9/0.2	2
PmB1	2.2/0.7	831/44	5730/300	-33.3/0.8	-36.3/0.4	2
Cooling Rate 3.6°F/h (2°C/h)						
BIT120AH	1.3/0.2	508/76	3499/524	-25.2/2.5	-31.8/1.3	2
BIT120ECO	1.6/0.3	582/10	4015/65	-27.7/0.6	-33.2/0.3	2
BIT65AH	2.0/0.5	523/23	3606/158	-18.0/1.4	-27.8/0.8	2
BIT80AH	1.2/	511	3524	-23.1	-30.6	1
BIT200AH	1.4/0.1	603/52	4158/356	-31.6/0.6	-35.4/0.4	2
PmB1	1.6/0.3	807/13	5566/90	-36.5/0.4	-38.1/0.2	2

3.3.3 Data Analysis

The mean TSRST fracture temperatures (cooling rate 2°C/h, 3.6°F/h) for test sections (adapted from the Sodankyla test sections) and the minimum pavement temperature in the field are given in Figure 3.5. The TSRST fracture temperatures of the field sections are all colder than the minimum pavement temperature of -20°C (-4°F). Hence, the cracking behavior of the test sections could be explained by the TSRST fracture temperatures.

3.4 Sodankyla, Finland

3.4.1 Field Results

The temperature data and the cracking observations were obtained from the local road authority of Sodankyla and the Technical Research Center of Finland (Kurki 1991).

3.4.1.1 Temperature Data

A temperature data logger was installed at a representative location for the test sections. Temperature was measured using thermocouples every 30 minutes at the surface, at a depth of 25 mm (1 in.) at the bottom of the asphalt concrete layer, and in the air. The coldest air temperature observed was -33°C (-27.4°F), and coldest temperature in the pavement was -24.5°C (-12.1°F) The recorded maximum cooling rate was 2.3°C (4.1°F/h). The Freezing Index for the period of November 9, 1990 to March 25, 1991 was 1488 degree centrigrade days (2677 degree Fahrenheit days).

3.4.1.2 Cracking Observations

Visual crack observations were performed occasionally during the coldest winter months for a 300 m (984.2 ft) long segment of each test section. A complete investigation was performed after the first winter for the entire length of the project. A total of 116 full cracks and 48 half cracks were recorded. The observations are listed in Appendix E and summarized in Table 3.5. Because the observations were not made daily, the exact cracking moment, and therefore, the cracking temperature are not known. The estimated cracking temperatures in the air and pavement (given in Appendix E) are the coldest temperatures that occurred between the observations. The temperatures given in Table 3.5 are the warmest cracking temperatures for each 300 m (984.2 ft) long observed test segment.

In addition to the fact that the actual moment of cracking was not recorded, the following conditions make it difficult to interpret the cracking frequencies and temperatures:

- The test sections were limited to one lane only, and a large number of full cracks extending over the entire pavement were observed. Cracks may have occurred on the other lane and advanced to the section in question. The variation in the length of the test sections further complicated the interpretation.

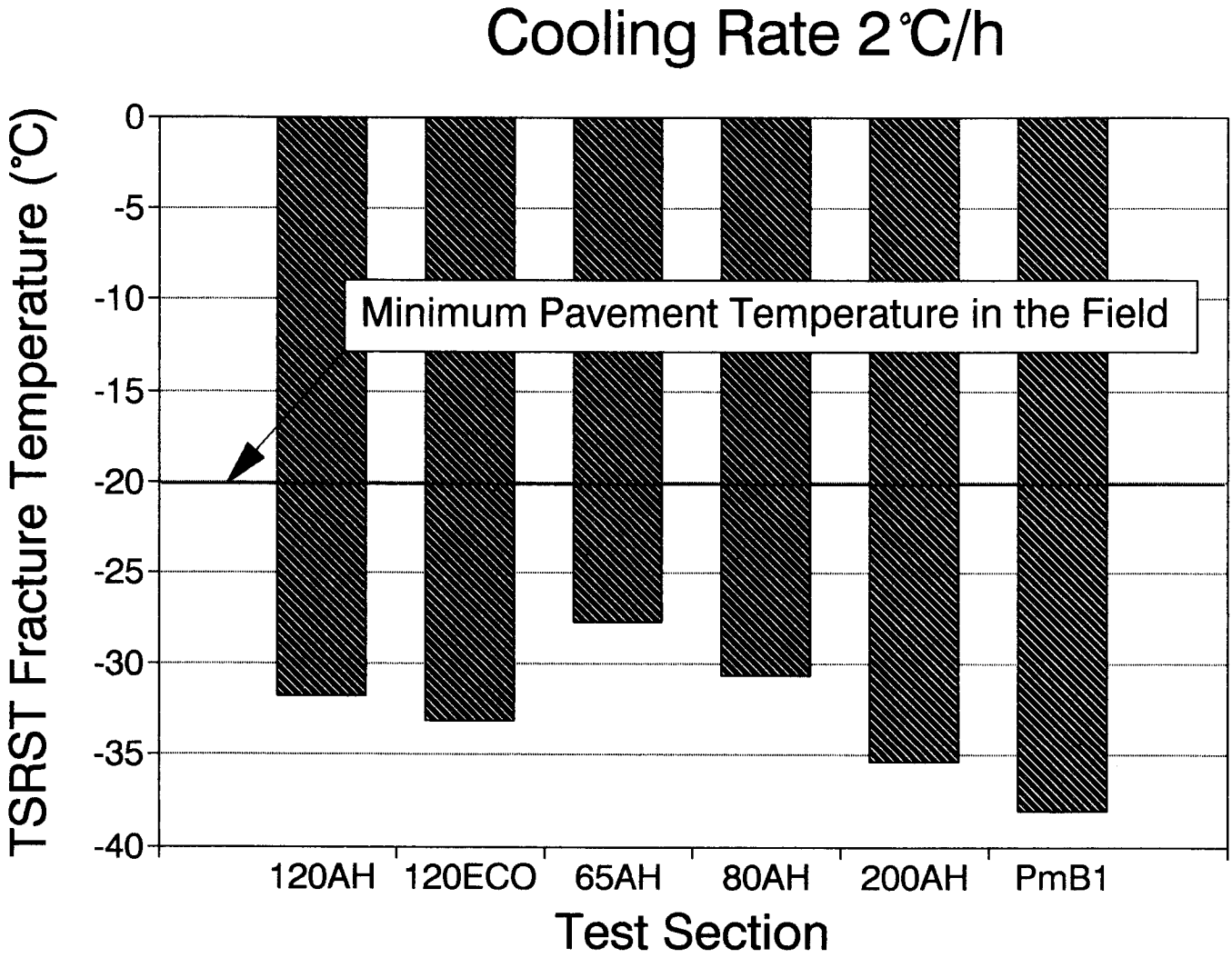

Figure 3.5. TSRST fracture temperatures and minimum pavement temperature for Peraseinajoki test sections

Table 3.5. Summary of crack observations for Sodankyla test sections

Asphalt	Length of Section (ft)	Length of Section (m)	Amount of Cracks	Cracking Index (1/500 ft)	Cracking Index (1/100 m)	Cracking Air Temperature (°F)	Cracking Air Temperature (°C)	Cracking Pavement Temperature (°F)	Cracking Pavement Temperature (°C)
BIT120AH	2490	759	15	3.01	1.98	-22.0	-30.0	-3.1	-19.5
B120LD	4547	1386	10	1.10	0.72	-27.4	-33.0	-12.1	-24.5
BIT120EC	2762	842	18	3.26	2.14	-13.0	-25.0	-4.0	-20.0
BIT120ARC	4127	1258	5	0.61	0.40	-26.5	-32.5	-8.5	-22.5
BIT65AH	1329	405	1	0.38	0.25	-4.0	-20.0	1.4	-17.0
BIT80AH	1293	394	7	2.71	1.78	-19.3	-28.5	-8.5	-22.5
BIT200AH	1834	559	2	0.55	0.36	-26.5	-32.5	-8.5	-22.5
PmB1	1312	400	8	3.05	2.00	-11.2	-24.0	-0.4	-18.0
BIT150AH	1991	607	15	3.77	2.47	-27.4	-33.0	-12.1	-24.5

- Only 300 m (984 ft) long segments were observed periodically. If the first crack occurred outside that segment, the cracking moment observed would relate to the second or possibly even the third or fourth crack.

- The transverse crack pattern in the pavement before the reconstruction was given in the construction documents. Approximately half of the cracks that occurred in the first winter appeared at the same locations as the existing cracks in the underlying pavements. Thus, a portion of the cracks should be considered reflection cracks.

- The cracking frequency in the preceding pavement was not constant (Figure 3.6), even though there was no variation in the materials. This leads to the conclusion that there is a variation in the conditions of the test sections.

- Ground thermal contraction rather than contraction in the asphalt concrete may have caused a number of the cracks in the pavement wearing course.

3.4.2 Laboratory Results

The TSRST results and test variables for each specimen are given in Appendix D, and the mean values for each data set are given in Table 3.6. The specimens were 51 × 51 × 305 mm (2 × 2 × 10 in.) beams produced at the mixing plant during construction and were tested in an unaged condition.

3.4.3 Data Analysis

A multiple regression analysis was performed to examine the association between the TSRST fracture temperature and cracking temperature and frequency in the field. Several prediction models for the cracking temperatures were considered, but only 28 percent of the variable cracking air temperature and 17 percent of the variable cracking pavement temperature could be explained by the TSRST fracture temperature. Possible reasons for the poor correlation are given in section 3.4.1.2 above.

The TSRST fracture temperatures for each section and the minimum pavement temperature are given in Figure 3.7. According to the data, none of the pavement sections should have cracked. However, compared with the conditions in Peraseinajoki, the minimum pavement temperature was 4.5°C (8°F) colder, and the Freezing Index at the surface of the pavement was more than twice as severe.

According to the multiple regression analysis, the cracking frequency increases with decreasing TSRST fracture temperature, which is not possible. The cracking frequency

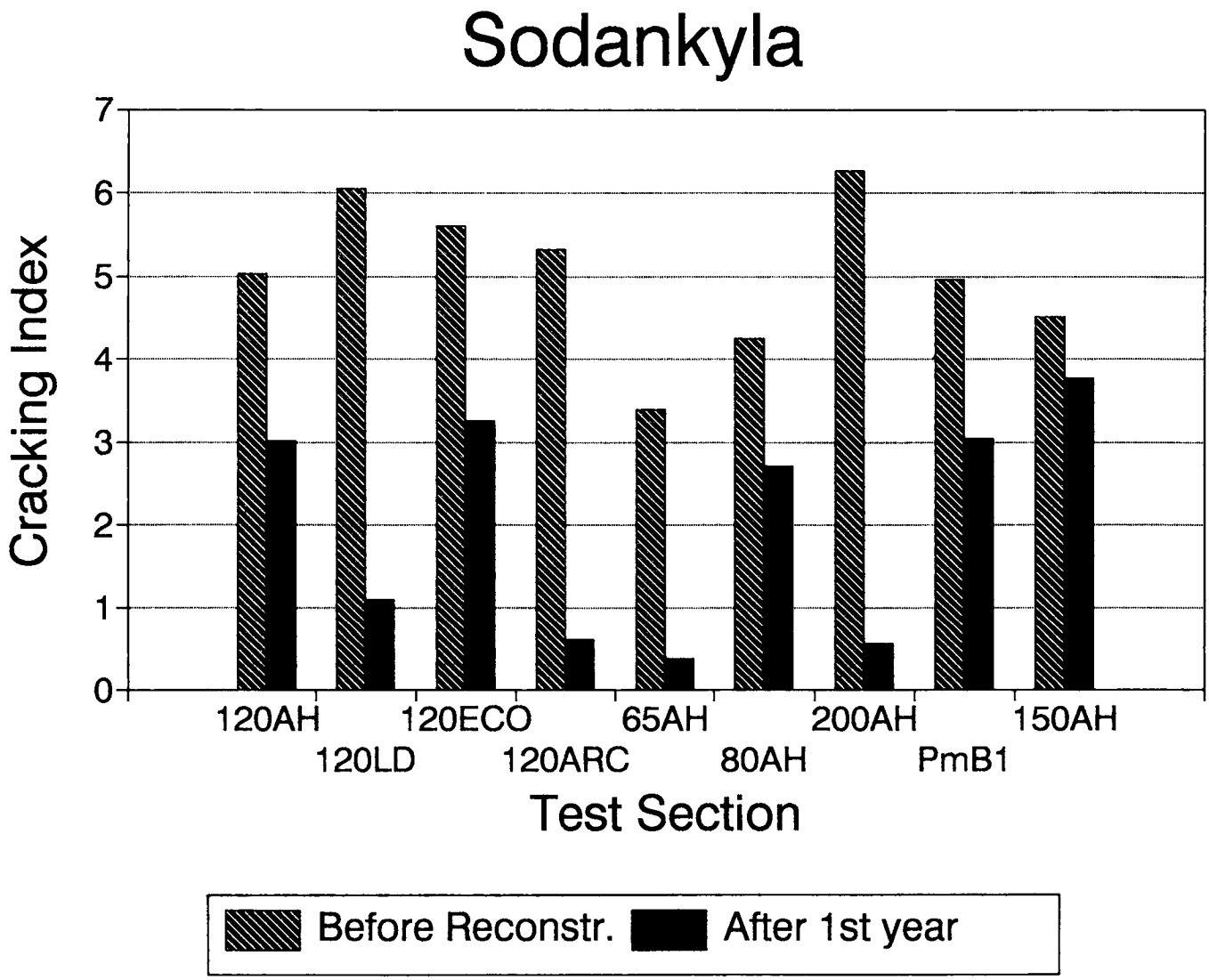

Figure 3.6. Cracking frequency before reconstruction and after first year for Sodankyla test sections

Table 3.6. Summary of TSRST results for Sodankyla test sections

Asphalt Cement	Mean Voids (VPAR) (%)	Mean Fracture Stress/ Std. Dev. (psi)	Mean Fracture Stress/ Std. Dev. (kPa)	Mean Fracture Temperature/ Std. Dev. (°F)	Mean Fracture Temperature/ Std. Dev. (°C)	Number of Observations
Cooling Rate 18°F/h (10°C/h)						
BIT120AH	1.6/0.1	285/123	1962/845	-24.3/1.8	-31.3/1.0	2
B120LD	1.1/0.2	582/77	4009/531	-24.9/0.0	-31.6/0.0.	2
BIT120ECO	1.2/0.1	523/104	3607/720	-20.0/4.8	-28.9/2.7	2
BIT120ARC	-	692/61	4772/424	-32.4/0.5	-35.8/0.3	2
BIT65AH	1.6/0.2	489/127	3369/880	-19.0/1.9	-28.4/1.1	2
BIT80AH	1.5/0.1	402/5	2768/33	-18.0/2.9	-27.8/1.6	2
BIT200AH	2.0/0.3	642/7	4425/48	-28.9/0.4	-33.9/0.2	2
PmB1	2.2/0.7	831/43	5730/300	-33.3/0.8	-36.3/0.4	2
BIT150AH	1.2/0.0	598/59	4125/408	-31.5/4.8	-35.3/2.7	2
Cooling Rate 3.6°F/h (2°C/h)						
BIT120AH	1.3/0.2	508/76	3499/524	-25.2/2.4	-31.8/1.3	2
B120LD	1.6/0.3	592/85	4080/585	-31.0/2.5	-35.0/1.4	2
BIT120ECO	1.6/0.1	582/10	4015/65	-27.7/0.6	-33.2/0.3	2
BIT120ARC	1.1/0.0	670/25	4620/165	-34.7/0.1	-37.1/0.1	2
BIT65AH	2.0/0.5	523/23	3606/158	-18.0/1.4	-27.8/0.8	2
BIT80AH	1.2	511	3524	-23.1	-30.6	1
BIT200AH	1.4/0.1	603/6	4158/356	-31.6/0.6	-35.4/0.3	2
PmB1	1.6/0.3	807/13	5566/90	-36.5/0.4	-38.1/0.2	2
BIT150AH	1.5/0.1	471/179	3250/1233	-30.2/4.4	-34.6/2.5	2

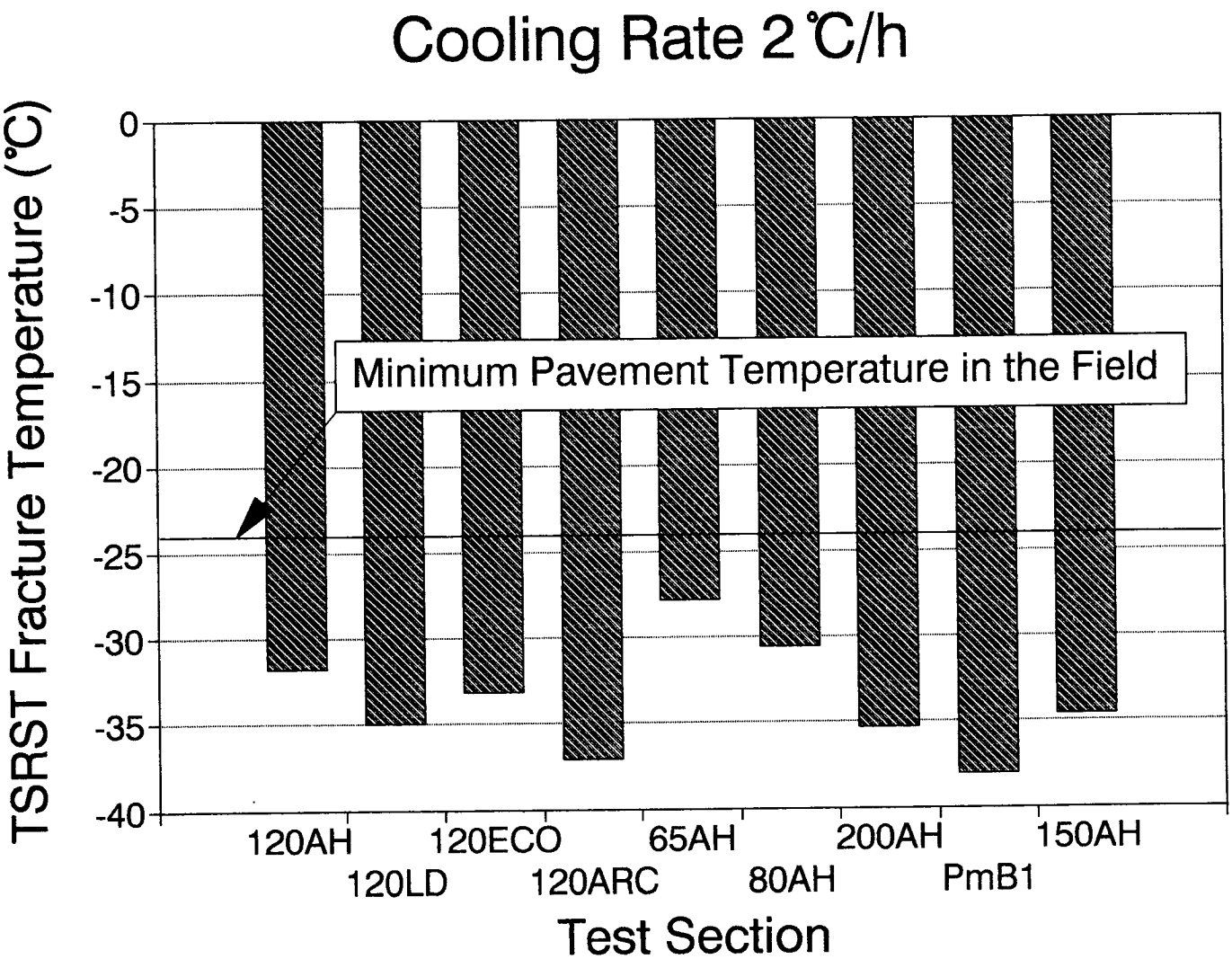

Figure 3.7. TSRST fracture temperatures and minimum pavement temperature for Sodankyla test sections

versus TSRST fracture temperature is given in Figure 3.8. By visual inspection of the results presented in Figure 3.8 and knowing the low-temperature behavior of the PmB (SBS modified) and BIT65AH (penetration grade 65, the lowest of the nine asphalts), the two data points are unreasonable. If these cases are omitted, the following model represents the relationship between the Cracking Index (cracks per 500 ft) and TSRST fracture temperature (FrT):

Mean{CI}	=	-10.56	-429.6 / FrT
S.E.		7.04	237.6
p-value in two-sided t-test			
		0.194	0.130

R^2 = 39%, Error of CI Estimate 0.75,

where CI = (Full + 0.5 × Half) Cracks / 500 ft,
FrT = fracture temperature (°C), cooling rate 2°C/h.

However, even if the two outliers are omitted, there is not enough evidence that the TSRST fracture temperature is associated with the Cracking Index (p-value in two-sided t-test is 0.13). Here, too, the geometry of the test sections, possible reflection cracking, ground thermal contraction, and varying conditions affected the data set.

In conclusion, factors other than the mixture properties apparently influenced the low-temperature cracking of the test sections. However, it is possible that the data set may be useful in a probabilistic analysis.

3.5 USACRREL

3.5.1 Field Results

The following temperature and cracking observations were presented by Kanerva et al. (1992).

3.5.1.1 Temperature Data

Temperatures in the pavement structure were measured using thermocouples placed at the surface and bottom of the asphalt concrete, in the midpoint of the base course, and at the top and bottom of the insulation layer.

The minimum temperature achieved at the surface of the pavement was -36.7°C (-34.0°F) and at the bottom of the pavement -32.8°C (-27°F). Pavement temperatures recorded when cracking occurred are given in Table 3.7. A typical temperature profile with detected cracking times is given in Figure 3.9. The three curves in Figure 3.9 represent the

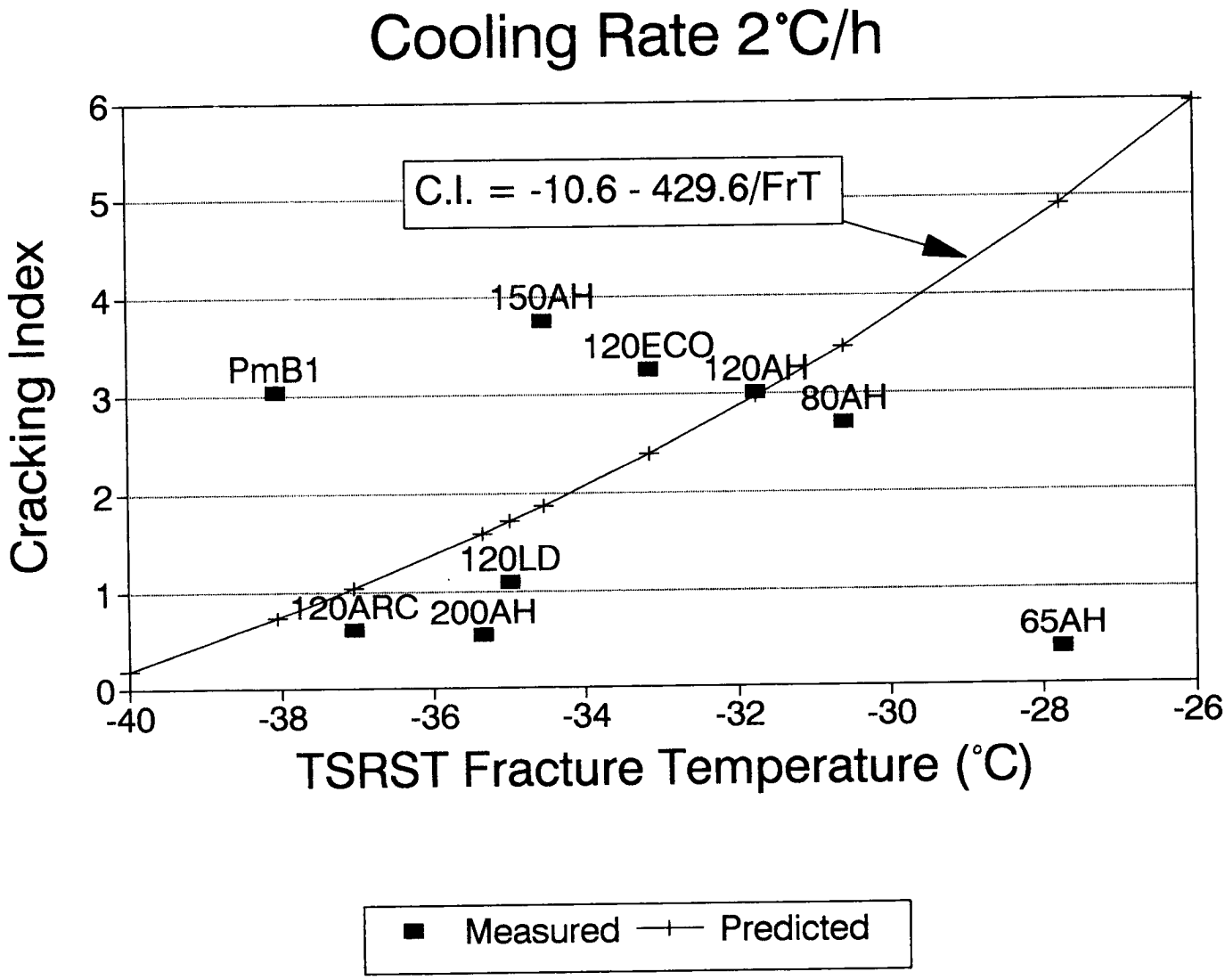

Figure 3.8. Cracking frequency versus TSRST fracture temperature for Sodankyla test sections

Table 3.7. Recorded crack observations for USACRREL test sections

Section ID	Station	Julian* Day	Time (hour:minute)	Surface Temperature (°F)	Surface Temperature (°C)	Bottom Temperature (°F)	Bottom Temperature (°C)
Ia	-38	221	3:45	-33.9	-36.6	-21.8	-29.9
		220	3:15	-33.3	-36.3	-17.0	-27.2
Ia	2.5	220	2:45	-31.0	-35.0	-16.6	-27.0
		220	11:45	-31.3	-35.2	-18.8	-28.2
		220	3:15	-30.7	-34.8	-16.6	-27.0
Ib	-38	220	12:00	-31.3	-35.2	-8.8	-22.7
		222	4:15	-33.0	-36.1	-14.7	-25.9
		220	18:30	-31.6	-35.3	-10.3	-23.5
Ib	2.5	220	8:44	-32.6	-35.9	-8.0	-22.2
		220	22:30	-33.2	-36.2	-11.0	-23.9
		220	5:00	-32.7	-35.9	-7.3	-21.8
Ib	30	219	2:20	-32.1	-35.6	-11.1	-23.9
		220	20:30	-33.2	-36.2	-16.5	-26.9
VI	-42	272	1:10	-30.3	-34.6	-13.1	-25.1
		272	1:10	-25.8	-32.1	-13.8	-25.4
VI	0	273	1:30	-27.9	-33.3	-15.8	-26.6
		273	10:30	-30.0	-34.4	-15.8	-26.6
		273	11:30	-29.7	-34.3	-15.8	-26.6
		274	3:45	-29.1	-33.9	-15.8	-26.6
		274	9:00	-29.2	-34.0	-15.9	-26.6

Continued on next page.

Table 3.7 (continued). Recorded crack observations for USACRREL test sections

Section ID	Station	Julian* Day	Time (hour:minute)	Surface Temperature (°F)	Surface Temperature (°C)	Bottom Temperature (°F)	Bottom Temperature (°C)
VII	2	284	19:30	-26.7	-32.6	-26.4	-32.4
		286	1:00	-27.7	-33.2	-26.9	-32.7
VIII	0	293	2:10	-33.2	-36.2	-23.9	-31.1
		293	2:00	-33.5	-36.4	-23.9	-31.1
		292	20:45	-30.7	-34.8	-21.2	-29.6
VIII	30	291	4:15	-26.8	-32.7	-12.5	-24.7
IX	-60	294	1:00	-33.5	-36.4	-24.3	-31.3
IX	30	298	2:30	-33.8	-36.6	-26.8	-32.7

*Julian Day = Sequential number of the day based on the 365.25 day Julian calendar year

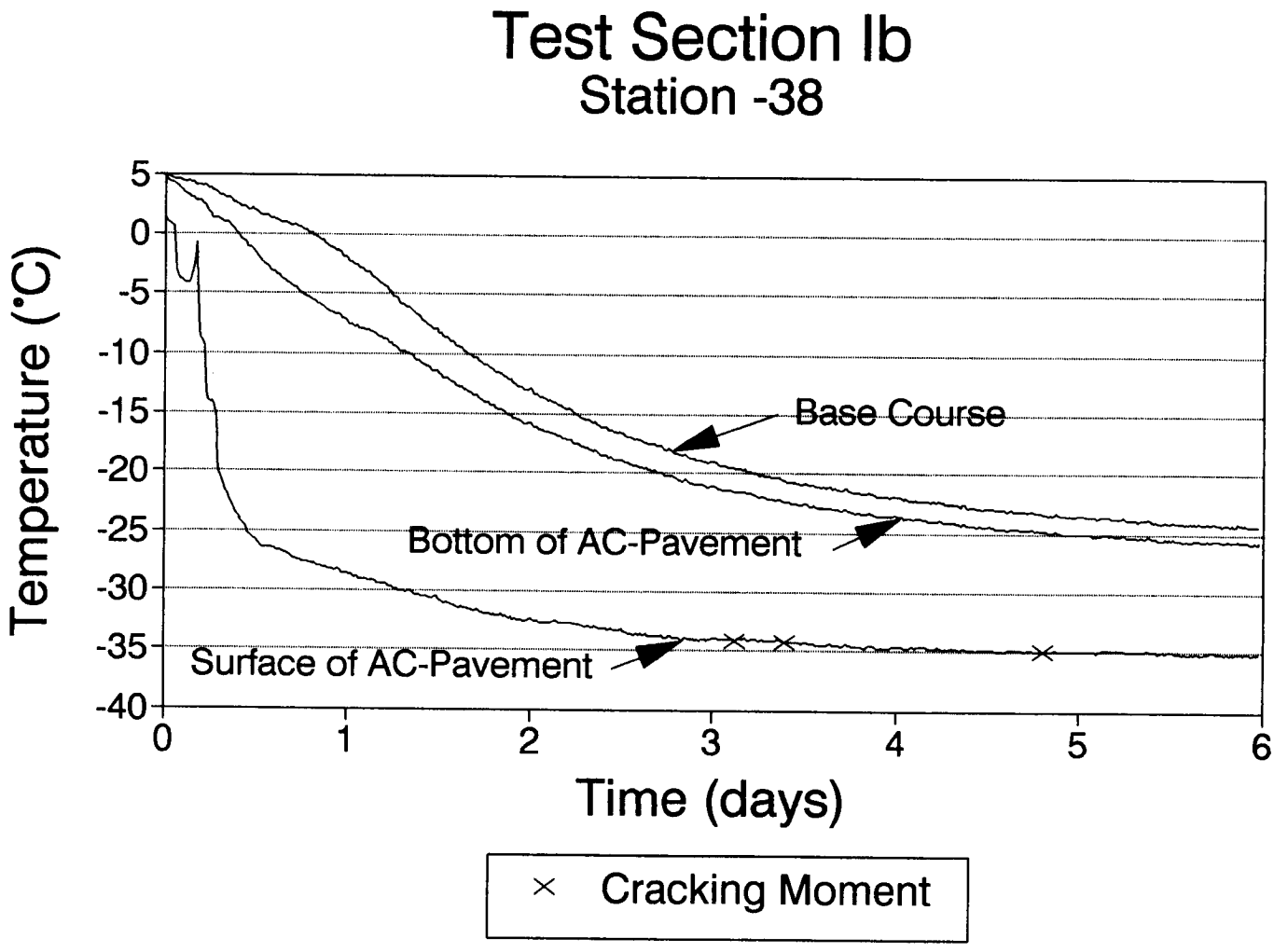

Figure 3.9. Temperature profile for USACRREL Section Ib at Station -38

temperatures at the surface and the bottom of the pavement and in the base course at a depth of 203 mm (8 in.) from the top of the pavement. The times at which cracks were detected are marked with symbols (x) on the temperature curve for the surface of the pavement.

3.5.1.2 Cracking Observations

The crack detection system consisted of two types of aluminum tape and hard-drawn copper wire attached to the pavement surface with adhesive. Seventeen cracks were observed in the nine sections. The cracks produced are shown in Figure 3.10, and the recorded observations are summarized in Table 3.7.

Based on the recorded temperature profiles, cracking generally did not occur before the minimum possible temperature for the cooling system was achieved. Therefore, the surface temperature was constant for a period of time before the onset of cracking. The surface temperature does not reflect the cracking temperature, but instead reflects the minimum temperature achieved by the cooling panels. However, the temperature at the bottom of the asphalt concrete layer decreased until cracking occurred in almost all cases. Hence, the stress due to the distribution of temperature in the pavement layer initiated cracking, rather than the stress associated with the surface temperature. Consequently, in this case, the temperature at the bottom of the asphalt pavement is a better indicator of the cracking temperature than the surface or average temperature. This temperature, termed the indicator cracking temperature, as well as the total number of cracks and the calculated Cracking Index [CI = (Full + 0.5 × Half Cracks) / 500 ft] are given in Table 3.8.

3.5.2 Laboratory Results

The TSRST results and test variables for each specimen are given in Appendix D, and the mean values for each data set are given in Table 3.9. The cylindrical specimens made in the laboratory were 57.2 mm (2.25 in.) in diameter, and the field specimens were 38.1 mm (1.5 in.) in diameter.

3.5.3 Data Analysis

Indicator cracking temperatures versus TSRST fracture temperatures for the test program are shown in Figures 3.11 to 3.13. Multiple regression analysis was performed to investigate the relationship between the cracking temperature of the test sections and TSRST fracture temperature of the corresponding mixture. Results of the regression analysis are given in Table 3.10. Based on the analysis, there is evidence ranging from slight to conclusive that the TSRST fracture temperature is associated with the pavement cracking temperature (CrT). For unaged laboratory samples that were tested using a cooling rate of 18°F/hour (10°C/h), the p-value in a two-sided t-test was 0.017, and 88 percent of the relationship could be explained. The following model represents the relationship:

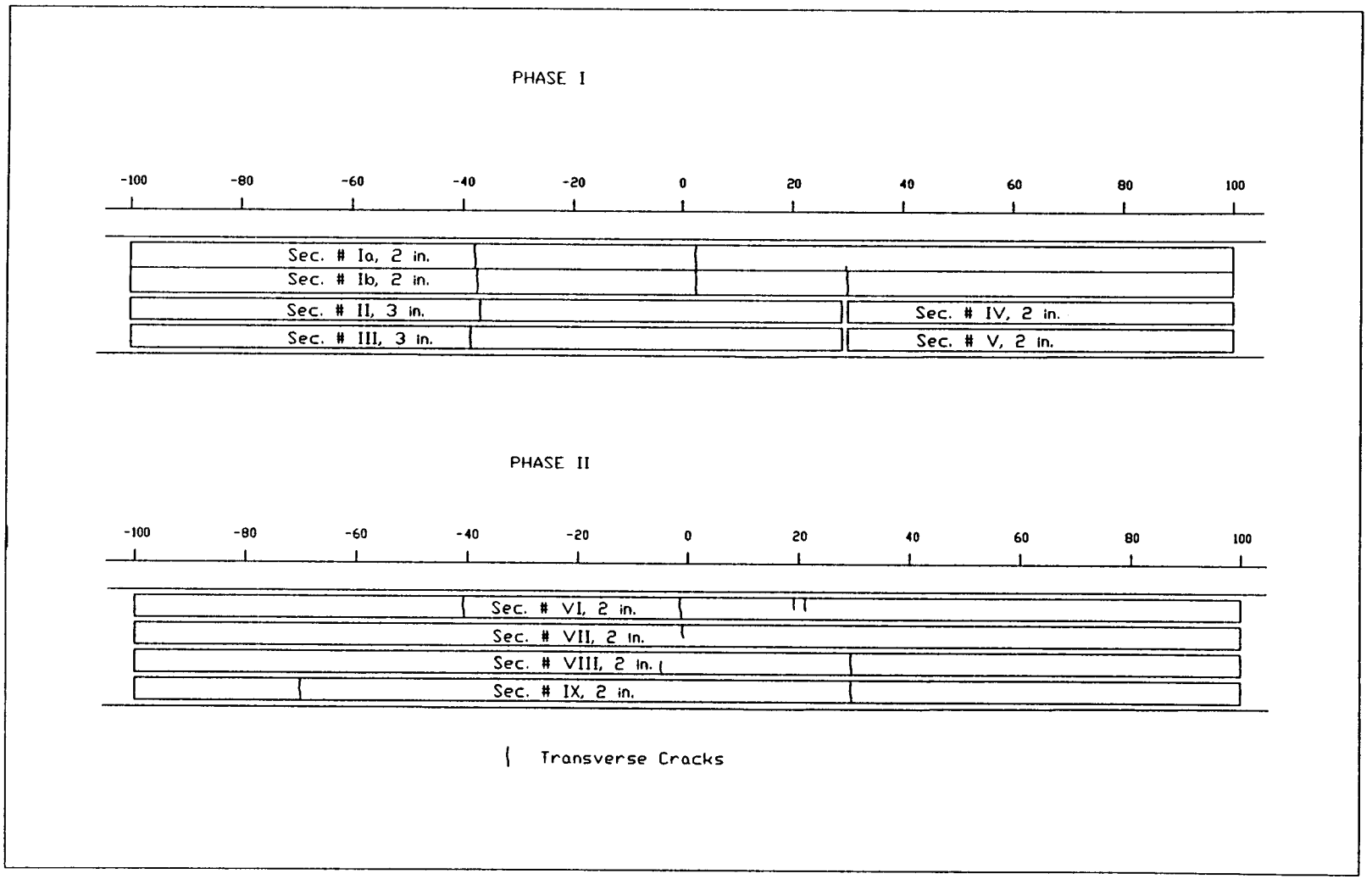

Figure 3.10. Crack map for USACRREL test sections

Table 3.8. Summary of crack observations for USACRREL test sections

Section ID	Asphalt Cement	Number of Cracks		Cracking Index	Cracking Temperature (°F)	Cracking Temperature (°C)
		Full	Half			
I	United AC-20	3	0	7.50	-7.3	-21.8
VI	Viking AC-20	2	2	7.50	-13.1	-25.1
VII	Cibro AC-20	0	1	1.25	-26.4	-32.4
VIII	Petro C. AC-20	1	1	3.75	-12.5	-24.7
IX	Viking AC-10	2	0	5.00	-24.3	-31.3

Table 3.9. Summary of TSRST results for USACRREL test sections

Unaged laboratory samples

Asphalt Cement	Mean Voids (VPAR) (%)	Mean Fracture Stress/ Std. Dev. (psi)	(kPa)	Mean Fracture Temperature/ Std. Dev. (°F)	(°C)	Number of Observations
Cooling Rate 18°F/h (10 C/h)						
United AC-2	3.7/0.7	424/24	2924/166	-13.3/0.4	-25.2/0.2	2
Viking AC-20	1.7/1.1	413/76	2847/521	-14.2/2.7	-25.7/1.5	2
Cibro AC-20	5.9/0.8	388/6	2675/45	-21.3/0.5	-29.6/0.3	2
Pet. C AC-20	3.8/1.1	381/0	2628/1	-16.8/2.5	-27.1/1.4	2
Viking AC-10	5.7/1.4	440/152	3034/1049	-18.9/3.1	-28.3/1.7	2
Cooling Rate 1.8°F/h (1°C/h)						
United AC-2	3.1/1.1	311/38	2142/264	-13.6/3.4	-25.4/1.9	2
Viking AC-20	2.0/0.5	388/20	2678/136	-19.1/0.0	-28.4/0.0	2
Cibro AC-20	3.8/0.1	316/40	2182/277	-22.4/0.8	-30.2/0.4	2
Pet. C AC-20	3.4	406	2798	-20.2	-29.0	1
Viking AC-10	5.8/0.1	311/28	2142/190	-25.6/0.8	-32.0/0.4	2

Short-term-aged laboratory samples

Asphalt Cement	Mean Voids (VPAR) (%)	Mean Fracture Stress/ Std. Dev. (psi)	(kPa)	Mean Fracture Temperature/ Std. Dev. (°F)	(°C)	Number of Observations
Cooling Rate 18°F/h (10°C/h)						
United AC-2	5.9/0.9	350/4	2410/28	-12.6/0.8	-24.8/0.4	2
Viking AC-20	5.0/1.0	253/82	1741/564	-12.6/1.3	-24.8/0.7	2
Cibro AC-20	6.0/1.3	299/9	2063/62	-18.9/0.8	-28.3/0.4	2
Pet. C. AC-20	3.4/0.3	365/8	2517/58	-10.9/1.2	-23.9/0.6	2
Viking AC-10	6.9/1.0	307/23	2115/156	-19.1/3.3	-28.4/1.8	2
Cooling Rate 1.8°F/h (1°C/h)						
United AC-2	5.8/0.5	345/28	2375/193	-15.3/0.9	-26.3/0.5	2
Viking AC-20	4.6/2.3	370/64	2551/445	-14.8/2.5	-26.0/1.4	2
Cibro AC-20	4.4/1.3	298/137	2054/947	-18.6/1.5	-28.1/0.8	2
Pet. C. AC-20	5.0/0.3	365/2	2514/12	-15.7/0.0	-26.5/0.0	2
Viking AC-10	5.6/0.6	275/4	1895/265	-20.9/1.8	-29.4/1.0	2

Continued on next page.

Table 3.9 (continued). Summary of TSRST results for USACRREL test sections

Field samples

Asphalt Cement	Mean Voids (VPAR) (%)	Mean Fracture Stress/ Std. Dev. (psi)	Mean Fracture Stress/ Std. Dev. (kPa)	Mean Fracture Temperature/ Std. Dev. (°F)	Mean Fracture Temperature/ Std. Dev. (°C)	Number of Observations
Cooling Rate 18°F/h (10°C/h)						
Viking AC-20	4.7/0.8	393/136	2709/936	-14.2/1.7	-25.7/0.9	4
Cibro AC-20	5.6/0.2	324/54	2232/374	-22.0/4.1	-30.0/2.3	4
Pet. C AC-20	5.2/0.3	378/48	2604/335	-15.7/2.5	-26.5/1.4	4
Viking AC-10	8.2/1.0	306/86	2107/591	-22.0/2.5	-30.0/1.4	3
Cooling Rate 1.8°F/h (1°C/h)						
Viking AC-20	8.60/0.3	294/42	2026/291	-20.3/2.7	-29.1/1.5	4
Cibro AC-20	6.3/0.2	275/88	1897/606	-32.1/4.2	-35.6/2.3	3
Pet. C Ac-20	5.0/1.0	278/64	1916/440	-22.3/3.6	-30.2/2.0	4
Viking AC-10	7.6/0.6	269/65	1854/451	-26.1/1.5	-32.3/0.8	4

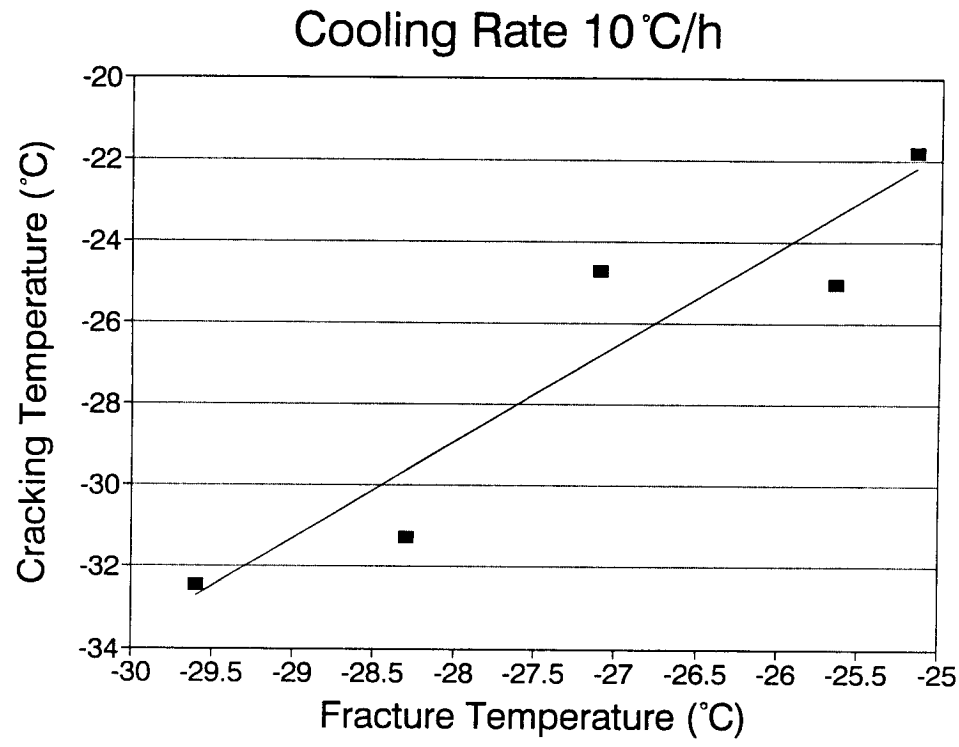

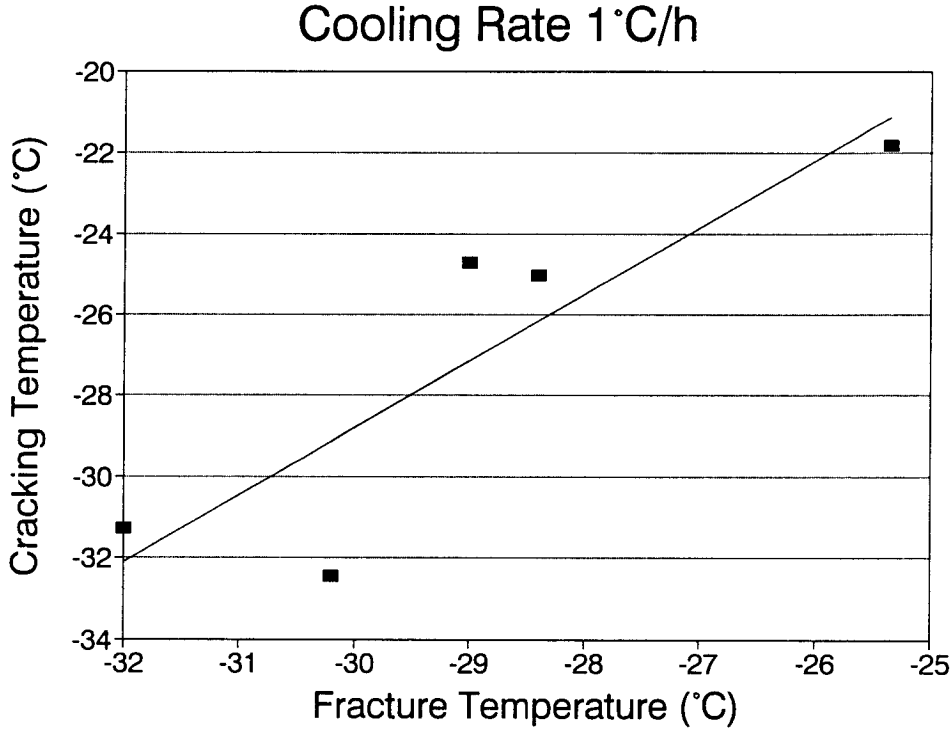

Figure 3.11. Cracking temperatures versus TSRST fracture temperatures for unaged USACRREL laboratory samples

Mean{CrT} = 37.16 + 2.36 * FrT
S.E. 13.48 0.49
p-value in two-sided t-test
0.027 0.017
R^2 = 88%, Error of CI Estimate 3.24,

where CrT = indicator cracking temperature (°C),
FrT = fracture temperature (°C), unaged samples, cooling rate 10°C/h.

Predicted cracking temperatures versus measured TSRST fracture temperatures values, are shown in Figure 3.14.

To investigate the correlation between the Cracking Index in the FERF and the TSRST fracture temperature, a multiple regression analysis was performed. The analysis was made with the TSRST fracture temperatures for the tests with a cooling rate of 10°C/h (18°F/h) for unaged samples. There is slight evidence that the TSRST fracture temperature is associated with the Cracking Index (p-value in two-sided t-test is 0.03). The following model represents the CI as a function of the FrT:

Mean{CI} = -31.50 - 988.64/FrT
S.E. 9.49 256.52
p-value in two-sided t-test
0.0450 0.0309
R^2 = 83% Error of CI Estimate 1.25,

where CI = (Full + 0.5 × Half Cracks) / 500 ft,
FrT = fracture temperature (°C), unaged samples, cooling rate 10°C/h.

Predicted Cracking Index versus the measured TSRST fracture temperatures values, are given in Figure 3.15.

According to the results (see Figures 3.11 to 3.13 and Table 3.10), a slow cooling rate (1° rather than 10°C/h) or short-term aging of the samples does not improve the relationship between the cracking temperature in the field and TSRST fracture temperature. The fracture temperatures for laboratory samples versus field samples are shown in Figure 3.16. The test sections were not aged in the field and, accordingly, the unaged laboratory samples are closer to the actual field samples with regard to TSRST fracture temperatures than the short-term aged samples.

Based on the USACRREL test program, where the environmental variables were closely controlled, the TSRST fracture temperature is an indicator of the pavement cracking temperature and frequency of cracking in the five mixtures tested.

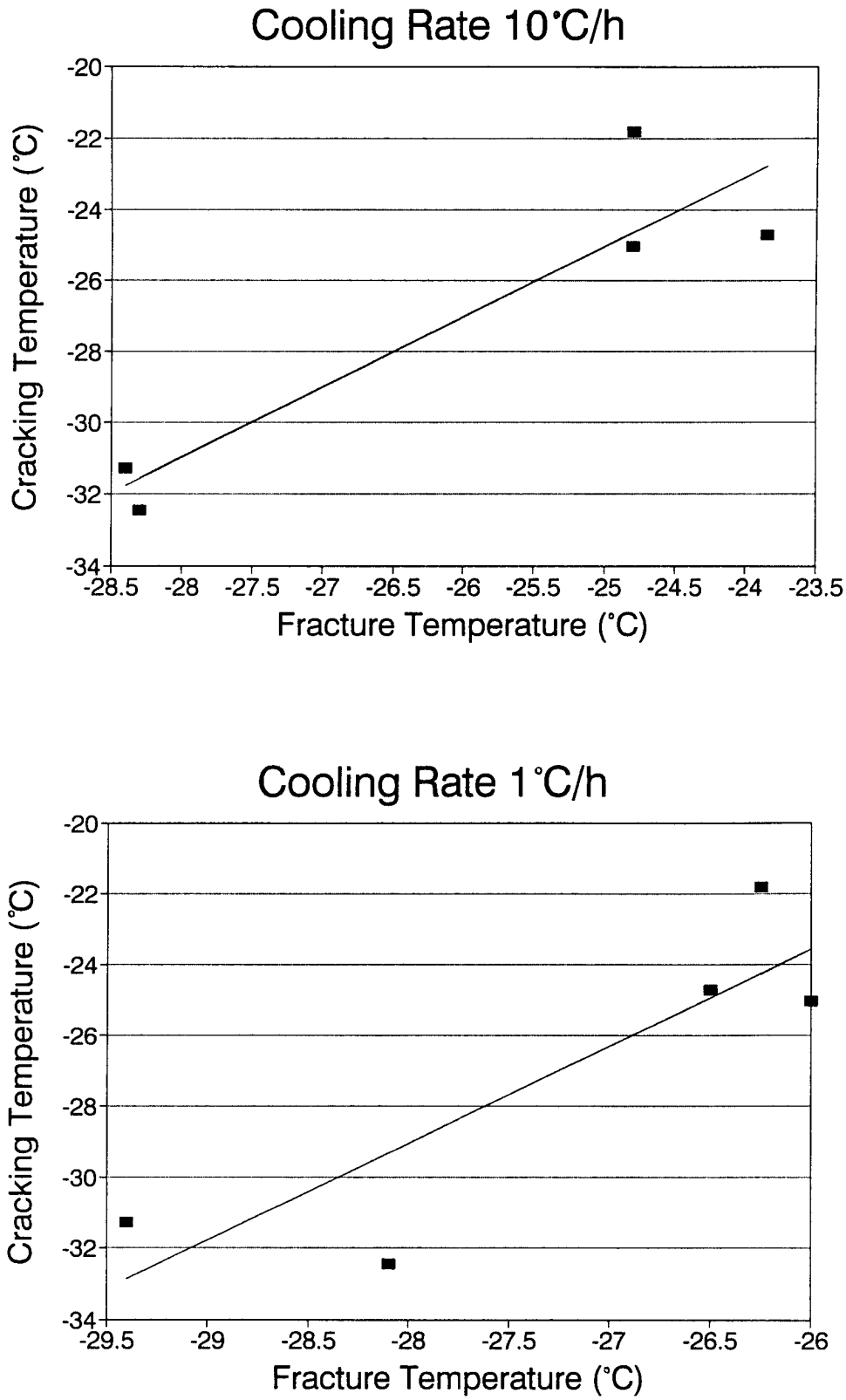

Figure 3.12. Cracking temperatures versus TSRST fracture temperatures for short-term USACRREL laboratory samples

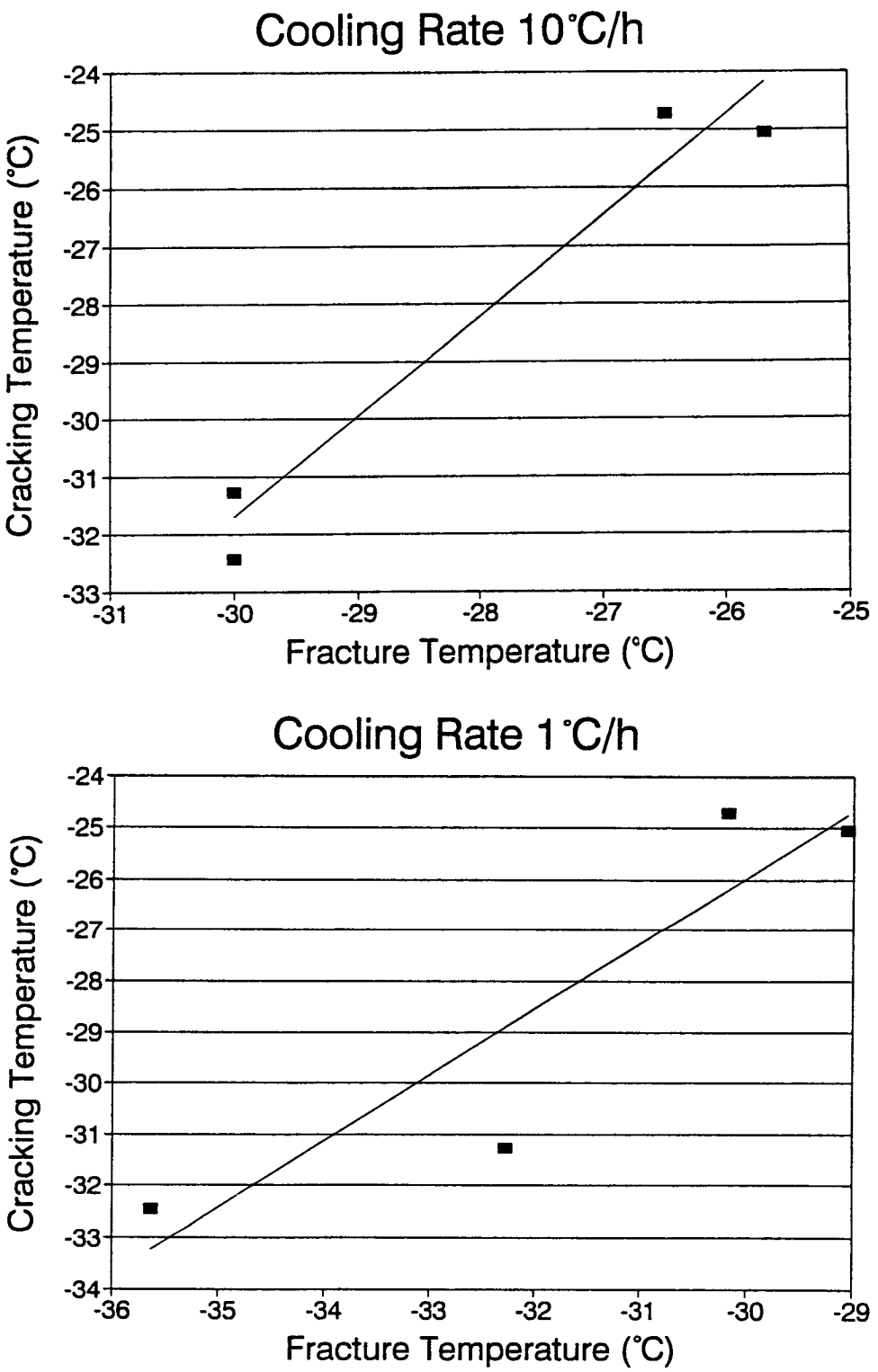

Figure 3.13. Cracking temperatures versus TSRST fracture temperatures for USACRREL field samples

Table 3.10. Results of regression analysis for USACRREL experiment

Aging	Cooling Rate (°C/h)	Origin	b_0	b_1	p-value	R^2 (%)	Stnd. Error of Est.
Unaged	10	Laboratory	37.16	2.36	0.018	88	1.80
Unaged	1	Laboratory	20.70	1.65	0.050	77	2.53
Short-term	10	Laboratory	24.20	1.97	0.026	85	2.04
Short-term	1	Laboratory	47.40	2.73	0.059	75	2.65
Unaged	10	Field	20.50	1.74	0.023	96	1.05
Unaged	1	Field	12.73	1.29	0.088	83	2.04

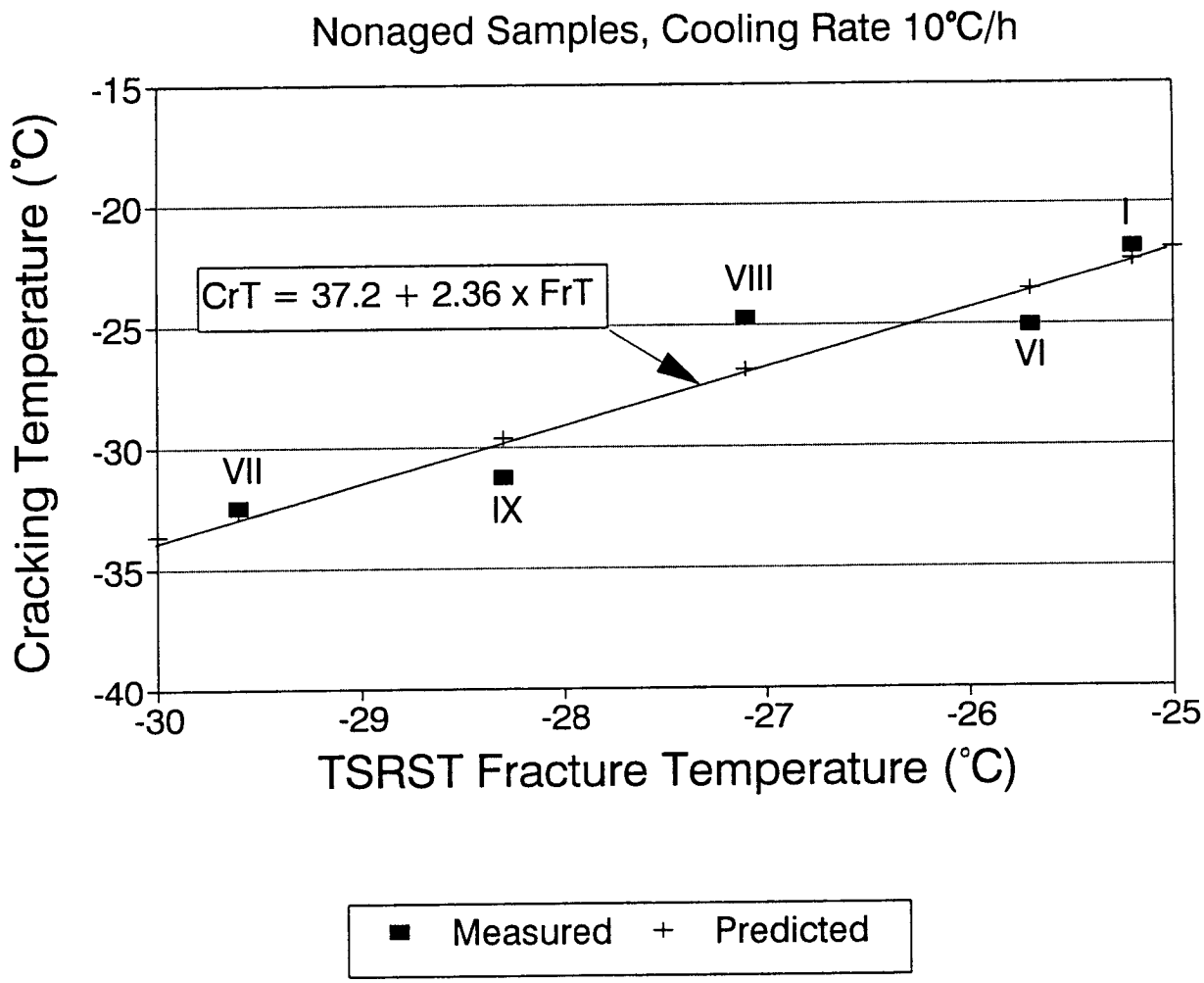

Figure 3.14. Predicted cracking temperatures for USACRREL test sections

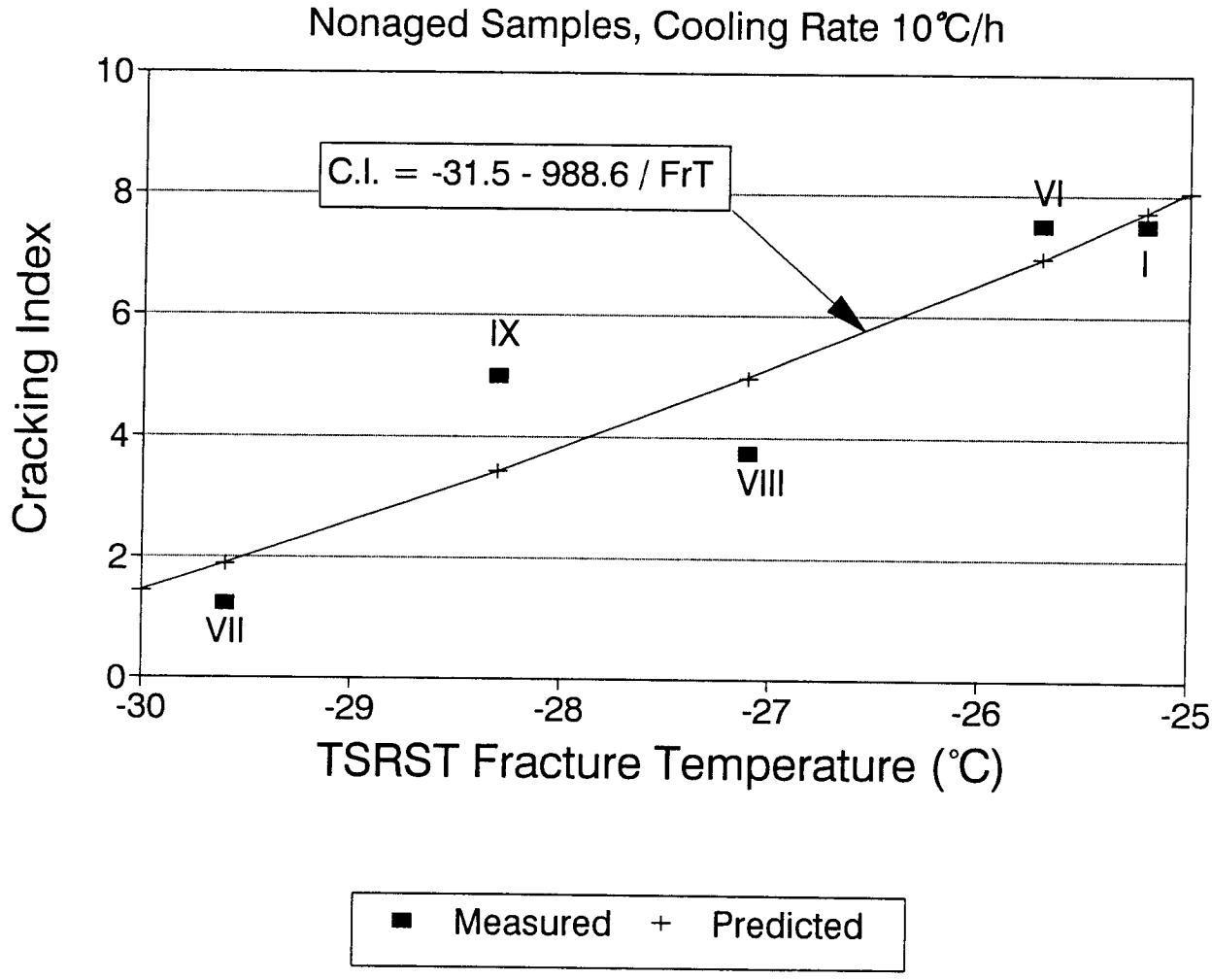

Figure 3.15. Predicted cracking index for USACRREL test sections

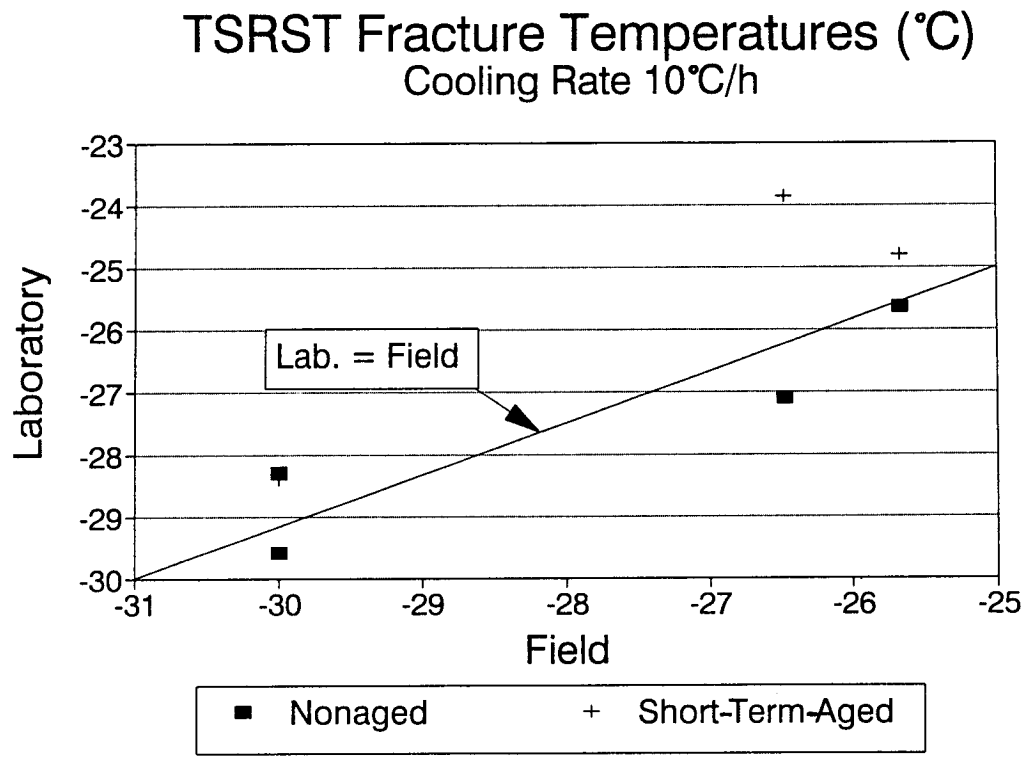

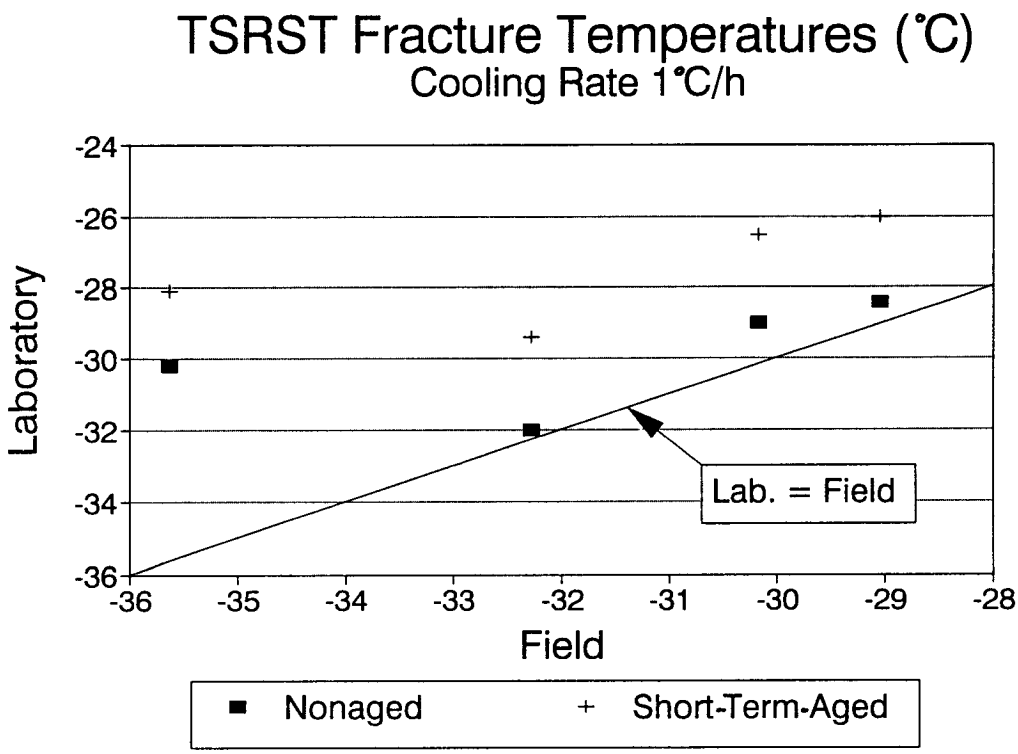

Figure 3.16. TSRST fracture temperatures of laboratory samples versus field samples for USACRREL test sections

4

Conclusions and Recommendations

4.1 Conclusions

Based on the data from the four test roads and USACRREL test sections, the following conclusions are appropriate:

- Cracking behavior of the test roads could be explained with TSRST fracture temperatures for Alaska, Pennsylvania, Peraseinajoki, and USACRREL. In Sodankyla, factors in addition to mixture properties affected low-temperature cracking. Hence, the TSRST can be used in the prediction of low-temperature cracking of asphalt-aggregate mixtures.

- Preliminary models to predict cracking frequency and temperature for the test roads were developed. This experience suggests that it is possible to develop a model that would predict the development of cracking in all climates.

4.2 Recommendations for Future Research

- A model to predict low-temperature cracking in all climates should be developed. In addition to TSRST fracture temperature, field aging, restraint conditions,and local temperature data should be used as input to the model.

- Additional research is necessary to validate the model. To accomplish the validation, full-scale test roads should be constructed and instrumented to measure pavement temperature and crack occurrence.

5

References

Arand, W. (1987). Influence of bitumen hardness on the fatigue behavior of asphalt pavements of different thickness due to bearing capacity of subbase, traffic loading, and temperature. *Proceedings,* 6th International Conference on Structural Behavior of Asphalt Pavements, University of Michigan.

Esch, D. C. (1990). Personal communication, October.

Esch, D. C. and D. Franklin (1989). Asphalt pavement crack control at Fairbanks International Airfield. *Proceedings*, 5th International Conference on Cold Regions Engineering, St. Paul, Minnesota.

Eaton, R. A. (1992). Frost effects research facility. FWHA Pavement Testing Workshop, University of Texas, Austin, Texas, July.

Fabb, T. R. J. (1974). The influence of mix composition, binder properties and cooling rate on asphalt cracking at low-temperature. *Proceedings,* Association of Asphalt Paving Technologists, Vol. 43.

Haas, R., F. Meyer, G. Assaf, and H. Lee (1987). A comprehensive study of cold climate airfield pavement cracking. *Proceedings,* Association of Asphalt Paving Technologists, Vol. 56.

Haas, R. C. and W. A. Phang (1990). Relationships between mix characteristics and low-temperature pavement cracking. *Proceedings,* Association of Asphalt Paving Technologists, Vol. 59.

Hills, J. F. and D. Brien (1966). The fracture of bitumens and asphalt mixes by temperature induced stresses. *Proceedings,* Association of Asphalt Paving Technologists, Vol. 35.

Janoo, V. C. (1989). Use of low viscosity asphalts in cold regions. *Proceedings,* 5th International Conference on Cold Regions Engineering, ASCE, St. Paul, Minnesota.

Jung, D. H., and T. S. Vinson (1992). Statistical analysis of low-temperature thermal stress restrained specimen test results. *Proceedings,* Canadian Technical Asphalt Association.

Kandhal, P. S., D. B. Mellott, and H. R. Basso, Jr. (1984). Durability study of viscosity graded AC-20 asphalts in Pennsylvania. Pennsylvania DOT, April.

Kanerva, H. K. and T. Nurmi (1991). Effects of asphalt properties on low-temperature cracking of asphalt pavements. *Proceedings,* ASTO Conference, Espo, Finland.

Kanerva, H. K., et al. (1992). Low-temperature cracking experiment at USACRREL frost effects research facility. Canadian Technical Asphalt Association Annual Conference, Victoria, British Columbia.

Kleemola, M. (1990). Personal communication, October.

Kurki, T. (1991). Personal communication, December.

Määttä, K., and S. Jussila (1990). Personal communication, July.

McLeod, N. W. (1972). A four year survey of low-temperature transverse pavement cracking on three Ontario test roads. *Proceedings,* Association of Asphalt Paving Technologists, Vol. 41, pp 424-493.

McLeod, N. W. (1987). Pen-Vis Number (PVN) as a measure of paving asphalt temperature susceptibility and its application to pavement design. *Proceedings,* Paving in Cold Areas Mining Workshop, Vol. 1, pp 147-240.

Monismith, C. L., G. A. Secor, and K. E. Secor (1965). Temperature induced stresses and deformations in asphalt concrete. *Proceedings,* Association of Asphalt Paving Technologists, Vol. 34, pp 248-285.

Saarela, A. (1991). ASTO test roads. VTT, Espoo, Finland, September.

Scheaffer, R. L. and J. T. McClave (1990). Probability and statistics for engineers, third edition. PWS Kent, Boston.

Appendix A
Mix Designs and Compositions for the Test Roads

ALASKA (Esch, 1990)

23rd Avenue and Peger Road

Target Mix Composition:

Sieve Size	Passing (%)
1" (25 mm)	
3/4" (19.0 mm)	100
3/8" (9.5 mm)	77
#4 (4.75 mm)	51
#10 (2.0 mm)	37
#40 (0.425 mm)	25
#200 (0.075 mm)	6

Asphalt Content (by wt of mix): 5.4 %

Actual Mix Composition:

Sieve Size	Passing (%)
1" (25 mm)	
3/4" (19.0 mm)	100
3/8" (9.5 mm)	72
#4 (4.75 mm)	47
#10 (2.0 mm)	35
#40 (0.425 mm)	25
#200 (0.075 mm)	8

Asphalt Content (by wt of mix): 5.0 %

Marshall Design Data:

23rd Avenue:

Optim. Unit Wt (lb/ft3)	150.8
Voids Filled (%)	88
Air Voids (%)	2
Stability (lbs)	1920
Flow	9.6

Peger Road:

Optim. Unit Wt (lb/ft3)	151.3
Voids Filled (%)	88
Air Voids (%)	2
Stability (lbs)	2450
Flow	11.0

PENNSYLVANIA (Kandhal, 1984)

Mix Composition

Sieve Size	Passing (%)
1/2" (12.7 mm)	100
3/8" (9.5 mm)	93
#4 (4.75 mm)	62
#8 (2.36 mm)	45
#16 (1.18 mm)	33
#30 (0.60 mm)	22
#50 (0.30 mm)	12
#100 (0.150 mm)	9
#200 (0.075 mm)	5

Asphalt Content (by wt of mix): 7.5 %

Marshall Design Data:

Theor. Max. Spec.Gr.	2.326
Specimen Spec.Gr.	2.278
VMA (%)	18.8
Air Voids (%)	2.1
Stability (lbs)	2075
Flow	13.3

PERASEINAJOKI (Kleemola 1990)

Mix Composition

Sieve Size	Passing (%)
3/4" (19.5mm)	96
1/2" (12.7mm)	75
3/8" (9.5mm)	62
#4 (4.75mm)	45
#8 (2.36mm)	33
#16 (1.18mm)	24
#30 (0.600mm)	20
#50 (0.300mm)	16
#200 (0.075mm)	10
Lime %	5

Asphalt Content by Weight of Mix:

BIT120AH	5.6%
BIT120ECO	5.6%
BIT65AH	5.7%
BIT80AH	5.7%
BIT200AH	5.6%
PmB1	5.8%

SODANKYLA (Määttä and Jussila 1990)

Mix Composition

Sieve Size	Passing (%)
3/4" (19.5mm)	100
1/2" (12.7mm)	82
3/8" (9.5mm)	69.5
#4 (4.75mm)	50.3
#8 (2.36mm)	37.5
#16 (1.18mm)	27.5
#30 (0.600mm)	20
#50 (0.300mm)	14.5
#200 (0.075mm)	9.2
Lime %	6

Asphalt Content by Weight of Mix:

BIT120AH	5.5%
B120LD	5.5%
BIT120ECO	5.5%
BIT120ARC	5.4%
BIT65AH	5.7%
BIT80AH	5.7%
BIT200AH	5.6%
PmB1	5.4%
BIT150AH	5.5%

USACRREL (Kanerva et al. 1992)

Target Mix Composition:

Sieve Size	Passing (%)
1" (25.0 mm)	100
3/4" (19.0 mm)	99
1/2" (12.7 mm)	82
3/8" (9.5 mm)	68
#4 (4.75 mm)	50
#8 (2.36 mm)	39
#16 (1.18 mm)	28
#30 (0.60 mm)	20
#50 (0.30 mm)	11
#200 (0.075 mm)	3.5

Asphalt Content (by wt of mix): 4.7 %

Marshall Design Data:

Theor. Max. Spec.Gr	2.601
VMA (%)	15.2
Air Voids (%)	4
Stability (lbs)	22660
Flow	10

Actual Mix Composition:

Sections I to V:

Sieve Size	Passing (%)
1" (25.0 mm)	100
3/4" (19.0 mm)	99.7
1/2" (12.7 mm)	83.1
3/8" (9.5 mm)	70.7
#4 (4.75 mm)	50.3
#8 (2.36 mm)	37.3
#16 (1.18 mm)	27.6
#30 (0.60 mm)	18.8
#50 (0.30 mm)	9.5
#200 (0.075 mm)	3.2

Asphalt Content (by wt of mix): 5.2 %

Sections VI to IX:

Sieve Size	Passing (%)
1" (25.0 mm)	100
3/4" (19.0 mm)	99.6
1/2" (12.7 mm)	82.7
3/8" (9.5 mm)	64.6
#4 (4.75 mm)	47.1
#8 (2.36 mm)	33.8
#16 (1.18 mm)	22.3
#30 (0.60 mm)	14
#50 (0.30 mm)	7.5
#200 (0.075 mm)	3.1

Asphalt Content (by wt of mix): 5.3 %

Appendix B
Mixing and Compaction Information for Laboratory Samples

ALASKA

MIXING DATA	For	AK1L1-8			
	Weight (g)		TEMPERATURE (C)		
DATE	Aggregate	Asphalt	Before	After	TARGET
9/11/91	8400	420	132	133	120-126

COMPACTION DATA			DATE:	4/3/92	
LAYER 1	PSI	75	100	150	TEMP.
	PASSES	4	12	16	
LAYER 2	PSI	75	150	325	
	PASSES	4	18	28	
LEVEL					
LOAD					

RICE Specific Gravity		
	1-4	4-7
WT.SAMPLE	1246	1242.9
WT.SAMPLE +H2O	6960.7	6953.7
RICE	2.491	2.465

Specimen I.D.	AIR	AIRP	H20P	H20	SSD	GmbSSD	GmbPAR	VSSD	VPAR
AK1L1	1649.6	1654.2	966.4	978.2	1652.6	2.446	2.416	1.79	2.98
AK1L2	1706.3	1711.0	998.7	1009.1	1706.9	2.445	2.413	1.82	3.11
AK1L3	1596.1	1601.1	932.6	941.9	1596.3	2.439	2.408	2.07	3.33
AK1L4	1593.7	1598.5	930.3	939.8	1594.7	2.434	2.404	2.29	3.46
AK1L5	1665.1	1670.3	976.3	987.5	1666.4	2.453	2.419	0.51	1.85
AK1L6	1649.8	1654.8	974.3	983.7	1650.6	2.474	2.444	-0.35	0.84
AK1L7	1665.1	1670.9	974.8	983.6	1665.7	2.441	2.414	0.97	2.06
AK1L8	1635.2	1639.9	960.8	969.5	1635.8	2.454	2.427	0.44	1.56

ALASKA

MIXING DATA	For	AK2L1-8			
	Weight (g)		TEMPERATURE (C)		
DATE	Aggregate	Asphalt	Before	After	TARGET
9/11/91	5573	280	132	125	120-126

COMPACTION DATA			DATE: 4/3/92		
LAYER 1	PSI	75	100	150	TEMP.
	PASSES	4	12	16	
LAYER 2	PSI	75	150	325	
	PASSES	4	18	28	
LEVEL LOAD					

RICE Specific Gravity		
	1-4	4-7
WT.SAMPLE	1247.2	1244.1
WT.SAMPLE +H2O	6964.5	6959.6
RICE	2.506	2.491

Specimen I.D.	AIR	AIRP	H20P	H20	SSD	GmbSSD	GmbPAR	VSSD	VPAR
AK2L1	1600.3	1605.3	939.8	945.9	1600.5	2.445	2.425	2.44	3.23
AK2L2	1626.3	1631.3	956.7	963.4	1626.5	2.453	2.431	2.13	3.00
AK2L3	1688.0	1693.9	997.2	1004.0	1688.3	2.467	2.446	1.56	2.40
AK2L4	1634.6	1639.0	962.6	969.1	1634.9	2.455	2.434	2.03	2.86
AK2L5	1651.4	1656.1	968.3	979.0	1654.7	2.444	2.419	1.88	2.86
AK2L6	1608.5	1613.2	942.5	951.1	1609.6	2.443	2.417	1.93	2.96
AK2L7	1606.3	1610.9	943.3	949.1	1606.9	2.442	2.425	1.96	2.65
AK2L8	1623.9	1627.9	953.3	958.1	1624.2	2.438	2.423	2.12	2.71

PENNSYLVANIA

MIXING DATA For PA1L1-2					
	Weight (g)		Temperature (C)		
DATE	Aggregate	Asphalt	Before	After	TARGET
9/13/91	8400	630	153	142	

COMPACTION DATA			DATE: 4/3/92		
LAYER	PSI	75	150	250	TEMP.
	PASSES	2	7	9	
LAYER	PSI	75	175	350	
	PASSES	4	16	26	
LEVEL LOAD					

RICE Specific Gravity	
WT.SAMPLE	1279.1
WT.SAMPLE +H2O	6941.1
RICE	2.313

Specimen I.D.	AIR	AIRP	H20P	H20	SSD	GmbSSD	GmbPA	VSSD	VPAR
PA1L1	1497.0	1502.0	839.6	847.8	1498.2	2.302	2.279	0.48	1.47
PA1L2	1478.3	1483.6	827.6	833.7	1479.6	2.289	2.274	1.04	1.69

PENNSYLVANIA

MIXING DATA For PA2L1-4					
	Weight (g)		Temperature (C)		
DATE	Aggregate	Asphalt	Before	After	TARGET
9/16/91	8400	630	153	150	

COMPACTION DATA			DATE: 9/16/91		
LAYER	PSI	75	150	250	TEMP.
	PASSES	2	7	9	
LAYER	PSI	75	175	350	
	PASSES	4	16	26	
LEVEL LOAD					

RICE Specific Gravity	
WT.SAMPLE	1248
WT.SAMPLE +H2O	6925.3
RICE	2.321

Specimen I.D.	AIR	AIRP	H20P	H20	SSD	GmbSSD	GmbPA	VSSD	VPAR
PA2L1	1574.4	1576.0	891.0	896.0	1575.0	2.319	2.304	0.10	0.72
PA2L2	1578.0	1580.0	899.0	903.0	1579.0	2.334	2.325	-0.57	-0.16
PA2L3	1580.3	1581.0	896.0	900.0	1581.0	2.321	2.310	0.02	0.49
PA2L4	1598.4	1600.0	910.0	915.0	1599.0	2.337	2.323	-0.68	-0.07

PENNSYLVANIA

MIXING DATA	For	PA3L1-4			
	Weight (g)		Temperature (C)		
DATE	Aggregate	Asphalt	Before	After	TARGET
9/16/91	8400	630	153	150	

COMPACTION DATA		DATE:	9/16/91		
LAYER	PSI	75	150	250	TEMP.
	PASSES	2	7	9	
LAYER	PSI	75	175	350	
	PASSES	4	16	26	
LEVEL LOAD					

RICE Specific Gravity	
WT.SAMPLE	1246.4
WT.SAMPLE +H2O	6925
RICE	2.324

Specimen I.D.	AIR	AIRP	H20P	H20	SSD	GmbSSD	GmbPA	VSSD	VPAR
PA3L1	1520.7	1523.0	860.0	864.0	1521.0	2.315	2.303	0.39	0.91
PA3L2	1520.4	1522.0	853.0	858.0	1521.0	2.000	2.279	13.93	1.93
PA3L3	1539.0	1541.0	870.0	877.0	1539.0	2.325	2.301	-0.05	0.97
PA3L4	1523.3	1525.0	857.0	860.0	1524.0	2.294	2.287	1.27	1.58

PENNSYLVANIA

MIXING DATA For PA4L1-4					
	Weight (g)		Temperature (C)		
DATE	Aggregate	Asphalt	Before	After	TARGET
9/12/91	8400	630	150	138	

COMPACTION DATA			DATE: 9/16/91		
LAYER	PSI	75	150	250	TEMP.
	PASSES	2	7	9	
LAYER	PSI	75	175	350	
	PASSES	4	16	26	
LEVEL LOAD					

RICE Specific Gravity	
WT.SAMPLE	1243.4
WT.SAMPLE +H2O	6923.1
RICE	2.323

Specimen I.D.	AIR	AIRP	H20P	H20	SSD	GmbSSD	GmbPA	VSSD	VPAR
PA4L1	1525.0	1527.0	856.0	861.0	1526.0	2.293	2.280	1.27	1.83
PA4L2	1362.2	1365.0	764.0	768.0	1362.0	2.293	2.278	1.27	1.91
PA4L3	1505.6	1507.0	844.0	849.0	1506.0	2.292	2.276	1.34	2.01
PA4L4	1540.6	1543.0	868.0	872.0	1541.0	2.303	2.291	0.86	1.35

PENNSYLVANIA

MIXING DATA For PA5L1-4					
	Weight (g)		Temperature (C)		
DATE	Aggregate	Asphalt	Before	After	TARGET
9/12/91	8400	630	150	139	

COMPACTION DATA			DATE: 9/16/91		
LAYER	PSI	75	150	250	TEMP.
	PASSES	2	7	9	
LAYER	PSI	75	175	350	
	PASSES	4	16	26	
LEVEL LOAD					

RICE Specific Gravity	
WT.SAMPLE	1248.6
WT.SAMPLE +H2O	6929.6
RICE	2.338

Specimen I.D.	AIR	AIRP	H20P	H20	SSD	GmbSSD	GmbPA	VSSD	VPAR
PA5L1	1524.1	1526.0	848.0	854.0	1524.0	2.275	2.255	2.71	3.56
PA5L2	1543.3	1545.0	870.0	875.0	1544.0	2.307	2.293	1.34	1.94
PA5L3	1522.3	1554.0	866.0	871.0	1554.0	2.229	2.332	4.68	0.26
PA5L4	1537.6	1540.0	868.0	872.0	1538.0	2.309	2.297	1.26	1.75

PENNSYLVANIA

MIXING DATA For PA6L1-4					
	Weight (g)		Temperature (C)		
DATE	Aggregate	Asphalt	Before	After	TARGET
9/13/91	8400	630	153	149	

COMPACTION DATA			DATE: 9/16/91		
LAYER	PSI	75	150	250	TEMP.
	PASSES	2	7	9	
LAYER	PSI	75	175	350	
	PASSES	4	16	26	
LEVEL LOAD					

RICE Specific Gravity	
WT.SAMPLE	1244.7
WT.SAMPLE +H2O	6923
RICE	2.319

Specimen I.D.	AIR	AIRP	H20P	H20	SSD	GmbSSD	GmbPA	VSSD	VPAR
PA6L1	1559.7	1561.0	883.0	888.0	1560.0	2.321	2.305	-0.08	0.60
PA6L2	1571.8	1573.0	888.0	894.0	1572.0	2.318	2.299	0.04	0.87
PA6L3	1592.6	1598.0	898.0	906.0	1594.0	2.315	2.295	0.19	1.05
PA6L4	1583.6	1585.0	897.0	901.0	1585.0	2.315	2.307	0.17	0.53

USACRREL

MIXING DATA For CR1L1-4					
	Weight (g)		TEMPERATURE (C)		
DATE	Aggregate	Asphalt	Before	After	TARGET
4/3/92	9175	504	155	145	150-155
4/3/92	9175	504	155	148	

COMPACTION DATA			DATE: 4/3/92		
LAYER	PSI	75	125	200	TEMP.
	PASSES	4	4	6	140-144
LAYER	PSI	75	200	325	
	PASSES	4	8	10	
LEVEL LOAD	40,000 lbs applied after compaction.				

RICE Specific Gravity	
Date	4/3/92
WT.SAMPLE	1113
WT.SAMPLE +H2O	6900
RICE	2.600

Specimen I.D.	AIR	AIRP	H20P	H20	SSD	GmbSSD	GmbPA	VSSD	VPAR
CR1L1	1612.7	1615.3	965.4	968.3	1613.3	2.5	2.5	3.9	4.2
CR1L2	1645.2	1647.4	997.8	1002.2	1646.1	2.6	2.5	1.7	2.2
CR1L3	1619.2	1621.7	972.0	975.7	1619.7	2.5	2.5	3.3	3.8
CR1L4	1638.5	1640.8	993.6	998.1	1639.1	2.6	2.5	1.7	2.3

USACRREL

MIXING DATA For CR1L5-8					
AGING	MIX @ 135 for 4 hrs.				
	Weight (g)		TEMPERATURE (C)		
DATE	Aggregate	Asphalt	Before	After	TARGET
5/16/92	9072	498	155	155	150-155
5/16/92	9072	498	155	151	

COMPACTION DATA			DATE	5/16/92	
LAYER	PSI	75	100	175	TEMP.
	PASSES	4	4	6	140-144
LAYER	PSI	75	150	250	
	PASSES	4	6	6	
LEVEL LOAD	12,000 lbs applied after compaction.				

RICE Specific Gravity	
Date	5/18/92
WT.SAMPLE	1113
WT.SAMPLE +H2O	6900
RICE	2.600

Specimen I.D.	AIR	AIRP	H20P	H20	SSD	GmbSSD	GmbPA	VSSD	VPAR
CR1L5	1603.1	1606.1	952.6	957.4	1604.3	2.48	2.47	4.7	5.2
CR1L6	1577.4	1580.8	928.3	933.2	1579.5	2.44	2.43	6.1	6.5
CR1L7	1598.1	1601.8	947.9	953.7	1599.8	2.47	2.46	4.9	5.4
CR1L8	1587.5	1591.2	936.9	943.6	1590.2	2.46	2.44	5.6	6.1

USACRREL

MIXING DATA For CR2L1-4					
	Weight (g)		Temperature (C)		
DATE	Aggregate	Asphalt	Before	After	TARGET
4/7/92	9107	509	158	152	153-158
4/7/92	9107	509	158	152	

COMPACTION DATA			DATE 4/7/92		
LAYER	PSI	75	125	200	TEMP.
	PASSES	4	4	8	144
LAYER	PSI	75	200	325	
	PASSES	4	8	10	
LEVEL LOAD	40,000 lbs applied after compaction.				

RICE Specific Gravity	
Date	4/9/92
WT.SAMPLE	1469.4
WT.SAMPLE +H2O	7116.5
RICE	2.587

Specimen I.D.	AIR	AIRP	H20P	H20	SSD	GmbSSD	GmbPA	VSSD	VPAR
CR2L1	1628	1630.3	983.4	986.6	1628.5	2.5	2.5	2.0	2.4
CR2L2	1647.9	1650.2	1005.1	1008.0	1648.8	2.6	2.6	0.6	0.9
CR2L3	1649.9	1652.3	1001.4	1005.0	1650.7	2.6	2.5	1.2	1.6
CR2L4	1635.3	1637.5	988.4	991.7	1635.8	2.5	2.5	1.9	2.3

USACRREL

MIXING DATA For CR2L5-8					
AGING	MIX @ 135 For 4 hrs.				
	Weight (g)		Temperature (C)		
DATE	Aggregate	Asphalt	Before	After	TARGET
5/16/92	9072	508	155	149	153-158
5/16/92	9072	508	155	150	

COMPACTION DATA		DATE	5/16/92		
LAYER	PSI	75	100	175	TEMP.
	PASSES	4	4	6	142-147
LAYER	PSI	75	150	250	
	PASSES	4	6	6	
LEVEL LOAD	12,000 lbs applied after compaction.				

RICE Specific Gravity	
Date	5/18/92
WT.SAMPLE	1469.4
WT.SAMPLE +H2O	7116.5
RICE	2.587

Specimen I.D.	AIR	AIRP	H20P	H20	SSD	GmbSSD	GmbPA	VSSD	VPAR
CR2L5	1608.2	1610.4	958.6	964.5	1610.3	2.49	2.48	3.8	4.3
CR2L6	1585.9	1588.0	935.9	941.3	1587.9	2.45	2.44	5.2	5.7
CR2L7	1628.3	1630.4	979.5	984.4	1629.6	2.52	2.51	2.5	3.0
CR2L8	1573.2	1575.3	924.7	931.4	1575.8	2.44	2.43	5.6	6.2

USACRREL

MIXING DATA For CR3L1-4					
	Weight (g)		Temperature (C)		
DATE	Aggregate	Asphalt	Before	After	TARGET
4/24/92	9080	508	1552	144	147-152
4/24/92	9080	508	152	143	

COMPACTION DATA			DATE 4/24/92		
LAYER	PSI	75	100	175	TEMP.
	PASSES	4	4	6	140
LAYER	PSI	75	150	275	
	PASSES	4	6	8	
LEVEL LOAD	12,000 lbs applied after compaction.				

RICE Specific Gravity	
Date	4/26/92
WT.SAMPLE	1401.9
WT.SAMPLE +H2O	7079.3
RICE	2.608

Specimen I.D.	AIR	AIRP	H20P	H20	SSD	GmbSSD	GmbPA	VSSD	VPAR
CR3L1	1582.1	1583.8	933.2	937.4	1583.1	2.5	2.4	6.0	6.5
CR3L2	1597.8	1599.4	950.3	954.6	1598.8	2.5	2.5	4.9	5.3
CR3L3	1628.3	1629.8	978.3	983.1	1629.3	2.5	2.5	3.4	3.9
CR3L4	1625.3	1626.9	977.7	981.2	1626.1	2.5	2.5	3.4	3.7

USACRREL

MIXING DATA	For	CR3L5-8			
AGING	MIX @ 135 for 4 hrs.				
	Weight (g)		TEMPERATURE (C)		
DATE	Aggregate	Asphalt	Before	After	TARGET
5/16/92	9072	508	150	148	148-152
5/16/92	9072	508	150	149	

COMPACTION DATA		DATE 5/16/92			
LAYER	PSI	75	100	175	TEMP.
	PASSES	4	4	6	138-142
LAYER	PSI	75	150	250	
	PASSES	4	6	6	
LEVEL LOAD	12,000 lbs applied after compaction.				

RICE Specific Gravity	
Date	5/18/92
WT.SAMPLE	1401.9
WT.SAMPLE +H2O	7079.3
RICE	2.608

Specimen I.D.	AIR	AIRP	H20P	H20	SSD	GmbSSD	GmbPA	VSSD	VPAR
CR3L5	1601.9	1604.1	954.1	959.1	1603.4	2.49	2.47	4.7	5.1
CR3L6	1573.7	1576.1	925.6	930.5	1574.7	2.44	2.43	6.3	6.9
CR3L7	1590.3	1592.8	943.3	948.1	1591.6	2.47	2.46	5.2	5.7
CR3L8	1626.2	1628.6	979.6	985.0	1627.2	2.53	2.52	2.9	3.5

USACRREL

MIXING DATA For CR4L1-4					
	Weight (g)		Temperature (C)		
DATE	Aggregate	Asphalt	Before	After	TARGET
5/16/92	9072	508	156	146	151-156
5/16/92	9072	508	156	145	

COMPACTION DATA			DATE 5/16/92		
LAYER	PSI	75	100	175	TEMP.
	PASSES	4	4	6	141-145
LAYER	PSI	75	150	250	
	PASSES	4	6	6	
LEVEL LOAD	12,000 lbs applied after compaction.				

RICE Specific Gravity	
Date	5/18/92
WT.SAMPLE	1469
WT.SAMPLE +H2O	7116.5
RICE	2.585

Specimen I.D.	AIR	AIRP	H20P	H20	SSD	GmbSSD	GmbPA	VSSD	VPAR
CR4L1	1599.8	1602.2	950.6	955	1600.9	2.48	2.47	4.2	4.6
CR4L2	1632.4	1635.2	981.2	985.7	1633.2	2.52	2.51	2.5	3.0
CR4L3	1607.8	1610.6	958.3	962.8	1608.7	2.49	2.48	3.7	4.2
CR4L4	1613.7	1616.4	966.9	970.5	1614.3	2.51	2.50	3.0	3.4

USACRREL

MIXING DATA	For	CR4L5-8			
AGING	MIX @ 135 for 4 hrs.				
	Weight (g)		Temperature (C)		
DATE	Aggregate	Asphalt	Before	After	TARGET
5/16/92	9072	508	155	149	151-156
5/16/92	9072	508	154	146	

COMPACTION DATA		DATE	5/16/92		
LAYER	PSI	75	100	175	TEMP.
	PASSES	4	4	6	141-145
LAYER	PSI	75	150	250	
	PASSES	4	6	6	
LEVEL LOAD	12,000 lbs applied after compaction.				

RICE Specific Gravity	
Date	5/16/92
WT.SAMPLE	1469
WT.SAMPLE +H2O	7116.5
RICE	2.589

Specimen I.D.	AIR	AIRP	H20P	H20	SSD	GmbSSD	GmbPA	VSSD	VPAR
CR4L5	1624.9	1627	973.3	977.9	1625.6	2.51	2.49	3.1	3.6
CR4L6	1632.0	1634.5	981.3	986.5	1633.0	2.52	2.51	2.5	3.1
CR4L7	1592.2	1594.4	942.9	946.9	1593.2	2.46	2.45	4.8	5.2
CR4L8	1601.8	1604.1	951.4	956.0	1602.8	2.48	2.46	4.3	4.8

USACRREL

MIXING DATA For CR5L1-4					
	Weight (g)		Temperature (C)		
DATE	Aggregate	Asphalt	Before	After	TARGET
7/13/92	9072	508	147	136	144-149
7/13/92	9072	508	147	134	

COMPACTION DATA			DATE	7/13/92	
LAYER	PSI	75	100	175	TEMP.
	PASSES	4	4	6	134-138
LAYER	PSI	75	150	250	
	PASSES	4	6	6	
LEVEL LOAD	12,000 lbs applied after compaction.				

RICE Specific Gravity	
Date	7/15/92
WT.SAMPLE	1467.2
WT.SAMPLE +H2O	7122.8
RICE	2.623

Specimen I.D.	AIR	AIRP	H20P	H20	SSD	GmbSSD	GmbPA	VSSD	VPAR
CR5L1	1567	1571	926.5	929.9	1567.6	2.46	2.45	6.3	6.7
CR5L2	1601.9	1606.3	960.4	965.3	1602.8	2.51	2.50	4.2	4.7
CR5L3	1579.7	1583.9	939.0	942.5	1580.5	2.48	2.47	5.6	5.9
CR5L4	1573.8	1578.0	936.8	942.4	1575.5	2.49	2.47	5.2	5.7

USACRREL

MIXING DATA For CR5L5-8					
AGING	MIX @ 135 for 4 hrs.				
	Weight (g)		Temperature (C)		
DATE	Aggregate	Asphalt	Before	After	TARGET
713/92	9072	508	147	136	144-149
7/13/92	9072	508	147	133	

COMPACTION DATA			DATE	7/13/92	
LAYER	PSI	75	100	175	TEMP.
	PASSES	4	4	6	134-138
LAYER	PSI	75	150	250	
	PASSES	4	6	6	
LEVEL LOAD	12,000 lbs applied after compaction.				

RICE Specific Gravity	
Date	7/15/92
WT.SAMPLE	1467.2
WT.SAMPLE +H2O	7122.8
RICE	2.623

Specimen I.D.	AIR	AIRP	H20P	H20	SSD	GmbSSD	GmbPA	VSSD	VPAR
CR5L5	1606.8	1611	959.9	970.7	1611.1	2.51	2.49	4.3	5.2
CR5L6	1594.5	1598.7	947.4	953.7	1596.8	2.48	2.47	5.5	6.0
CR5L7	1562.9	1567.2	917.8	922.4	1564.1	2.44	2.42	7.1	7.6
CR5L8	1584.2	1588.4	939.6	944.4	1586.0	2.47	2.46	5.9	6.2

Appendix C
Specific Gravities and Void Contents for Field Samples

ALASKA

RICE Specific Gravity			
Date 23 JULY 9	SLAB 1A	SLAB 2B	SLAB 3B
Layer Thickness (in.)	2.25	1.75	4
Weight	1569	919	2052
Weight in H20	7144	6758	7424
RICE	2.452	2.444	2.434
	AVERAGE		2.443

Specimen	Area (in.2)	AIR	AIRP	H20P	H20	SSD	GmbSSD	GmbPAR	VSSD	VPAR
AK1F1	4.53	1719.1	1723.3	987.3	996.4	1720.5	2.4	2.4	3.2	4.1
AK1F2	4.10	1567.2	1571.5	893.9	903.2	1569.6	2.4	2.3	4.1	5.0
AK1F3	2.33	887.5	891.7	507.3	513.3	888.5	2.4	2.3	3.2	4.4
AK1F4	2.40	899.6	903.9	505.7	515.1	902.7	2.3	2.3	5.0	6.4
AK1F5	5.42	1569.6	1574.0	900.6	909.0	1570.1	2.4	2.3	2.5	3.5
AK1F6	4.22	1625.4	1629.6	937.3	942.9	1625.7	2.4	2.4	2.2	2.9
AK1F7	3.98	1534.3	1538.2	887.2	890.0	1534.8	2.4	2.4	2.2	2.5
AK1F8	3.98	1522.9	1526.7	878.0	881.2	1523.6	2.4	2.4	2.6	2.9
AK1F9	3.76	1456.9	1461.1	843.7	850.0	1457.1	2.4	2.4	1.4	2.3
AK1F10	4.04	1586.6	1590.7	918.9	925.8	1586.9	2.4	2.4	1.4	2.3
AK1F11	3.98	1531.0	1534.9	886.4	889.8	1531.6	2.4	2.4	2.0	2.4
AK1F12	3.98	1527.5	1531.3	881.3	885.0	1528.1	2.4	2.4	2.4	2.8

SODANKYLA, FINLAND

RICE Specific Gravity			
Date 6 JULY 92	TRIAL 1	TRIAL 2	TRIAL 3
Weight	1346	894	837
Weight in H20	7023	6749	6717
RICE	2.502	2.483	2.499
		AVE	2.495

Specimen	AIR	AIRP	H20P	H20	SSD	GmbSSD	GmbPA	VSSD	VPAR
FS1F1	1659.6	1661.6	983.1	992	1660.4	2.5	2.5	0.5	1.6
FS1F2	1686.3	1688.6	999.8	1008.7	1687.4	2.5	2.5	0.4	1.5
FS1F5	1647.4	1649.2	978.6	986.1	1648.1	2.5	2.5	0.2	1.2
FS1F6	1607.3	1612.8	952.3	961.8	1607.8	2.5	2.5	0.3	1.5
FS2F1	1674.5	1677.0	994.9	1001.4	1675.1	2.5	2.5	0.4	1.2
FS2F2	1668.3	1670.1	993.3	999.4	1669.3	2.5	2.5	0.2	0.9
FS2F5	1617.3	1618.4	957.3	965.8	1618.0	2.5	2.5	0.6	1.8
FS2F6	1514.7	1520.3	898.1	905.3	1515.5	2.5	2.5	0.5	1.4
FS3F1	1553.5	1555.6	922.3	930.0	1554.2	2.5	2.5	0.2	1.3
FS3F2	1622.8	1624.5	964.1	970.4	1623.4	2.5	2.5	0.4	1.2
FS3F5	1638.6	1640.5	971.1	979.1	1639.6	2.5	2.5	0.5	1.6
FS3F6	1548.1	1553.5	917.7	925.8	1548.8	2.5	2.5	0.4	1.5
FS4F1									
FS4F2									
FS4F5									
FS4F6	1719.0	1724.7	1022.1	1027.8	1719.7	2.5	2.5	0.4	1.0
FS5F1	1621.7	1624.3	961.2	967.4	1622.5	2.5	2.5	0.8	1.5
FS5F2	1618.3	1620.6	957.1	964.1	1619.1	2.5	2.4	1.0	1.8
FS5F5	1639.2	1641.5	970.9	977.6	1640.1	2.5	2.5	0.8	1.6
FS5F6	1545.6	1552.9	910.5	922.4	1546.5	2.5	2.4	0.7	2.3
FS6F1	1639.5	1642.0	972.9	981.9	1640.3	2.5	2.5	0.2	1.4

SODANKYLA, FINLAND

RICE Specific Gravity			
Date 6 JULY 92	TRIAL 1	TRIAL 2	TRIAL 3
Weight	1346	894	837
Weight in H20	7023	6749	6717
RICE	2.502	2.483	2.499
		AVE	2.495

Specimen	AIR	AIRP	H20P	H20	SSD	GmbSSD	GmbPA	VSSD	VPAR
FS6F2	1670.2	1672.3	989.7	998.5	1671.4	2.5	2.5	0.5	1.6
FS6F5	1666.6	1668.4	990.1	997.8	1667.4	2.5	2.5	0.2	1.2
FS6F6	1655.5	1661.1	978.1	990.1	1656.2	2.5	2.4	0.4	1.9
FS7F1	1611.6	1613.4	954.2	961.4	1612.1	2.5	2.5	0.7	1.7
FS7F2	1622.2	1624.3	957.1	964.8	1622.9	2.5	2.4	1.2	2.2
FS7F5	1664.9	1666.9	988.6	994.8	1666.1	2.5	2.5	0.6	1.3
FS7F6	1638.8	1644.3	972.0	980.4	1639.6	2.5	2.5	0.3	1.4
FS8F1	1648.9	1653.6	969.1	981.5	1649.8	2.5	2.4	1.1	2.7
FS8F2	1621.5	1624.5	960.2	967.5	1622.4	2.5	2.5	0.7	1.7
FS8F5	1664.2	1667.1	987.2	993.8	1665.1	2.5	2.5	0.6	1.4
FS8F6	1570.8	1576.3	929.2	935.4	1571.6	2.5	2.5	1.0	1.8
FS9F1	1675.4	1677.7	995.5	1003.1	1676.2	2.5	2.5	0.2	1.2
FS9F2	1656.6	1659.2	984.1	992.2	1657.2	2.5	2.5	0.1	1.2
FS9F5	1669.0	1671.4	988.9	997.9	1669.6	2.5	2.5	0.4	1.6
FS9F6	1526.2	1531.8	905.3	912.6	1526.7	2.5	2.5	0.4	1.4

RICE Specific Gravity	Section + Station (ft)					
Date 11 Feb. 92	VII + 0	VII + 60	IX + 30	VII + 0	VI + 30	VIII+60
Weight	1112.2	1524.5	1478.5	1401.9	1469.4	1429.7
Weight in H20	6899.5	7158.6	7139.2	7079.3	7116.5	7091.6
RICE	2.600	2.624	2.667	2.608	2.587	2.585
		AVE	2.612			

Specimen	AIR	AIRP	H20P	H20	SSD	GmbSSD	GmbPA	VSSD	VPAR
CR2F4	686.0	687.7	396.3	399.4	687.2	2.38	2.37	7.9	8.4
CR2F3	680.5	682.6	391.9	396.7	682.1	2.38	2.36	7.8	8.8
CR2F1	698.5	700.5	412.9	414.7	699.1	2.46	2.45	5.1	5.4
CR2F2	692.9	694.8	409.7	412.2	693.8	2.46	2.45	4.9	5.4
CR2F5	702.2	704.1	416.6	419.2	702.4	2.48	2.46	4.2	4.9
CR2F6	707	709.2	422.9	425.3	707.8	2.50	2.49	3.3	3.7
CR2F7									
CR2F8									
CR3F1	716.5	720.4	426.3	429.5	716.8	2.49	2.47	3.6	4.4
CR3F2	712.4	716.3	422.9	426.0	712.6	2.49	2.46	3.9	4.8
CR3F3	708.7	712.6	419.0	423.5	709.8	2.48	2.45	4.3	5.3
CR3F4	707.9	711.7	418.7	422.6	708.4	2.48	2.45	4.3	5.3
CR3F5	708.4	712.1	420.5	432.9	708.6	2.57	2.46	0.7	4.8
CR3F6	708.7	710.7	420.7	423.3	708.9	2.48	2.46	4.1	4.8
CR3F7	698.5	700.6	411.8	413.3	699.0	2.44	2.44	5.5	5.8
CR3F8									
CR4F1	710.0	713.8	419.2	422.5	710.2	2.47	2.45	4.6	5.5
CR4F2	709.9	713.6	420.6	423.1	710.1	2.47	2.46	4.4	5.0
CR4F3	695.3	697.5	408.2	411.3	696.1	2.44	2.42	5.6	6.3
CR4F4	698.6	700.8	412.8	414.6	699.8	2.45	2.45	5.3	5.4
CR4F5									

USACRREL

RICE Specific Gravity	Section + Station (ft)					
Date 11 Feb. 92	VII + 0	VII + 60	IX + 30	VII + 0	VI + 30	VIII+60
Weight	1112.2	1524.5	1478.5	1401.9	1469.4	1429.7
Weight in H20	6899.5	7158.6	7139.2	7079.3	7116.5	7091.6
RICE	2.600	2.624	2.667	2.608	2.587	2.585
		AVE	2.612			

Specimen	AIR	AIRP	H20P	H20	SSD	GmbSSD	GmbPA	VSSD	VPAR
CR4F6									
CR4F7	711.1	713.1	423.2	425.2	711.3	2.49	2.47	3.9	4.5
CR4F8	704.3	706.4	420.4	422.1	704.5	2.49	2.48	3.6	4.0
CR5F1	707.7	711.6	419.0	423.9	709.6	2.48	2.46	4.3	5.1
CR5F2	695.2	698.9	407.8	413.1	697.2	2.45	2.42	5.4	6.4
CR5F3	682.6	684.7	403.0	406.0	683.6	2.46	2.44	5.0	5.6
CR5F4	693.0	695.1	413.0	414.8	693.3	2.49	2.48	3.8	4.3
CR5F5									
CR5F6	709.6	713.4	418.8	422.7	710.0	2.47	2.44	4.5	5.6
CR5F7	693.7	695.9	413.0	414.6	694.1	2.48	2.47	4.1	4.4
CR5F8	697.1	699.1	414.2	416.5	697.3	2.48	2.47	4.1	4.7

Appendix D
TSRST Results for Each Sample

Specimen I.D.	Asphalt Cement	Voids (VPAR) (%)	Cylinder=1 Beam=0	Laborat.=1 Field=0	Cooling Rate (C/h)	Aging None=N Short=S Long=L	Device A,B,C	Fracture Stress (psi)	Fracture Stress (kPa)	Fracture Temperature (F)	Fracture Temperature (C)	Location
AK1F1	AC-5	4.1	0	0	1.1	N	A	496.1	3420.6	-17.9	-27.7	1A
AK1F2	AC-5	5.0	0	0	1.6	N	C	298.1	2055.4	-14.3	-25.7	1B
AK1F3	AC-5	4.4	0	0	1.5	N	B	457.3	3153.1	-20.9	-29.4	2A
AK1F4	AC-5	6.4	0	0	1.1	N	A	484.6	3341.3	-20.7	-29.3	2B
AK1F5	AC-5	3.5	0	0	1.5	N	C	488.8	3370.3	-19.5	-28.6	3A trans.
AK1F6	AC-5	2.9	0	0	1.4	N	B	416.1	2869.0	-14.1	-25.6	3A trans.
AK1F7	AC-5	2.5	1	0	1.5	N	B	484.1	3337.9	-17.7	-27.6	3A trans.
AK1F8	AC-5	2.9	1	0	1.5	N	C	427.5	2947.6	-16.4	-26.9	3A trans.
AK1F9	AC-5	2.3	0	0	1.5	N	B	518.2	3573.0	-18.4	-28	3B paral.
AK1F10	AC-5	2.3	0	0	1.4	N	A	447.6	3086.2	-13.4	-25.2	3B paral.
AK1F11	AC-5	2.4	1	0	1.5	N	A	517.2	3566.1	-19.3	-28.5	3B paral.
AK1F12	AC-5	2.8	1	0	1.4	N	C	504.5	3478.5	-18.2	-27.9	3B paral.
AK1L1	AC-5	3.0	0	1	8.6	N	C	422.2	2911.1	-11.4	-24.1	
AK1L2	AC-5	3.1	0	1	10.1	N	B	544.4	3753.6	-16.4	-26.9	
AK1L3	AC-5	3.3	0	1	1.3	N	A	667.8	4604.5	-24.0	-31.1	
AK1L5	AC-5	1.9	0	1	8.6	N	C	487.2	3359.2	-10.5	-23.6	
AK1L6	AC-5	0.8	0	1	10.1	N	B	589.9	4067.4	-19.3	-28.5	
AK1L7	AC-5	2.1	0	1	1.3	N	A	697.9	4812.0	-21.5	-29.7	
AK2L1	AC2.5	3.2	0	1	8.9	N	C	712.6	4913.4	-22.2	-30.1	
AK2L2	AC2.5	3.0	0	1	9.0	N	C	656.6	4527.3	-23.6	-30.9	
AK2L3	AC2.5	2.4	0	1	1.2	N	A	588.0	4054.3	-23.8	-31.0	
AK2L5	AC2.5	2.9	0	1	8.7	N	C	328.2	2262.6	-11.9	-24.4	
AK2L6	AC2.5	3.0	0	1	10.3	N	C	453.8	3129.0	-17.1	-27.3	
AK2L7	AC2.5	2.7	0	1	1.2	N	A	636.0	4385.2	-24.2	-31.2	

Specimen I.D.	Asphalt Cement	Voids (VPAR) (%)	Cylinder=1 Beam=0	Laborat.=1 Field=0	Cooling Rate (C/h)	Aging None=N Short=S Long=L	Device A,B,C	Fracture Stress (psi)	(kPa)	Fracture Temp. (F)	(C)	Obs. Ref. No.
PA1L1	T1	1.5	0	1	4.5	N	C	528.6	3644.7	-1.3	-18.5	
PA1L2	T1	1.7	0	1	8.7	N	B	347.3	2394.6	-2.7	-19.3	
PA2L1	T2	0.72	0	1	9.0	N	C	448.0	3089.0	-9.0	-22.8	
PA2L2	T2	0	0	1	8.8	N	C	483.3	3332.4	-8.7	-22.6	
PA2L3	T2	0.49	0	1	4.5	N	C	663.1	4572.1	-17.1	-27.3	
PA2L4	T2	0	0	1	4.5	N	C	697.2	4807.2	-17.1	-27.3	
PA3L1	T3	0.91	0	1	9.0	N	C	519.5	3582.0	-9.6	-23.1	
PA3L2	T3	1.93	0	1	8.7	N	C	607.9	4191.5	-12.8	-24.9	
PA3L3	T3	0.97	0	1	4.5	N	C	661.3	4559.7	-14.8	-26.0	
PA3L4	T3	1.58	0	1	4.5	N	C	633.1	4365.2	-16.1	-26.7	
PA4L1	T4	1.83	0	1	9.1	N	C	618.3	4263.2	-14.1	-25.6	
PA4L2	T4	1.91	0	1	9.0	N	C	571.7	3941.9	-13.4	-25.2	1
PA4L3	T4	2.01	0	1	4.5	N	C	618.8	4266.6	-13.2	-25.1	
PA4L4	T4	1.35	0	1	4.3	N	B	446.6	3079.3	-10.1	-23.4	
PA5L1	T5	3.56	0	1	9.0	N	C	547.1	3772.3	-2.9	-19.4	
PA5L2	T5	1.94	0	1	8.0	N	C	566.9	3908.8	-4.2	-20.1	
PA5L3	T5	0.26	0	1	4.5	N	C	554.0	3819.8	-5.1	-20.6	
PA5L4	T5	1.75	0	1	4.5	N	C	589.6	4065.3	-4.7	-20.4	
PA6L1	T6	0.6	0	1	9.2	N	C	711.7	4907.2	-17.5	-27.5	
PA6L2	T6	0.87	0	1	9.0	N	C	628.1	4330.7	-15.3	-26.3	
PA6L3	T6	1.05	0	1	5.1	N	A	675.0	4654.1	-16.8	-27.1	
PA6L4	T6	0.53	0	1	5.0	N	A	675.4	4656.9	-18.2	-27.9	

Observations:

1 Length of the sample 9 in.

Specimen I.D.	Asphalt Cement	Voids (VPAR) (%)	Cylinder=1 Beam=0	Laborat.=1 Field=0	Cooling Rate (C/h)	Aging None = N Short= S Long=L	Device A,B,C	Fracture Stress (psi)	(kPa)	Fracture Temp. (F)	(C)	Obs. Ref. No.
FS1F1	BIT120AH	1.6	0	0	9.8	N	A	197.8	1364.0	-25.5	-32.0	
FS1F2	BIT120AH	1.5	0	0	8.7	N	B	371.2	2559.4	-23.1	-30.6	
FS1F5	BIT120AH	1.2	0	0	1.9	N	A	561.2	3869.5	-26.9	-32.7	
FS1F6	BIT120AH	1.5	0	0	1.9	N	A	453.7	3128.3	-23.4	-30.8	
FS2F1	B120LD	1.2	0	0	10.1	N	C	527.0	3633.7	-24.9	-31.6	
FS2F2	B120LD	0.9	0	0	10.0	N	C	635.9	4384.5	-24.9	-31.6	
FS2F5	B120LD	1.8	0	0	1.5	N	C	651.7	4493.5	-32.8	-36.0	
FS2F6	B120LD	1.4	0	0	1.8	N	A	531.7	3666.1	-29.2	-34.0	
FS3F1	BIT120ECO	1.3	0	0	10.2	N	C	449.3	3097.9	-16.6	-27.0	
FS3F2	BIT120ECO	1.2	0	0	9.0	N	C	596.9	4115.6	-23.4	-30.8	
FS3F5	BIT120ECO	1.6	0	0	1.9	N	A	589.0	4061.2	-27.2	-32.9	
FS3F6	BIT120ECO	1.5	0	0	1.8	N	A	575.6	3968.8	-28.1	-33.4	
FS4F1	BIT120ARC	-	0	0	10.5	N	C	648.7	4472.8	-32.8	-36.0	
FS4F2	BIT120ARC	-	0	0	10.4	N	C	735.6	5072.0	-32.1	-35.6	
FS4F5	BIT120ARC	1.1	0	0	1.5	N	C	652.6	4499.7	-34.8	-37.1	
FS4F6	BIT120ARC	-	0	0	1.9	N	A	687.4	4739.6	-34.6	-37.0	
FS5F1	BIT65AH	1.5	0	0	8.7	N	B	398.3	2746.3	-20.4	-29.1	
FS5F2	BIT65AH	1.8	0	0	8.9	N	C	578.6	3989.4	-17.7	-27.6	
FS5F5	BIT65AH	1.6	0	0	2.0	N	A	506.8	3494.4	-17.0	-27.2	
FS5F6	BIT65AH	2.3	0	0	1.7	N	A	539.3	3718.5	-18.9	-28.3	
FS6F1	BIT80AH	1.4	0	0	9.3	N	B	404.9	2791.8	-15.9	-26.6	
FS6F2	BIT80AH	1.6	0	0	8.9	N	B	398.1	2744.9	-20.0	-28.9	
FS6F5	BIT80AH	1.2	0	0	2.1	N	A	511.1	3524.0	-23.1	-30.6	
FS6F6	BIT80AH	-	0	0	2	N						
FS7F1	BIT200AH	1.7	0	0	9.0	N	C	636.8	4390.7	-28.7	-33.7	
FS7F2	BIT200AH	2.2	0	0	10.5	N	C	646.7	4459.0	-29.2	-34.0	
FS7F5	BIT200AH	1.3	0	0	1.5	N	C	639.6	4410.0	-32.1	-35.6	
FS7F6	BIT200AH	1.4	0	0	2	N	C	566.6	3906.7	-31.2	-35.1	
FS8F1	PmB1	2.7	0	0	9.1	N	C	861.9	5942.5	-33.9	-36.6	
FS8F2	PmB1	1.7	0	0	9.0	N	C	800.3	5518.1	-32.8	-36.0	

Specimen I.D.	Asphalt Cement	Voids (VPAR) (%)	Cylinder=1 Beam=0	Laborat.=1 Field=0	Cooling Rate (C/h)	Aging None = N Short= S Long=L	Device A,B,C	Fracture Stress (psi)	(kPa)	Fracture Temp. (F)	(C)	Obs. Ref. No.
FS8F5	PmB1	1.4	0	0	1.9	N	A	798.0	5502.1	-36.2	-37.9	
FS8F6	PmB1	1.8	0	0	1.9	N	A	816.4	5629.1	-36.8	-38.2	
FS9F1	BIT150AH	1.2	0	0	9.1	N	C	556.4	3836.4	-28.1	-33.4	
FS9F2	BIT150AH	1.2	0	0	10.1	N	A	640.1	4413.5	-35.0	-37.2	
FS9F5	BIT150AH	1.6	0	0	1.5	N	C	344.8	2377.4	-27.0	-32.8	1
FS9F6	BIT150AH	1.4	0	0	1.5	N	C	597.8	4121.8	-33.3	-36.3	

Observations:

1 Something wrong in the test

Specimen I.D.	Asphalt Cement	Voids (VPAR) (%)	Cylinder=1 Beam=0	Laborat.=1 Field=0	Cooling Rate (C/h)	Aging None=N Short=S Long=L	Device A,B,C	Fracture Stress (psi)	(kPa)	Fracture Temp. (F)	(C)	Obs. Ref. No.
CR1L1	Unit AC-20	4.2	1	1	8.7	N	C	441.2	3042.1	-13.0	-25.0	
CR1L2	Unit AC-20	2.2	1	1	10.3	N	C	407.1	2807.0	-13.5	-25.3	
CR1L3	Unit AC-20	3.8	1	1	1.3	N	A	337.8	2329.1	-16.1	-26.7	
CR1L4	Unit AC-20	2.3	1	1	1.3	N	A	283.6	1955.4	-11.2	-24.0	
CR1L5	Unit AC-20	5.2	1	1	10.1	S	C	352.5	2430.5	-12.1	-24.5	
CR1L6	Unit AC-20	6.5	1	1	10.1	S	C	346.7	2390.5	-13.2	-25.1	
CR1L7	Unit AC-20	5.4	1	1	1.5	S	C	364.3	2511.8	-15.9	-26.6	1
CR1L8	Unit AC-20	6.1	1	1	1.6	S	C	324.6	2238.1	-14.6	-25.9	
CR2F1	Viki AC-20	5.4	1	0	10.5	N	C	327.6	2258.8	-13.5	-25.3	
CR2F2	Viki AC-20	5.4	1	0	10.3	N	C	595.8	4108.0	-15.0	-26.1	
CR2F3	Viki AC-20	8.8	1	0	1.2	N	A	285.8	1970.6	-16.6	-27.0	2
CR2F4	Viki AC-20	8.4	1	0	1.2	N	A	247.3	1705.1	-22.4	-30.2	3
CR2F5	Viki AC-20	4.3	1	0	10.4	N	C	338.4	2333.3	-12.3	-24.6	
CR2F6	Viki AC-20	3.7	1	0	10.3	N	C	310.0	2137.5	-16.1	-26.7	
CR2F7	Viki AC-20	-	1	0	1.2	N	A	292.7	2018.2	-22.2	-30.1	
CR2F8	Viki AC-20	-	1	0	1.5	N	C	349.6	2410.5	-20.0	-28.9	4
CR2L1	Viki AC-20	2.4	1	1	10.1	N	C	466.3	3215.1	-16.1	-26.7	
CR2L2	Viki AC-20	0.9	1	1	8.9	N	C	359.4	2478.1	-12.3	-24.6	
CR2L3	Viki AC-20	1.6	1	1	1.3	N	A	402.3	2773.9	-19.1	-28.4	
CR2L4	Viki AC-20	2.3	1	1	1.4	N	A	374.4	2581.5	-19.1	-28.4	
CR2L5	Viki AC-20	4.3	1	1	10.2	S	C	310.4	2140.2	-11.7	-24.3	
CR2L6	Viki AC-20	5.7	1	1	8.6	S	A	194.7	1342.5	-13.5	-25.3	5
CR2L7	Viki AC-20	3	1	1	1.5	S	C	324.4	2236.7	-13.0	-25.0	
CR2L8	Viki AC-20	6.2	1	1	1.2	S	A	415.6	2865.6	-16.6	-27.0	
CR3F1	Cibr AC-20	5.3	1	0	10.4	N	B	286.5	1975.4	-16.6	-27.0	
CR3F2	Cibr AC-20	5.6	1	0	10.4	N	B	273.0	1882.3	-21.3	-29.6	
CR3F3	Cibr AC-20	6.2	1	0	1.0	N						
CR3F4	Cibr AC-20	6.2	1	0	1.2	N	A	238.4	1643.8	-27.6	-33.1	
CR3F5	Cibr AC-20	5.7	1	0	10.4	N	C	345.2	2380.2	-24.3	-31.3	
CR3F6	Cibr AC-20	5.7	1	0	10.4	N	C	390.1	2689.7	-25.8	-32.1	
CR3F7	Cibr AC-20	6.6	1	0	1.2	N	A	211.6	1459.0	-35.9	-37.7	
CR3F8	Cibr AC-20	-	1	0	1.6	N	C	375.5	2589.1	-33.0	-36.1	

Specimen I.D.	Asphalt Cement	Voids (VPAR) (%)	Cylinder=1 Beam=0	Laborat.=1 Field=0	Cooling Rate (C/h)	Aging None=N Short=S Long=L	Device A,B,C	Fracture Stress (psi)	(kPa)	Fracture Temp. (F)	(C)	Obs. Ref. No.
CR3L1	Cibr AC-20	6.5	1	1	10.3	N	C	392.5	2706.3	-21.6	-29.8	
CR3L2	Cibr AC-20	5.3	1	1	10.4	N	C	383.3	2642.9	-20.9	-29.4	
CR3L3	Cibr AC-20	3.9	1	1	1.3	N	A	279.0	1923.7	-21.8	-29.9	
CR3L4	Cibr AC-20	3.7	1	1	1.3	N	A	335.8	2315.3	-22.9	-30.5	
CR3L5	Cibr AC-20	5.1	1	1	10.4	S	C	305.6	2107.1	-18.4	-28.0	
CR3L6	Cibr AC-20	6.9	1	1	9.8	S	A	292.8	2018.9	-19.5	-28.6	
CR3L7	Cibr AC-20	5.3	1	1	1.5	S	C	395.0	2723.5	-19.7	-28.7	
CR3L8	Cibr AC-20	3.5	1	1	1.1	S	A	200.8	1384.5	-17.5	-27.5	6
CR4F1	PetC AC-20	5.4	1	0	10.2	N	C	393.3	2711.8	-19.1	-28.4	
CR4F2	PetC AC-20	4.9	1	0	8.8	N	A	438.1	3020.7	-13.4	-25.2	
CR4F3	PetC AC-20	6.2	1	0	1.3	N	A	335.2	2311.2	-21.1	-29.5	
CR4F4	PetC AC-20	5.4	1	0	1.2	N	A	215.6	1486.6	-22.7	-30.4	
CR4F5	PetC AC-20	-	1	0	10.3	N	C	351.0	2420.1	-15.0	-26.1	
CR4F6	PetC AC-20	-	1	0	10.3	N	C	328.1	2262.2	-15.2	-26.2	
CR4F7	PetC AC-20	4.4	1	0	1.4	N	C	330.4	2278.1	-18.4	-28.0	
CR4F8	PetC AC-20	3.9	1	0	1.2	N	A	230.2	1587.2	-27.0	-32.8	
CR4L1	PetC AC-20	4.6	1	1	10.4	N	C	381.3	2629.1	-18.6	-28.1	
CR4L2	PetC AC-20	3	1	1	10.2	N	C	381.1	2627.7	-15.0	-26.1	
CR4L3	PetC AC-20	4.2	1	1	1.5	N	C					
CR4L4	PetC AC-20	3.4	1	1	1.5	N	C	405.8	2798.0	-20.2	-29.0	
CR4L5	PetC AC-20	3.6	1	1	9.9	S	C	371.0	2558.0	-11.7	-24.3	
CR4L6	PetC AC-20	3.1	1	1	10.3	S	C	359.1	2476.0	-10.1	-23.4	
CR4L7	PetC AC-20	5.2	1	1	1.6	S	C	365.8	2522.2	-15.7	-26.5	
CR4L8	PetC AC-20	4.8	1	1	1.6	S	C	363.4	2505.6	-15.7	-26.5	
CR5F1	Viki AC-10	8	1	0	10.6	N	A	226.1	1559.0	-23.1	-30.6	
CR5F2	Viki AC-10	9.2	1	0	10.0	N						
CR5F3	Viki AC-10	8.4	1	0	1.2	N	A	187.2	1290.7	-25.8	-32.1	
CR5F4	Viki AC-10	7.1	1	0	1.2	N	A	258.1	1779.6	-24.9	-31.6	
CR5F5	Viki AC-10	-	1	0	10.4	N	C	396.3	2732.5	-23.8	-31.0	
CR5F6	Viki AC-10	7.3	1	0	10.5	N	C	294.5	2030.6	-19.1	-28.4	
CR5F7	Viki AC-10	7.5	1	0	1.6	N	C	344.7	2376.7	-28.3	-33.5	
CR5F8	Viki AC-10	7.5	1	0	1.5	N	C	285.8	1970.6	-25.4	-31.9	

Specimen I.D.	Asphalt Cement	Voids (VPAR) (%)	Cylinder=1 Beam=0	Laborat.=1 Field=0	Cooling Rate (C/h)	Aging None=N Short=S Long=L	Device A,B,C	Fracture Stress (psi)	(kPa)	Fracture Temp. (F)	(C)	Obs. Ref. No.
CR5L1	Viki AC-10	6.7	1	1	10.1	N	B	547.7	3776.4	-16.8	-27.1	
CR5L2	Viki AC-10	4.7	1	1	9.5	N	A	332.5	2292.6	-21.1	-29.5	
CR5L3	Viki AC-10	5.9	1	1	1.7	N	C	330.1	2276.0	-26.1	-32.3	
CR5L4	Viki AC-10	5.7	1	1	1.7	N	B	291.2	2007.8	-25.1	-31.7	
CR5L5	Viki AC-10	5.2	1	1	1.6	S	A	247.6	1707.2	-19.7	-28.7	
CR5L6	Viki AC-10	6	1	1	1.1	S	A	302.0	2082.3	-22.2	-30.1	
CR5L7	Viki AC-10	7.6	1	1	10.0	S	C	322.7	2225.0	-21.5	-29.7	
CR5L8	Viki AC-10	6.2	1	1	9.4	S	A	290.7	2004.4	-16.8	-27.1	

Observations:

1 Change of the nitrogen bottle during the test
2 Damaged sample
3 The sample may be damaged
4 Change of the nitrogen bottle during the test
5 Fracture stress may be wrong
6 Fracture stress may be wrong

Appendix E
Cracking Observations for Sodankyla Test Sections

In the following tables, cracks that are limited to one lane only are marked in the column of the corresponding lane. Cracks that exist over the whole width of the pavement are marked in the column "Both Lanes."

BIT120AH, located on the Right Lane

Station (m)	Number of Cracks: Left Lane	Right Lane	Both Lanes	Length (m)	Initiation Point	Initiation Date (Julian)	Air Temp. (C)	Pavem. Temp. (C)	Air Temp. (F)	Pavem. Temp. (F)
8801										
8815			1	8.5						
8967			1	8.5						
9044			1	8.5						
9145			1	8.5						
9184	1			4	Edge					
9242			1	8.5	Center	35	-28.5	-22.5	-19.3	-8.5
9263			1	8.5		36	-28.5	-22.5	-19.3	-8.5
9305	1			3	Center	86	-26	-16	-14.8	3.2
9310			1	7.5	Center	86	-26	-16	-14.8	3.2
9348	1			3	Center	86	-26	-16	-14.8	3.2
9350		1		4		86	-26	-16	-14.8	3.2
9395		1		4		74	-25	-16	-13	3.2
9405	1			3.5	Center	74	-25	-16	-13	3.2
9409		1		3.5	Center	32	-30	-19.5	-22	-3.1
9439		1		3	Center	74	-25	-16	-13	3.2
9441		1		4.25		36	-28.5	-22.5	-19.3	-8.5
9445	1			4.25		86	-26	-16	-14.8	3.2
9461			1	7	Center	74	-25	-16	-13	3.2
9471	1			3.5	Edge	86	-26	-16	-14.8	3.2
9504	1			3.5	Edge					
9527		1		4	Center					
9530			1	8.5						
9560										
Total	7	6	9							

B120LD, located on the Left Lane

Station (m)	Number of Cracks Left Lane	Right Lane	Both Lanes	Length (m)	Initiation Point	Initiation Date (Julian)	Air Temp. (C)	Pavem. Temp. (C)	Air Temp. (F)	Pavem. Temp. (F)
12104										
12195		1		4.25						
12450			1	8.5						
12660		1		4	Center	36	-28.5	-22.5	-19.3	-8.5
12661	1			4	Center	50	-33	-24.5	-27.4	-12.1
12750		1		4.25	Edge	39	-23.5	-20	-10.3	-4
13160			1	8.5						
13298			1	8.5						
13342			1	8.5						
13359			1	8.5						
13389			1	8.5						
13404			1	8.5						
13428			1	8.5						
13452			1	8.5						
13490										
Total	1	3	9							

BIT120ECO, located on the Right Lane

Station (m)	Number of Cracks Left Lane	Right Lane	Both Lanes	Length (m)	Initiation Point	Initiation Date (Julian)	Air Temp. (C)	Pavem. Temp. (C)	Air Temp. (F)	Pavem. Temp. (F)
9960										
10162			1	8.5						
10183			1	8.5						
10242		1		3	Center	331	-25	-20	-13	-4
10262	1			2	Center					
10265			1	7.5	Center	35	-28.5	-22.5	-19.3	-8.5
10268	1			3	Center	74	-25	-16	-13	3.2
10286			1	7.5	Center	35	-28.5	-22.5	-19.3	-8.5
10295	4		1	8.5		36	-28.5	-22.5	-19.3	-8.5
10298		1		2	Center	86	-26	-16	-14.8	3.2
10340			1	8.5		86	-26	-16	-14.8	3.2
10350			1	8.5		343	-20	-17	-4	1.4
10360			1	8.5		36	-28.5	-22.5	-19.3	-8.5
10388	1			5	Edge	36	-28.5	-22.5	-19.3	-8.5
10406			1	8.5	Center	35	-28.5	-22.5	-19.3	-8.5
10417	1			5	Edge	36	-28.5	-22.5	-19.3	-8.5
10467			1	8.5		35	-28.5	-22.5	-19.3	-8.5
10512			1	8.5						
10525			1	8.5						
10552			1	8.5						
10604			1	8.5						
10708			1	8.5						
10791			1	8.5						
10802										
Total	8	2	16							

BIT120ARC, located on the Right Lane

Station (m)	Number of Cracks			Length (m)	Initiation Point	Initiation Date (Julian)	Air Temp. (C)	Pavem. Temp. (C)	Air Temp. (F)	Pavem. Temp. (F)
	Left Lane	Right Lane	Both Lanes							
11196										
11352		1		4	Center	11	-32.5	-22.5	-26.5	-8.5
11747	1			4	Center	63	-22	-18	-7.6	-0.4
11752			1	8	Center	11	-32.5	-22.5	-26.5	-8.5
11840		1		4	Center	86	-26	-16	-14.8	3.2
12195		1		4.25						
12450			1	8.5						
12454										
Total	1	3	2							

BIT65AH, located on the Left Lane

Station (m)	Number of Cracks			Length (m)	Initiation Point	Initiation Date (Julian)	Air Temp. (C)	Pavem. Temp. (C)	Air Temp. (F)	Pavem. Temp. (F)
	Left Lane	Right Lane	Both Lanes							
11140										
11352	1			4		343	-20	-17	-4	1.4
11352		1		4	Center	11	-32.5	-22.5	-26.5	-8.5
11545										
Total	1	1	0							

BIT80AH, located on the Left Lane

Station (m)	Number of Cracks			Length (m)	Initiation Point	Initiation Date (Julian)	Air Temp. (C)	Pavem. Temp. (C)	Air Temp. (F)	Pavem. Temp. (F)
	Left Lane	Right Lane	Both Lanes							
10802										
10964	1			4	Edge	86	-26	-16	-14.8	3.2
10967			1	7	Center	35	-28.5	-22.5	-19.3	-8.5
11014	1			2	Center	63	-22	-18	-7.6	-0.4
11018	1			2	Center	63	-22	-18	-7.6	-0.4
11021			1	7	Center	322	-28.5	-22.5	-19.3	-8.5
11080			1	8.5	Center	86	-26	-16	-14.8	3.2
11083		1		3	Center					
11090		1		1	Center					
11122			1	8	Center	35	-24	-19	-11.2	-2.2
11196										
Total	3	2	4							

BIT200AH, located on the Left Lane

Station (m)	Number of Cracks: Left Lane	Right Lane	Both Lanes	Length (m)	Initiation Point	Initiation Date (Julian)	Air Temp. (C)	Pavem. Temp. (C)	Air Temp. (F)	Pavem. Temp. (F)
11545										
11747	1			4	Center	63	-22	-18	-7.6	-0.4
11752			1	8	Center	11	-32.5	-22.5	-26.5	-8.5
11840		1		4	Center	86	-26	-16	-14.8	3.2
12104										
Total	1	1	1							

BIT150AH, located on Both Lanes

Station (m)	Number of Cracks: Left Lane	Right Lane	Both Lanes	Length (m)	Initiation Point	Initiation Date (Julian)	Air Temp. (C)	Pavem. Temp. (C)	Air Temp. (F)	Pavem. Temp. (F)
13410										
13428			1	8.5						
13452			1	8.5	Edge					
13492			1	8.5						
13525			1	8	Edge					
13538			1	8						
13566			1	8.5						
13588			1	8.5						
13610			1	7	Center	86				
13687	1			2	Center					
13690			1	8.5		50	-33	-24.5	-27.4	-12.1
13710			1	8.5		50	-33	-24.5	-27.4	-12.1
13764			1	8.5		113	-24	-14	-11.2	6.8
13784			1	8.5		86	-26	-16	-14.8	3.2
13809		1		4.25		113	-24	-14	-11.2	6.8
13906			1	8.5						
14017			1	8.5						
Total	1	1	14							

PmB1, located on the Right Lane

Station (m)	Number of Cracks: Left Lane	Right Lane	Both Lanes	Length (m)	Initiation Point	Initiation Date (Julian)	Air Temp. (C)	Pavem. Temp. (C)	Air Temp. (F)	Pavem. Temp. (F)
9560										
9562			1	8.5						
9580			1	8.5						
9644			1	7.5		35	-28.5	-22.5	-19.3	-8.5
9683			1	7.5		35	-28.5	-22.5	-19.3	-8.5
9711			1	6.5		74	-25	-16	-13	3.2
9780			1	8.5		36	-28.5	-22.5	-19.3	-8.5
9850			1	8.5		50	-33	-24.5	-27.4	-12.1
9910			1	8.5		324	-24	-18	-11.2	-0.4
9960										
Total	0	0	8							